Interpretation of pressuremeter test results in frozen soils

Ladanyi, B.

Internal Report (National Research Council Canada. Division of Building Research); no. DBR-IR-401, 1972-12-01

NATIONAL RESEARCH COUNCIL OF CANADA
DIVISION OF BUILDING RESEARCH

INTERPRETATION OF PRESSUREMETER TEST RESULTS IN FROZEN SOILS

by

B. Ladanyi
(Centre d'Ingénierie Nordique de
l'Ecole Polytechnique)

Internal Report No. 401
of the
Division of Building Research

Ottawa
December 1972

PREFACE

In designing foundations and other engineering structures for use in permafrost areas, there has been an increasing need for new methods and instruments to evaluate frozen soil properties in the field. The purpose of the present research project is to investigate whether and how one particular soil testing instrument, known as the "Ménard Pressuremeter", could be used to furnish field data for the evaluation of rheological properties of frozen soils.

To realize this objective an agreement was signed in June 1971 between the Division of Building Research of the National Research Council of Canada (DBR/NRC) and the Centre d'Ingénierie Nordique de l'Ecole Polytechnique de Montréal (CINEP), in which the former agreed to provide all the equipment and technical assistance required for the field studies, and the latter the research supervision and interpretation of test results. The project began 1 June 1971 and ended 31 May 1972.

The first phase was carried out during the months of June and July 1971, and involved field investigations with the pressuremeter both at the DBR/NRC site in Ottawa and at two permafrost sites at Thompson, Manitoba. Personnel involved in carrying out the first (field) phase of the project were: G.H. Johnston, Research Officer, Geotechnical Section DBR/NRC; Dr. B. Ladanyi, Director, CINEP (Project Supervisor); and J.C. Plunkett, Technical Officer, Geotechnical Section DBR/NRC.

An interim progress report, covering the first phase, was presented to the Division in October 1971.

The second phase of the project, carried out between August 1971 and May 1972, comprised the development of a theory and a practical method for determining creep properties of frozen soils from pressuremeter test results as well as the calculation of all results obtained in the field according to the proposed method.

Ottawa,
December 1972

N. B. Hutcheon
Director

TABLE OF CONTENTS

INTERPRETATION OF PRESSUREMETER TEST RESULTS IN FROZEN SOILS

by

B. Ladanyi
(Centre d'Ingénierie Nordique de
l'Ecole Polytechnique)

SCOPE OF THE PROJECT

The purpose of this project was to investigate the suitability of the pressuremeter as an instrument for evaluating creep properties of frozen soils.

Such a study was considered necessary for the following two reasons:

(1) Although the potential capacity of the pressuremeter for studying creep behavior of soils has been recognized from its beginning by Ménard (1957), it has never been shown how the instrument and the test should be used for determining basic creep parameters of the soil, and

(2) When the present research project was undertaken there was no published account available on pressuremeter tests in frozen soils and the problems that might be encountered in performing such tests.

At present there is a large amount of literature available on the test procedure, the performance, and the interpretation of test results for pressuremeter tests performed in nearly all common types of unfrozen soils and rocks. Moreover, several types of pressure-cells and measuring equipment have been developed by Ménard and his co-workers to cover the needs of various ground conditions.

Nevertheless, in order to be able to use the pressuremeter for evaluating creep properties of frozen soils, a certain number of practical problems had to be solved first, such as:

(1) how to drill the borehole for the test without seriously disturbing the natural temperature field in the ground surrounding the borehole;

(2) how to monitor the temperature variation at the contact between the probe and the ground throughout the test; and

(3) how to perform the test to obtain a maximum amount of creep information without exceeding the practical limits of probe extension and test duration.

To meet these requirements, some modification in instrumentation and the current test procedure were found to be necessary. They will be described in the following chapters.

INSTRUMENTATION

A pressuremeter type G was used in the tests. It consists essentially of a pressure-volume control device and a probe connected together by a coaxial plastic tubing (Figure 1). The pressure-volume control device had a 700 cm^3 volume capacity and 0 to 25 kg/cm^2 pressure range. The probe was of NX type (60 mm) with a metallic extensible protection jacket. The diameter of the central (measuring) part of the empty probe with the protection jacket was 66 mm. A more detailed drawing of the pressure-volume control and the probe (without jacket) can be seen in Figure 2. According to the operation manual, the length of the measuring cell is about 21 cm.

In comparison with a commercially available instrument the pressuremeter used in these tests had the following additions and modifications:

(1) The supplier was asked to add a fine adjustment valve to the pressure control system. This would enable a more accurate control of pressure in the probe, especially when performing long-term creep tests at constant pressure. The new valve, inserted between Nos. 15 and 17 in Figure 2(a), was found to perform satisfactorily for these types of tests.

(2) It was considered that for temperature control during the test it would be sufficient to check the temperature at three points on the exterior surface of the probe in contact with the wall of the borehole: one at each end, and one in the middle of the probe. For that purpose,

thermocouples made at the DBR/NRC laboratory in Ottawa, were fixed to the probe. The two upper thermocouples were affixed by plastic tapes; the one at the lower end of the cell, considered to be the most important, was mounted in the exterior wall of a specially fabricated cylindrical bakelite piece fixed to the lower end of the probe. The thermocouple leads were conducted through the inside of the cell and along the rods to the measuring instrument at the ground surface. The bakelite end piece was meant to provide the insulation necessary to isolate the temperature measurement in the borehole wall from the heat transfer along the steel rods and the probe. In use, it was found that the lowest thermocouple performed satisfactorily, while the upper two were often torn off the probe during its introduction into the borehole. Obviously, the system used in this series of tests, while satisfying the immediate needs, will have to be improved in any final design of a special probe for use in frozen soils.

(3) In order to keep the fluid to be injected into the probe during the test at low temperature, the fluid (a mixture of 10 per cent ethylene glycol and 90 per cent water) in the volumeter was put in a foamed-plastic box, and surrounded with crushed ice (Figure 3).

BOREHOLE DRILLING METHOD

The pressuremeter test results are known to be affected considerably by the quality of the borehole drilling job. In fact, it has been found that the state of disturbance of the borehole wall, which depends to a great extent on the drilling method, has a direct bearing on the shape of the pressuremeter curve from which all soil information is eventually deduced. According to Jezequel et al (1968), the value of pressuremeter modulus deduced from the initial portion of the curve is particularly affected by drilling disturbance and improper hole diameter, while the value of the limit pressure seems to be affected only slightly.

In general, in any type of soil, the borehole should be made in such a way that a minimum of mechanical disturbance is produced in the surrounding ground. Moreover, at the level of the test, the shape of the hole should be as close as possible to a right circular cylinder with the diameter only slightly larger than that of the pressuremeter probe. Various methods have been proposed in order to achieve this result, some of which are described in the booklet: "Essai pressiométrique normal" and elsewhere in the literature (Jezequel et al, 1968).

In cohesive soils and at shallow depths the most recommended method consists of drilling the hole by means of a manual auger drill which is usually supplied with the pressuremeter. While this is often sufficient for practical purposes, other methods of obtaining a good borehole in clays have been mentioned such as the combination of auger drilling and Shelby tube sampling. The tube sampling is carried out immediately before the pressuremeter test with its main purpose being to make a clean cylindrical hole that will tightly fit the pressuremeter probe.

In the present field study one such combined method was used. Usually, the hole was drilled to about 2 ft above the required test level by using a motorized drilling rig. The rest of the hole was made by pushing into the ground a special sampling tube having an inside-turned sharpened end. In preliminary tests in Leda clay in Ottawa, a special thin-walled sampler was used for that purpose; in frozen soil, in Thompson, having a much greater strength, a thick-walled tube with an outside diameter of $2\frac{3}{4}$ in. and a wall thickness of $\frac{1}{4}$ in. had to be used. Its cutting edge was tapered towards the inside and indented to facilitate the soil cutting by rotation. It was hoped that the particular method of sharpening the cutting edge would confine most of the soil disturbance to the inside of the tube. Similar tubes have been used by others for the same purpose and are known as "Delmag driven samplers" (Jezequel et al, 1968).

NUMBER AND TYPE OF TESTS

In order to test the equipment and the method before departing for Thompson, a series of 5 pressuremeter tests were made in Leda clay at the DBR/NRC site in Ottawa in June 1971. In Thompson, 20 more tests were made during July 1971 of which 14 were at the "Thompson 1" permafrost site in a varved frozen clay-silt soil, 3 were made at "Thompson 2" in a frozen clay, and 3 more at "Thompson 1" in unfrozen varved soil. All the tests have been designated by two numbers, the first denoting the number of the borehole, and the second, the number of the test in the borehole.

All the tests were made with only one pressuremeter equipment (No. 727 G) and one jacketed NX probe.

SOIL CONDITIONS AT THE SITE

At the Thompson 1 site, where the majority of tests were performed, within the depth interval investigated, i. e., between 5 and 14 ft, the soil was a varved clay of low to medium plasticity composed

of dark brown clay layers from $\frac{1}{2}$ to 1 in. thick, and tan-coloured silt layers increasing in thickness with depth from 1 to 3 in.

The most significant ice segregation was found in the top 13 ft and was usually associated with the dark layers. Ice lenses were mainly horizontal and varied in thickness from hairline to a maximum of about $\frac{1}{2}$ in. The ground temperature at the site, below the active layer, i.e., between 5 and 30 ft, was fairly uniform varying between 31.5 and 31.8° F and was found to be essentially isothermal throughout the year.

TESTING PROGRAM

Standard Tests

Before starting a proper long-term testing of soil at each site it was necessary to carry out several short-term tests to investigate the general character of the particular soil. Such short-term tests are similar to Ménard's standard or normal pressuremeter tests, used in current soil testing practice. In such a test the pressure in the probe is increased up to the limit pressure in about 10 to 20 pressure increments, each pressure level being kept constant for no longer than 2 min. At each stage, volume readings are taken 30 sec, 1 min and 2 min after each pressure increase. Typical loading diagrams from such tests performed in this work are shown in Figure 4 (Tests DBR I-1, II-1 and II-2), in Figure 5 (Test 1-1), Figure 9 (Tests 8-1 to 8-3) and Figure 11 (Test 12-1). It will be seen that, while the time intervals were 2 min per stage in all tests, the load increments in a particular test were sometimes smaller at the beginning of the test, which had the purpose of better describing the shape of the pressuremeter curve at low pressures where the effect of eventual soil disturbance is felt mostly.

Long-Term Tests

In order to investigate the long-term behavior of the soil, several types of tests were tried.

A. One-stage creep tests

These tests consisted of rapidly bringing the pressure to a given high level and leaving it there as long as possible. Some such tests were simply standard tests the last stage of which was kept constant from 20 min to several hours. Loading diagrams of such tests are, for example, Figure 5 (Tests 1-2 and 2-1), Figure 8 (Tests 5-1

and 6-1), and Figure 11 (Test 12-2). Still more rapid loading up to the creep stage was attempted in tests Nos. 7-1 (Figure 8) and 11-1 (Figure 10). Tests Nos. 4-1 and 4-2 (Figure 7) also fall in the category of one-stage creep tests, even if their first stage was a little different (4 min instead of 2 min per stage).

B. Multi-stage creep tests

A multi-stage creep test consists of bringing the pressure rapidly up to an initial creep level by standard procedure and then increasing it to the limit in stages, each being kept constant for 15 or more minutes. Loading diagrams of such tests are shown in Figure 4 (Tests DBR III-1 and IV-1), Figure 6 (Tests 2-2 and 2-3), and in Figure 10 (Tests 9-1 and 10-1).

C. Equal-stage creep tests

Equal-stage creep tests are similar to the multi-stage creep tests the difference being that they are not preceded by a rapid pressure increase. Only two such tests were carried out, viz., Test 3-1 (Figure 6) and 3-2 (Figure 7).

It should be noted that each creep test has to be planned in advance so that the required creep information at a given pressure level or levels is obtained without exceeding the volume capacity of the probe, which is 700 cm^3 maximum.

TESTING PROCEDURE

As the standard testing procedure is described in the Operation Manual supplied by the producer ("Pressiomètre type G"), only a few particular aspects will be given here.

(1) Zero Point Determination

Zero point is the volume reading when all the water is squeezed out from the measuring part of the probe. The zero reading was checked before each new test. The water column was deliberately kept at high level (zero at 30 to 50 cm^3) so that the whole capacity of the volumeter and the probe could be used.

(2) Calibration Curve Determination

The calibration curve of the probe reflects the extension resistance of the probe and the flow resistance of the hydraulic system. In

the Operation Manual a standard rapid loading procedure is recommended for the calibration curve determination. This procedure corresponds well to the conditions of a standard pressuremeter test. As some lag in response due to the flow resistance is usually observed during calibration, it was considered that a long-term calibration curve should be used in connection with long-term pressuremeter tests. This procedure was followed as much as possible. The effect of this detail on the pressuremeter curve was, however, quite small.

The calibration curve was determined at least once each morning before starting a new series of tests, and sometimes was re-checked after the tests were completed.

(3) Temperature Stabilization

As the frozen ground temperature at Thompson was only slightly lower than 32° F (i. e., from about 31. 5 to 31. 8° F), while the outside air temperature during the tests was mainly between 60 and 70° F, some temperature disturbance and even some thawing of the walls of the borehole may have been produced during the drilling and sampling operation. This was shown by a temperature check made immediately after lowering the probe into the borehole. Usually the temperature stabilized within about an hour and remained below freezing thereafter. Most of the tests were, therefore, preceded by a temperature stabilization period of from 30 minutes to one hour.

(4) Pressure and Volume Corrections

For the apparatus and the range of pressure used in the tests the volume correction due to expansion of the tubing is very small and can be ignored, according to the Operation Manual.

The gauge pressure, however, must be corrected for the piezometric head and the extension resistance of the probe. The correction is made according to the formula:

$$p_c = p_m - q_i (V_m) + q_{pz} \qquad (1)$$

in which:

p_c = corrected (applied) pressure;

p_m = pressure reading at the gauge;

$qi\ (V_m)$ = extension resistance of the probe, read from the calibration curve for the injected volume, V_m;

V_m = volume reading minus zero-point reading = total injected volume;

q_{pz} = piezometric pressure due to the column of the water, calculated from

$$q_{pz} = (H + h - h_o)\ \gamma_w \qquad (2)$$

where

H = difference in elevation between the centre of the probe and the ground surface at the top of the borehole;

h = difference in elevation between the pressure gauge and the top of the borehole;

h_o = height of the probe centre during the determination of the calibration curve.

PLOTTING OF PRESSUREMETER CURVE

The results of an ordinary pressuremeter test are usually plotted as a "corrected pressuremeter curve" (Figure 12) defined as

$$V_m = f\ (p_c) \qquad (3)$$

where V_m denotes the total volume of liquid injected into the measuring cell from the start of pressure application and p_c is the applied pressure corrected for the inflation resistance of the probe and for the piezometric head, according to Eq. (1).

The strength determination method adopted in this report uses, as the basis, the "true pressuremeter curve" as would be obtained in an ideal pressuremeter test starting from the original ground pressure, p_o.

The true pressuremeter curve represents a relationship of the form

$$\Delta V = f(p_c - p_o) \tag{4}$$

where p_o denotes the original total lateral ground pressure at the level of the test, and

$$\Delta V = V_m - V_{mo} \tag{5}$$

where V_{mo} is the volume of the liquid injected in the probe at $p_c = p_o$. In practice, the true pressuremeter curve is obtained from the former by shifting the origin from 0 to $0'$, as shown in Figure 12.

Figure 13 shows the same pressuremeter curve from Figure 12 (obtained in Leda clay at the DBR/NRC site in Ottawa) replotted in a semi-log plot of log $(\Delta V/V)$ vs $(p_c - p_o)$, as proposed by Gibson and Anderson (1961). The values of $\Delta V/V$ have been obtained by dividing ΔV values in Figure 12 by $V = V_o + \Delta V$, where V_o denotes the volume of the measuring section of the probe at the moment when the pressure in the probe has attained the original ground pressure p_o. The volume V_o was obtained as a sum

$$V_o = V_{empty} + V_{mo} \tag{6}$$

of the volume of the empty measuring section of the probe ($V_{empty} \approx 718$ cm^3 for the probe used in the tests) and the volume V_{mo} of the water injected at $p_c = p_o$. The role of the semi-log plot in the determination of soil parameters will be shown later.

USE OF PRESSUREMETER TEST RESULTS IN CURRENT PRACTICE

In current pressuremeter practice the basic information that a pressuremeter test is supposed to furnish is, according to Ménard, limited to three parameters: (1) the limit pressure, p_ℓ ; (2) the creep pressure, p_f ; and (3) the pressuremeter modulus, E_p. The values of the three parameters are read directly on, or deducted from, the corrected pressuremeter curve p_c vs V_m, as shown in Figure 12.

For foundation design purposes, the parameters are then substituted into proper empirical expressions, proposed by Ménard (1963), enabling the settlement and the bearing capacity of foundations and other earth structures to be estimated.

In other words, in current practice, an attempt is rarely made to determine basic soil properties from the pressuremeter test results. The test is regarded rather as a model test or an in situ loading test from which, after some corrections due mainly to scale and shape effects, direct conclusions can be drawn as to the behavior of full-scale foundations.

In the past, however, several methods have been proposed by Ménard and others (Gibson and Anderson, 1961; Ladanyi, 1963b) for determining; from the test certain basic soil parameters such as the undrained cohesion of clays and the angle of internal friction of sands. The purpose of the present work being the determination of some basic and rather unconventional soil properties, the currently recommended test interpretation procedure could not have been used but had to be replaced by a specially developed procedure.

OUTLINE OF THE PROPOSED INTERPRETATION METHOD

There are essentially two methods that can be used for determining time-dependent deformation and strength properties from pressuremeter tests carried out in frozen soils.

On the one hand, a series of pressuremeter tests carried out with equal pressure increments but with different lengths of time per increment in each test can be made in a frozen soil. The pressuremeter curves resulting from such tests may be regarded as the results of a series of loading tests with different times to failure or different average loading rates. Using a convenient interpretation method, one can determine from such tests time-dependent values of certain parameters such as the pressuremeter modulus E_p and the peak compression strength q_p. This method, while not requiring any new theory, nevertheless lacks generality and implies a large amount of in situ testing that may become time-consuming and impractical.

A second method, that seems more practical, consists of performing systematic stress-controlled pressuremeter creep tests in frozen soils from which certain basic parameters in the general creep equation of the soil can be determined. Once the creep equation is known, it can be used either directly for solving certain creep problems in the particular frozen soil, or indirectly for calculating and plotting isochronous pressuremeter curves. The latter can subsequently be interpreted in the same manner as those obtained by direct testing in the first method.

In the following, a general interpretation method applicable to any pressuremeter curve will be shown first. Subsequently, a procedure enabling the determination of creep parameters in the general creep equation will be shown.

INTERPRETATION OF SHORT-TERM PRESSUREMETER TESTS

From a soil mechanics point of view, a frozen soil is essentially a (c, ϕ)-material with a relatively strong time-and-temperature-dependent cohesion and a much less time-and-temperature-dependent angle of friction. As very little is yet known about intergranular stresses in frozen soils, c and ϕ are assumed to be total stress parameters. Moreover, if the soil is fine-grained and ice-saturated the volumetric component of the deformation will be so small that it can be neglected in the calculation. With these assumptions, a pressuremeter curve in frozen soil can be interpreted by using the method described in the following.

It has been known for quite some time that in metal plasticity (Nádai, 1931), the problem of expansion of a thick-walled cylinder could be solved approximately for any given stress-strain law of the material if the cylinder is considered as an assemblage of a great number of thin concentric cylinders, all of them responding to a common stress-strain law. At a given expansion of the bore, any particular such thin cylinder will be strained to a given point on the common stress-strain curve. Owing to the fact that the assumption of volume constancy enables the average strain in each cylinder to be directly related to the expansion of the bore, the complete pressure-expansion curve can be obtained by a numerical integration method.

The method is described, among others, in Nádai (1931, Chap. 29; 1950, Chap. 31) and in Hill (1950, pp. 122-123). Several approximate methods of this type have been reviewed by Morrison (1948), including

a method due to Shepherd (1948) for the converse calculation, that of deriving the stress-strain curve in shear from the known pressure-expansion relationship.

It is essentially this method, with small variations, that has been used by the author for a number of years to solve several cavity expansion problems both in sands (Ladanyi, 1961, 1963b) and in clays (Ladanyi, 1963a, 1966).

Theory

The state of stress and strain around a cylindrical cavity expanding from zero radius in an infinite medium can be obtained by integrating the differential equation of equilibrium valid for the cylindrical symmetry and no body forces case

$$\frac{d\sigma_r}{dr} + \frac{\sigma_r - \sigma_\theta}{r} = 0 \tag{7}$$

where σ_r and σ_θ are total principal stresses in radial and circumferential direction, respectively, while r is any radius measured from the centreline of the cavity.

Assuming, as shown schematically in Figures 14a and b, that the medium is composed of an assemblage of thin concentric cylinders and that in any such cylinder between the radii r_i and r_{i+1}, the mobilized undrained plane strain compression strength,

$$q_{i,i+1} = (\sigma_1 - \sigma_3)_{i,i+1} , \tag{8}$$

corresponds to the average shear strain in that cylinder,

$$\gamma_{i,i+1} = (\varepsilon_1 - \varepsilon_3)_{i,i+1} , \tag{9}$$

Eq. (7) can be integrated for one such cylinder to give

$$\int_i^{i+1} d\sigma_r = -\int_i^{i+1} (\sigma_r - \sigma_\theta)_{i,i+1} \frac{dr}{r} = -q_{i,i+1} \int_i^{i+1} \frac{dr}{r} \tag{10}$$

or

$$\sigma_{ri} - \sigma_{r,i+1} = q_{i,i+1} \ln \frac{r_{i+1}}{r_i} \tag{11}$$

For a given stress-strain curve, and by substituting the proper boundary conditions, Eq. (10) enables the complete state of stress and strain around the cavity to be found.

In order to solve the converse case of strength determination from a pressuremeter curve, Eq. (11) could be written as

$$q_{i,i+1} = \frac{\sigma_{ri} - \sigma_{r,i+1}}{\ln r_{i+1} - \ln r_i} \tag{12}$$

It has been pointed out by Hill (1950, p. 115) and explained in more detail in Ladanyi (1963a, pp. 143-146) that, due to the particular symmetry of the problem, the pressure-expansion curve can be directly deduced from a solution giving the complete state of stress and strain around a cavity expanding from zero radius. This is possible because only radial stresses are acting at any concentric cylindrical surface within the mass so that any such surface can be considered as the bore of a cylinder undergoing an expansion equal to the radial displacement u_r due to the increase of radial stress from zero to σ_r. For that reason, the radial stresses σ_{ri} and $\sigma_{r,i+1}$ in Eq. (12) can also be considered as two pressures, p_{i+1} and p_i, applied in the bore at two successive stages of a pressuremeter test.

On the other hand, the term in the denominator of Eq. (12) can be expressed in terms of the displacements as follows:

The denominator can be written as

$$\ln \frac{r_{i+1}}{r_i} = \ln \left(\frac{r}{a}\right)_{i+1} - \ln \left(\frac{r}{a}\right)_i \tag{13}$$

where a denotes the current bore radius. If the cavity is expanded continuously from $a_o = 0$ to a, the relationship between the relative distance r/a and the corresponding radial displacement at that distance, u_r, can be obtained simply by equalizing the volume of the expanded cavity with that displaced at the distance r/a, as shown in Ladanyi (1961, 1963a). Denoting the radial distance of a material point before the expansion by r' (Figure 14b), and the distance of the same material point after the expansion by r, so that

$$r = r' + u_r \quad , \tag{14}$$

the volume equality between the cavity expansion and the displacement annulus yields

$$\left(\frac{r}{a}\right)^2 = \frac{\left(1 + \frac{u_r}{r'}\right)^2}{\left(1 + \frac{u_r}{r'}\right)^2 - 1} \tag{15}$$

By virtue of the same similarity principle as for stresses, the relative displacements $(u_r/r')_i$ and $(u_r/r')_{i+1}$ corresponding to the stresses σ_{ri} and $\sigma_{r,i+1}$ can be considered as relative expansions, $(\Delta a/a_o)_i$ and $(\Delta a/a_o)_{i+1}$ of a borehole with initial radius a_o produced at two successive stages of a pressuremeter test at borehole pressures of p_i and p_{i+1}, respectively (Figure 14c). In terms of the volume expansion of the borehole, the term $(1 + u_r/r')^2$ in Eq. (15) can be written as

$$\left(1 + \frac{u_r}{r'}\right)^2 = \left(1 + \frac{\Delta a}{a_o}\right)^2 = \frac{V}{V_o} = \frac{1}{1 - \frac{\Delta V}{V}} \tag{16}$$

where $V_o = a_o^2 \pi L$ is the initial and $V = a^2 \pi L$ is the current volume of the measuring length L of the borehole. Substituting Eq. (16) into Eq. (15) and then into Eq. (13) the latter becomes

$$\ln \frac{r_{i+1}}{r_i} = \frac{1}{2} \left[\ln \left(\frac{\Delta V}{V} \right)_i - \ln \left(\frac{\Delta V}{V} \right)_{i+1} \right] \tag{17}$$

Finally, with Eq. (17), one gets from Eq. (12)

$$q_{i,i+1} = \frac{p_i - p_{i+1}}{\frac{1}{2} \left[\ln \left(\frac{\Delta V}{V} \right)_i - \ln \left(\frac{\Delta V}{V} \right)_{i+1} \right]} \tag{18}$$

Eq. (18) is analogous to Eq. (26) in Gibson and Anderson (1961), if in the latter small elastic strains due to the elastic hole closure before the test are neglected. The difference with the latter, however, is that in developing Eq. (16) no assumption has been made either on the shape of the stress-strain curve or on the yield criterion of the soil.

Stress-Strain Curve

Equation (18) enables the average mobilized strength $q_{i,\,i+1}$ to be determined from any two points of the observed pressure-expansion curve. The corresponding average shear strains $\gamma_{i,\,i+1}$ can be obtained by a reasoning similar to that in case of displacements. As in the case of cylindrical cavity expansion from zero initial radius, the value of the engineering shear strain γ is related to r/a by, (Ladanyi, 1961):

$$\gamma = \left(\frac{a}{r} \right)^2 \tag{19}$$

it follows from Eqs. (15), (16) and (19) that

$$\gamma = \frac{\Delta V}{V} \tag{20}$$

The average shear strain $\gamma_{i,i+1}$ corresponding to the average mobilized principal stress difference $q_{i,i+1}$ is then

$$\gamma_{i,i+1} = \frac{1}{2}\left[\left(\frac{\Delta V}{V}\right)_i + \left(\frac{\Delta V}{V}\right)_{i+1}\right] \tag{21}$$

It should be noted that the stress-strain relationship $q = f(\gamma)$ obtained by this procedure, i.e., by applying Eqs. (18) and (21) to an actual pressuremeter curve, represents a relationship between stresses and strains under constant-volume plane-strain conditions. The information can, however, easily be transformed into the more usual axial symmetry case, as found in a conventional triaxial test, if the validity of the von Mises yield criterion is assumed in the whole plastic portion of the test. Thus, in order to find from the plane-strain stress-strain curve, deduced from Eqs. (18) and (21), the corresponding undrained compression curve under axial symmetry conditions, the following relationships should be used (Ladanyi, 1967a):

$$q_a = \frac{\sqrt{3}}{2}\, q_{ps} \tag{22}$$

and

$$\gamma_a = \frac{3}{2}\, \varepsilon_{1a} = \frac{\sqrt{3}}{2}\, \gamma_{ps} \tag{23}$$

or, if the axial strain ε_{1a} is used instead of the shear strain,

$$\varepsilon_{1a} = \gamma_{ps} / \sqrt{3} \tag{24}$$

where subscript ps denotes the plane-strain information deduced from Eqs. (18) and (21), and subscript a that corresponding to an axial symmetry case. Figure 15 shows one such stress-strain curve deduced from a pressuremeter test in Leda clay (Figures 12 and 13).

Vector Curve in Mohr Plot

On the other hand, because both the major principal stress ($\sigma_{ri} = p_i$) and the principal stress difference (q_i) are known at any moment of the test, the information can be used for plotting a series of Mohr circles and a vector curve in Mohr plot. Figure 16 shows one such plot obtained from a pressuremeter test in Leda clay, the pressuremeter curve of which is shown in Figure 12. The plot is made in terms of plane-strain information, which means that, for any interval i, i+1

$$\sigma_1 = \tfrac{1}{2}[(p_c - p_o)_i + (p_c - p_o)_{i+1}] \tag{25}$$

and

$$\sigma_3 = \sigma_1 - (\sigma_1 - \sigma_3)_{ps} = \sigma_1 - q_{i,i+1} \tag{26}$$

where $q_{i,i+1}$ is given by Eq. (18).

While a semi-graphical method for drawing Mohr circles from a pressuremeter curve has been shown already by Ménard (1957), the true meaning of the plot has never been pointed out. To properly understand the plot one should remember that, in a pressuremeter test, the soil initially responds in a pseudo-elastic manner and then in a plastic manner up to large deformations. In Figure 16, the pseudo-elastic behaviour is shown by the first three circles (1, 2, 3) which increase in diameter but have their centres very close to the origin, as it is anticipated by Lamé's theory of expansion of a cylindrical hole in an infinite elastic medium. Any eventual deviation of actual centres from

the origin gives, in fact, a check of the value of p_o assumed in the calculation.

The following two circles, 4 and 5, are failure circles and correspond to the peak strength of the soil. As the soil tested was a saturated clay, the peak strength envelope in terms of total stresses should be a straight line parallel with the σ-axis and passing through the points 4 and 5. The remaining circles 6 to 11 are all in the plastic domain and correspond to ever increasing plastic deformations. For a sensitive clay, as in Figure 16, the diameters of Mohr circles can be seen to decrease, showing how the strength of the clay drops off with increasing distortion. It is, however, obvious that the latter circles have no common failure envelope since each of them corresponds to a different plastically deformed material with a different degree of disturbance. In fact, each circle from 6 to 11 has a separate undrained strength envelope parallel with σ-axis.

This result shows clearly why the original Ménard's method of deducing Mohr circles from the pressuremeter curve with the purpose of determining the failure envelope of the soil presented difficulties in interpretation most often. In fact, the results show that the circles will follow one single failure envelope only if the soil has an ideally-plastic post-failure behavior. If, on the contrary, the post-failure behavior of the soil is either strain-hardening or strain-softening, which is very often the case, the circles will not have a common failure envelope and the determination of the failure parameters c and ϕ from one single pressuremeter curve will be very difficult or impossible. Nevertheless, it is considered that plotting both the stress-strain curve and the Mohr circles as described here, is the best available method for a proper understanding of a short-term pressuremeter test.

The method just described can be used for finding strength parameters of frozen soil from any stage-loaded pressuremeter test with equal time intervals for each stage. Unfortunately, in practice, because of the volume limitation of the probe combined with the requirement that at least ten points are necessary for drawing a pressuremeter curve, the longest time per stage was 15 minutes. This is clearly too short a time to be able to draw any conclusions concerning the possibility of extrapolation of the results to long-time periods. In order to obtain the latter information, the creep behavior of frozen soil in a pressuremeter test had to be studied in more detail, both theoretically and experimentally, from the point of view of general creep theory, as shown in the following.

INTERPRETATION OF PRESSUREMETER CREEP TESTS

According to Hult (1966), there are essentially two practical methods for generalizing experimental creep information. The first one, applicable to long-term creep tests in which the steady-state creep strain greatly exceeds the instantaneous and the primary creep strains, consists of linearizing the creep curves and of considering the total strain at anytime as being a sum of a pseudo-instantaneous and a steady-state creep strain. The method was applied to the creep of frozen soils by Ladanyi, 1972, and was used subsequently by Johnston and Ladanyi, 1972, for generalizing creep information obtained in a series of long-term pull tests performed on grouted rod anchors in permafrost.

The second method, applicable to relatively short-term creep tests, considers the creep information as being essentially of a primary (or "stationary") creep type and attempts to extrapolate it to longer times using a convenient creep curve fitting method. As the creep time that can be realized in a pressuremeter test does not usually exceed several hours, the test should be considered as a short-term creep test to which the second method is applicable.

According to the second method, the creep data obtained in a pressuremeter test can be generalized by using, as a basis, the solution of the problem of stationary creep under internal pressure of a cylindrical cavity of infinite length located in an infinite medium. However, before showing the solution of the problem, it seems appropriate for the purpose of clarity, to make some general comments and to point out the assumptions on which the solution was based. The following general considerations on creep follow closely the line of thought expressed by Hult (1966).

The term "stationary creep" is sometimes used as a synonym for secondary creep, that is creep with a constant rate of strain. However, in this report a more general definition of the term proposed by Hult will be adopted. By that definition, a state of stationary creep is the one where the space distribution of stress in the body remains constant with time.

The strain in a creep process, at constant stress and temperature, is often formally split up into two parts:

$$\varepsilon = \varepsilon^{(i)} + \varepsilon^{(c)} \tag{27}$$

where $\epsilon^{(i)}$ is the instantaneous (elastic and plastic) strain and $\epsilon^{(c)}$ is the creep strain. The form of $\epsilon^{(i)}$, discussed by Hult (1966), will not be considered here because it is of secondary importance to the problem at hand.

The form of the creep law governing the creep strain $\epsilon^{(c)}$ depends upon the portion of the creep curve under consideration. If secondary (steady state) creep is of the main concern, the creep rate will depend only on stress σ and temperature T, so that the creep law may simply be written as

$$\frac{d\epsilon^{(c)}}{dt} = G(\sigma, T) \tag{28}$$

If, on the other hand, the considered creep process is mainly in the primary creep domain, the creep rate will also depend on the time t. For the creep strain, one can write then

$$\epsilon^{(c)} = f(\sigma, t, T) \tag{29}$$

In order to arrive at an incremental strain form, the time derivative of Eq. (29) is formed

$$\frac{d\epsilon^{(c)}}{dt} = g(\sigma, t, T) \tag{30}$$

where $g = \partial f / \partial t$, since σ and T are assumed to be constant.

Elimination of t between (29) and (30) yields

$$\frac{d\epsilon^{(c)}}{dt} = h(\sigma, \epsilon^{(c)}, T) \tag{31}$$

The expressions (29), (30) and (31) are fully equivalent for constant σ and T. For varying σ and T , however, they give different predictions. Comparison with experiments shows that in a majority of cases, Eq. (31) gives predictions closer to reality than Eq. (30). A law of the form of Eq. (30) is often termed a time-hardening creep law as opposed to Eq. (31) which is termed a strain-hardening creep law.

Solution of creep problems is greatly simplified if Eq. (29) can be written in the form

$$\varepsilon^{(c)} = \Phi(\sigma, T)\, \Psi(t) \tag{32}$$

For constant σ and T , differentiation with respect to t yields the time-hardening creep law

$$\frac{d\varepsilon^{(c)}}{dt} = \Phi(\sigma , T) \frac{d\Psi(t)}{dt} \tag{33}$$

If $\Psi(t)$ is a monotonically increasing function of time, introduction here of the transformed time

$$\tau = \Psi(t) \tag{34}$$

transforms the creep law into

$$\frac{d\varepsilon^{(c)}}{d\tau} = \Phi(\sigma, T) \tag{35}$$

which is a generalization of the secondary-creep law, Eq. (28). Hence, calculations made for the case of secondary creep can immediately be transformed to the case of time-hardening creep. An additional simplification is obtained if, as the time proceeds, the creep strain becomes

much larger than the instantaneous strain, so that one can write:

$$\varepsilon \approx \Phi(\sigma, T)\, \Psi(t) \tag{36}$$

In a structure where a constant state of stress prevails during a creep process, (stationary creep), and the strains are governed by Eq. (36), the ratio between the strains at two arbitrary points, 1 and 2, remains constant:

$$\frac{\varepsilon_1}{\varepsilon_2} \approx \frac{\Phi(\sigma_1, T_1)}{\Phi(\sigma_2, T_2)} \tag{37}$$

The same strain ratio prevails in the structure if instead the material were elastic according to

$$\varepsilon = \Phi(\sigma, T)\, C \tag{38}$$

Hence, the stress and strain distributions in structures subject to stationary creep can be formed by analyzing a corresponding problem of elasticity. This procedure by which the time element is eliminated from the analysis, is often termed the elastic analogy for stationary creep. (Hoff, 1954). It simply implies that an elastic strain is made to correspond to a creep strain rate.

The primary creep of high temperature metals, ice and frozen soils can often conveniently be described by a law of the form

$$\varepsilon^{(c)} = K \sigma^a t^b \qquad (b < 1) \tag{39}$$

where K , a, and b are temperature-dependent material constants. In this report, Eq. (39) will be written in Hult's (1966) notation,

generalized to multiaxial state of stress:

$$\epsilon_e^{(c)} = [\dot{\epsilon}_c(1+\mu)]^{1/(1+\mu)} (\sigma_e/\sigma_c)^{m/(1+\mu)} t^{1/(1+\mu)} \tag{40}$$

where ϵ_e and σ_e are the equivalent creep strain and the equivalent stress, respectively, $\dot{\epsilon}_c$ is an arbitrary, conveniently selected, strain rate, σ_c is the creep modulus in units of stress, while m and μ are creep exponents. The values of creep parameters σ_c, m and μ can be obtained by a convenient plotting of creep curves as described by Hult (1966, pp. 34-37).

In order to solve the problem at hand, it is convenient to introduce into Eq. (40) the transformed time unit

$$\tau = t^{1/(1+\mu)} \tag{41}$$

which enables Eq. (40) to be transformed into an ordinary power law

$$\frac{d\epsilon_e^{(c)}}{d\tau} = K \sigma_e^n \tag{42}$$

where

$$K = \left[\frac{\dot{\epsilon}_c(1+\mu)}{\sigma_c^m}\right]^{1/(1+\mu)} \tag{43}$$

and

$$n = m/(1+\mu) \tag{44}$$

The solution, based on the power law of creep (Eq. (42)), of the problem of creep expansion of a cylindrical cavity under plane-strain condition can easily be obtained by elastic analogy from the corresponding solution in non-linear elasticity. Complete solutions of the particular problem can be found in several textbooks (e. g., Nádai, 1950; Odquist, 1966; Drucker, 1967).

To solve the problem of processing the pressuremeter creep data, the only relationship needed from the solution is one relating the creep cavity expansion rate with the applied internal pressure, which is, according to Odquist (1966),

$$\frac{dr}{d\tau} = \left(\frac{\sqrt{3}}{2}\right)^{n+1} K\, r \left[\frac{2}{n}(p_i - p_o)\right]^n \tag{45}$$

where r is the current radius of the cavity, p_i is the constant applied internal pressure and p_o is the pressure acting at infinity. If p_i is replaced by p_c according to the notation adopted for the corrected pressure in the borehole, Eq. (45) can be written as

$$\frac{dr}{r} = G(p_c - p_o)\, d\tau \tag{46}$$

where, according to Eqs. (43) and (44),

$$G(p_c - p_o) = \left(\frac{\sqrt{3}}{2}\right)^{\left(1+\frac{m}{1+\mu}\right)} \left[\frac{\dot{\varepsilon}_c(1+\mu)}{\sigma_c^m}\right]^{1/(1+\mu)} \left[\frac{2(1+\mu)}{m}(p_c - p_o)\right]^{m/(1+\mu)} \tag{47}$$

For a finite interval of time at a constant stress, Eq. (46) can be integrated to give

$$\ln r = G(p_c - p_o)\,\tau + C \tag{48}$$

Taking $r = r_{i-1}$ at $\tau = 0$, i.e., at the beginning of the considered i-th creep stage, the integration constant C can be eliminated and Eq. (48) becomes

$$\ln\left(\frac{r}{r_{i-1}}\right) = G(p_c - p_o)\,\tau \tag{49}$$

Since for a cylindrical cavity

$$(r/r_{i-1})^2 = V/V_{i-1} \quad , \tag{50}$$

Eq.(49) becomes finally

$$\frac{V}{V_{i-1}} = \exp[2\,G(p_c - p_o)\,t^{\,1/(1+\mu)}] \tag{51}$$

where, (Figure 17), V_{i-1} denotes the cavity volume at $t = 0$, i.e., at the start of a given constant-pressure creep stage, and $V = V_{i-1} + \Delta V_c$ denotes the volume of the cavity at any time t after the step-increase of pressure $(p_c - p_o)$ in the stage i.

In order to be able to determine the creep parameters μ, m and σ_c, the semi-graphical procedure described by Hult (1966) for primary creep case can be followed. Taking first a natural and then an ordinary logarithm of Eq. (51) one gets

$$\log\left(\ln \frac{V}{V_{i-1}}\right) = \log 2G(p_c - p_o) + \frac{1}{1+\mu} \log t \tag{52}$$

showing that pressuremeter creep curves should linearize if $(\ln V/V_{i-1})$ is plotted against time in a log-log plot. (Figure 18). According to Eq. (52), in such a plot, the slope of the creep straight-lines is equal to $1/(1+\mu)$ or (Figure 18),

$$1 + \mu = A/B \tag{53}$$

The intercept at the unit time (t = 1 min in Figure 18) of any creep line, each of them corresponding to a different value of pressure $(p_c - p_o)$, is then equal to $2G\,(p_c - p_o)$.

In order to determine the parameters m and σ_c, Eq. (47) may be written as

$$\log 2G(p_c - p_o) = \log M - \frac{m}{1+\mu} \log \sigma_c + \frac{m}{1+\mu} \log(p_c - p_o) \tag{54}$$

where

$$\log M = \log 2 + (1 + \frac{m}{1+\mu})\log \frac{\sqrt{3}}{2} + (\frac{1}{1+\mu})\log \dot{\varepsilon}_c(1+\mu) + \\ + \frac{m}{1+\mu} \log \frac{2(1+\mu)}{m} \tag{55}$$

Equation (54) shows that plotting of $2G\,(p_c - p_o)$ against $(p_c - p_o)$ in a log-log plot will give a straight-line with the slope equal to $m/(1+\mu)$. In Figure 18 such a plot is shown superimposed upon the former. The new straight-line has a slope

$$D/C = m/(1+\mu) \tag{56}$$

and its intercept N, read at unit value of $(p_c - p_o)$ (at 1 kg/cm^2 in Figure 18), is according to Eq. (54) equal to

$$N = M / \sigma_c^{m/(1+\mu)} \tag{57}$$

Since, for an arbitrary assumed $\dot{\varepsilon}_c$, and with known μ and m, the value of M can be calculated from Eq. (55), the value of σ_c is

$$\sigma_c = (M/N)^{(1+\mu)/m} \tag{58}$$

Once the creep parameters μ, m and σ_c have been determined, they can be substituted into Eq. (40) to get a general creep equation of the soil. The latter can subsequently be used either for extrapolating the pressuremeter creep data to longer time intervals, or, in association with an estimated creep failure strain, can serve for predicting the long-term strength of frozen soil. In the latter case, if ε_{ef} denotes the equivalent failure strain and σ_{ef} the equivalent creep strength, Eq. (40) yields

$$\sigma_{ef} = \sigma_c \left[\frac{\varepsilon_{ef}^{(1+\mu)}}{\dot{\varepsilon}_c (1+\mu)\, t} \right]^{1/m} \tag{59}$$

If, on the other hand, the theory is to be used only for extrapolating the pressuremeter creep curves to longer time intervals, it should be noted that the following relationship exists between the (V/V_{i-1})-ratio, determined from Eq. (51), and the ratio $\Delta V/V$ necessary for plotting the extrapolated pressuremeter curve as in Figure 13:

$$\frac{\Delta V}{V} = \frac{V - V_o}{V} = \frac{(V/V_{i-1})V_{i-1} - V_o}{(V/V_{i-1})V_{i-1}} = 1 - \frac{V_o/V_{i-1}}{V/V_{i-1}} \tag{60}$$

where, (Figure 17), V_o is the initial volume of the borehole at $(p_c - p_o) = 0$, and V_{i-1} is the cumulative borehole extension at the end of the preceding stage, equal to the sum of extrapolated borehole extensions in all previous stages.

TEST RESULTS

Figures 19 to 70 show all the results of the series of pressuremeter tests carried out in the frozen varved soil at Thompson. Moreover, the most important numerical data and calculated parameters are compiled in Table 1. Both in Figures 19 to 70 and in Table 1, the tests are presented in chronological order, and follow their consecutive numbering system as explained earlier. Altogether, 19 Thompson tests are shown in the figures and the table (Test DBR II-1 was made in Leda clay in Ottawa).

As general information, Table 1 contains the following data for each test: depth below the ground surface; thickness of various layers of silt, clay and ice from visual inspection of the samples taken by a tube sampler; minimum soil temperature measured at the contact with the probe during the test; and, in the last column, the figure numbers connected with the test. The remaining numerical data in Table 1 are results of calculation, and will be discussed later. The applied load - time sequence for each test was given earlier in Figures 4 to 11.

The results shown graphically in Figures 19 to 70 have been divided into two groups: Figures 19 to 57 show essentially only short-term information obtained in the tests with 2 to 15 minutes duration per stage. Figures 58 to 70 show all data connected with creep and used subsequently for predicting the long-term performance of the frozen soil.

In the first group of short-term data (Figures 19 to 57), only three kinds of plots are shown:

(1) Standard pressuremeter curve in terms of V_m (cm^3) vs p_c (kg/cm^2). The origin $0'$ of the true pressuremeter curve is also indicated.

(2) Mohr circles and the vector curve, showing the true loading sequence to which an element of soil was subjected in a particular test. The plot also contains a tentative failure envelope, to be discussed later.

(3) For some of the tests the plane-strain stress-strain curve in terms of $(\sigma_1 - \sigma_3)_{ps}$ vs γ_{ps}, is also shown.

The second group of figures (58 to 70) contains the results of all sustained loading tests, both multi-stage and one-stage, as well as those in which only the last stage was held constant for a certain longer period of time. All multi-stage creep data have been used for obtaining the creep parameters by using the method shown in Figure 18.

A more detailed discussion of the test results follows.

DISCUSSION OF TEST RESULTS

A. Short-Term Information

As mentioned earlier, from a conventional pressuremeter test with a sufficient number of short-term stages, one can obtain certain short-term information on the deformation modulus and the strength of soil. Usually, for each such test, the pressuremeter curve is plotted in terms of V_m vs p_c, as shown in Figures 19 to 57. As the next thing, it is necessary to estimate on the curve the position of the true origin $0'$, from which the true pressuremeter data in terms of ΔV and $(p_c - p_o)$ are calculated.

According to Ménard (1957), the position of $0'$ should coincide with the point of inflexion observed on the pressuremeter curve. This is, however, considered to be a highly unreliable method, because it can be shown that unloading (assumed by Ménard), and remolding and temperature disturbance of a layer of soil surrounding the borehole (which occurs in the majority of tests), have about the same effect on the shape of the pressuremeter curve. In other words, the point of inflexion of the curve has, in most cases, nothing to do with the original lateral pressure p_o.

After having realized this fact, it was decided to calculate the value of p_o independently and to put the true origin $0'$ at the intersection between the vertical line through p_o and the extension of the straight-line portion of the pressuremeter curve, as shown in Figure 19 and other similar figures. This is considered to be a first step towards correcting the effects of temperature disturbance, thought to have caused the convex shape of the initial portion of the pressuremeter curve. After this correction, the error due to temperature disturbance is, however, not yet quite eliminated. An approximate analysis of the effect of an eventual weaker zone around the borehole on the values of certain calculated parameters is shown in the Appendix. The analysis

shows that the error is usually not very important and that it can be reasonably estimated. Nevertheless, every possible means should be used in future tests for keeping the temperature disturbance of the borehole at a minimum.

The value of the total lateral pressure p_o was taken in each test to be equal to the total overburden pressure, i. e., it was assumed that total $K_o = 1$. There is, unfortunately, still a complete lack of knowledge about the real value of the lateral pressure in the permafrost strata. The foregoing assumption on the value of p_o is, nevertheless, considered to be an acceptable first approximation, because it can be anticipated that the strata have retained some residual lateral stresses after the last glaciation. The calculated p_o values are shown in column (5) of Table 1.

From the true pressurementer curve, a set of Mohr circles was calculated for each test, using Eqs. (18), (25) and (26). Figure 20 shows one such plot for Test 1 - 1, and is followed by similar plots for all other tests. As expected, the Mohr circles in any one of the tests did not follow a single failure envelope but reflected at the same time the strength mobilization and the shape of the stress-strain curve of the soil. One additional feature that showed up in these tests was that the tensile strength of the soil seemed to play an important role in the behavior of soil in a pressuremeter test.

Figure 32 shows a typical example of a test illustrating this point. As in most other tests, the particular test started with two concentric Mohr circles, as would be expected according to the Lamé's theory for a linear-elastic material. The next two circles are displaced laterally, showing a plastic flow effect. However, after that, the circles continued to increase in diameter until the value of σ_3 reached again, on the negative σ-axis, the same point as before. A similar behavior may be observed also in Figures 28, 30, 35, 37, 50 and 52.

It is thought that this behavior is caused by the following sequence of events: At low loads the frozen soil behaves quasi-elastically with σ_1 increasing and σ_3 decreasing by the same amount. When, however, σ_3 attains the tensile strength of the soil, radial cracks appear and σ_3 becomes zero. With further increasing σ_1 the blocks between the cracks fail in unconfined compression (as anticipated by Ladanyi, 1967b). When the cracks are thus healed, the soil can again sustain tensile stresses until the tensile strength is

attained for the second time. This alternative, and often random, failing of the soil in tension and in shear is thought to be the reason for the generally irregular variation of the Mohr circles during the tests. In order to follow the sequence of Mohr circles more easily, they have been connected by a vector curve showing the variation of $\frac{1}{2}(\sigma_1 - \sigma_3)$ with $\frac{1}{2}(\sigma_1 + \sigma_3)$ in the tests.

As may be seen in all the Mohr circle plots shown in Figures 19 to 57, contrary to what was thought by Ménard (1957) and Gibson and Anderson (1961), a pressuremeter test does not usually furnish enough information to determine the failure envelope of the soil. Nevertheless, in this report, the Mohr circle plots have been used for estimating the minimum short-term values of the tensile strength T_o and the cohesion c. To estimate the two parameters the Mohr circles have been enclosed by a bi-linear failure envelope composed of a Coulomb straight-line and a vertical tension cut-off. For the Coulomb line, a friction angle of 15° was assumed in all silty soils, and 0° in the soils composed mostly of clay. The values of T_o and c were then read from the plot by taking into account that the plot should, in fact, be referred to the original pressure p_o shown by the dashed line. This was necessary because the Mohr circles were plotted in terms of $(p_c - p_o)$.

Columns (7) to (9) in Table 1 show the values of short-term strength parameters obtained from the Mohr circle plots in such a manner. In addition, column (6) gives the values of the pressuremeter modulus E_p, calculated from the straight-line portions of the pressuremeter curves by using the formula (valid for $\nu = 0.5$),

$$E_p = 3 \frac{\Delta p}{\Delta(\Delta V/V)} \tag{61}$$

Looking at Table 1, it may be seen that the over-all variation of short-term parameters in the tests was approximately as follows:

Frozen varved soil:

E_p	from	250	to	800 kg/cm^2
c	"	5	to	14 "
T_o	"	-1.5	to	-12 "

Unfrozen varved soil: E_p from 60 to 80 kg/cm^2
c " 2 to 5 "
T_o " -1 to -5 "

As expected, a given type of soil when frozen is stronger and much less deformable than the same soil in an unfrozen state. It is also interesting to note that the tensile strength of frozen soil is about the same as its shear strength. Frozen varved clay (Tests 12-1 and 12-2), was found to be a little weaker and more deformable than frozen varved silt at the same temperature.

In addition to the Mohr circles, the short-term pressuremeter information was also used for calculating a number of plane-strain stress-strain curves. (Figures 23, 26, 33, 46, 55). The curves obtained are seen to be generally flat-topped and sometimes show a convex pre-peak portion which may be due to soil disturbance. The unusual shape of the curve in Figure 33 is thought to be due to an initial tensile failure after which the peak strength was not reached.

When considering the stress-strain curves, attention is drawn to the fact that their true shape may be slightly different if a correction for an eventual disturbed zone is made. In the Appendix, a correction method is proposed and a typical result is shown in Figure A-1 (b).

B. Long-Term Information

Creep information from all pressuremeter tests involving time intervals longer than 2 min per stage, is shown in Figures 58 to 70. In the figures, the logarithmic creep measure, $\ln (V/V_{i-1})$, is plotted against the time, t, in a log-log plot. In such a plot, creep curves at each stage become nearly straight lines, which enables the information to be generalized and put into an analytical form, as described previously.

In order to be able to apply the foregoing analysis, two conditions are necessary: (1) Creep curves should linearize in a log-log plot; and (2) Creep curves for different sustained pressures should be parallel to each other.

As may be noted in Figures 58 to 70, neither of the two conditions was completely satisfied in the tests. In fact, the creep curves were found to curve up slightly at low pressures and down at high

pressures. Moreover, the creep lines were frequently not quite parallel, diverging with increasing time. Nevertheless, they appear to linearize better in one-stage tests (Figure 66) than in multi-stage tests, and show a tendency to become more parallel after about 15 minutes. Having these two experimental facts in view it was decided, for the purpose of generalization of creep information, to consider the creep curves as becoming parallel after 15 minutes in each stage (as in Figure 60), and having an average slope ($A/B = 1 + \mu$) for the considered pressure interval. The creep lines were then projected back from 15 min to 1 min, to get the values of $2G(p_c - p_o)$ according to Eq. (52). The latter values were then plotted against $(p_c - p_o)$ to get a set of points through which an average (dash-dotted) line was drawn. The line, according to Eqs. (54) to (57), enables the determination of the ratio $D/C = m/(1+\mu)$ and the intercept N at $p = 1$ kg/cm^2 (Eq. 57). From the latter, and after calculating the value of M (Eq. 55), the creep modulus σ_c was finally determined.

The values of the creep parameters $1+\mu$, m, and σ_c, determined in that manner, are shown in Table 1, columns 10 to 12. It should be noted that in all the calculations the arbitrary strain rate $\dot{\epsilon}_c$ was taken equal to 10^{-5} min^{-1}.

As explained earlier, when the three parameters are known, a general creep equation, such as Eq. (40), can be written for each test. It may be noted in Table 1 that the value of $(1+\mu)$, with one single exception, remained essentially between 1.5 and 2.5, while the value of m varied from about 2 to 4. There was a much larger variation in σ_c, from about 4.5 to 24.0 kg/cm^2.

In addition to the creep equation, the calculated creep parameters also enable an estimate to be made of the time-dependent strength of the soil, according to Eq. (59), if the concept of a constant strain at failure is adopted. For illustration purposes, a failure strain $\epsilon_{ef} = 0.10$ was assumed here.

A list of resulting creep and time-dependent strength equations, respectively, for the 6 complete pressuremeter creep tests follows. (Valid for t in minutes and σ_{ef} in kg/cm^2).

Test No.	Equation
3 - 1	$\varepsilon_e = 2.185 \times 10^{-3}(\sigma_e/5.13)^{1.52}\ t^{0.56}$
	$\sigma_{ef} = 62.4\ t^{-0.368}$
3 - 2	$\varepsilon_e = 3.55 \times 10^{-3}\ (\sigma_e/10.93)^{2.04}\ t^{0.52}$
	$\sigma_{ef} = 56.4\ t^{-0.254}$
4 - 1	$\varepsilon_e = 1.8 \times 10^{-3}\ (\sigma_e/4.44)^{1.17}\ t^{0.58}$
	$\sigma_{ef} = 137\ t^{-0.49}$
4 - 2	$\varepsilon_e = 4.07 \times 10^{-3}\ (\sigma_e/24.0)^{1.08}\ t^{0.51}$
	$\sigma_{ef} = 466\ t^{-0.47}$
9 - 1	$\varepsilon_e = 0.96 \times 10^{-3}(\sigma_e/5.0)^{2.10}\ t^{0.63}$
	$\sigma_{ef} = 46\ t^{-0.30}$
10 - 1	$\varepsilon_e = 0.87 \times 10^{-3}\ (\sigma_e/4.71)^{2.08}\ t^{0.64}$
	$\sigma_{ef} = 44.5\ t^{-0.305}$

To illustrate how frozen soil strength decreases with time, the values of σ_{ef} have been calculated for time intervals of 30 minutes and 1 year and are shown in columns (13) and (14) of Table 1. It can be noted that, within a year, the apparent strength of such a soil may drop to less than one tenth of its short-term value.

CONCLUSIONS AND RECOMMENDATIONS

This study of the pressuremeter test as a means for obtaining creep information of frozen soils in situ, enabled the following conclusions to be made:

(1) After some minor modifications, the existing pressuremeter equipment proved to be suitable for performing creep tests under the conditions found at the site. It is not known, however, how the same equipment would perform at very low temperatures and in other types of frozen soils, such as glacial till.

(2) The borehole drilling method and the hole preparation for the tests was found fairly satisfactory. Some temperature disturbance could not, however, be avoided, and special care is recommended in all similar future studies.

(3) To get proper short-term information from the tests, a new interpretation method had to be developed. The method enabled the determination of short-term strength parameters and the stress-strain curve from each pressuremeter test.

(4) A method also had to be found for the determination of creep parameters from the pressuremeter creep data. The method has proved feasible for the determination of creep parameters of frozen soils in situ and the prediction of long-term strength. In order to get sufficient creep information for the proposed method to be applicable it is recommended, on the basis of this experience, that, in addition to conventional short-term pressuremeter tests, the following two creep tests be performed: (a) An equal-stage creep test with about 15 min per stage, such as Tests 3-1 and 3-2; and (b) Two or three one-stage creep tests, such as Test 7-1, at different pressure levels for checking the linearity of creep lines for long-time intervals.

(5) The interpretation method requires knowledge of the total lateral pressure in the ground before the test. In certain cases the value of this pressure can be reasonably predicted from geological or experimental information. In permafrost strata the value of the lateral pressure is still unknown and its determination in situ should be attempted in future pressuremeter investigations of this kind.

REFERENCES

Drucker, D.C. 1967. Introduction to mechanics of deformable solids. McGraw-Hill.

Essai pressiométrique normal. Mode opératoire MS.IS-2. DUNOD, Paris, 1971.

Gibson, R.E. and Anderson, W.F. 1961. In-situ measurement of soil properties with the pressuremeter. Civil Engrg & Publ. Works Rev., London, May 1961, pp. 615-618.

Hill, R. 1950. The mathematical theory of plasticity. University Press, Oxford.

Hoff, N.J. 1954. Approximate analysis of structures in the presence of moderately large creep deformations. Quart. Appl.Math., 12, pp. 49-55.

Hult, J.A.H. 1966. Creep in engineering structures. Blaisdell Publ. Co., Waltham, Mass., 115 p.

Jezequel, J., Lemasson, H. & Touzé, J. 1968. Le pressiomètre Louis Ménard. Boul. Liaison Lab. Rout.,P. et Ch., No.32, Paris, pp.97-120.

Johnston, G.H. and Ladanyi, B. 1972. Field tests of grouted rod anchors in permafrost. Can. Geotech. J., 9, pp.176-194.

Ladanyi, B. 1961. Etude théorique et expérimentale de l'expansion dans un sol pulvérulent d'une cavité présentant une symétrie sphérique ou cylindrique. Annales des Trav.Publ.de Belgique, pp.105-148,365-406.

Ladanyi, B. 1963 a. Expansion of a cavity in a saturated clay medium. Proc. ASCE, 89, SM4, pp.127-161.

Ladanyi, B. 1963 b. Evaluation of pressuremeter tests in granular soils. Proc. 2nd Panam. Conf. Soil Mech. Found. Engrg, Sao Paulo, Vol. 1, pp. 3-20.

Ladanyi, B. 1966. Short term behavior of clay around a circular tunnel. Rapport S-8, Dépt.de Génie Civil, Univ. Laval, Québec.

Ladanyi, B. 1967 a. Discussion on plane strain tests on a saturated remolded clay, by D.J.Henkel and N.H.Wade, Proc. ASCE, 93, SM5, pp. 322-325.

Ladanyi, B. 1967 b. Expansion of cavities in brittle media. Int.J. Rock Mech. Min. Sci., Vol.4, pp. 301-328.

Ladanyi, B. 1972. An engineering theory of creep of frozen soils. Can. Geotech. J., Vol.9, pp. 63-80.

Ménard, L. 1957. Mesures in-situ des propriétée physiques des sols. Annales des Ponts et Chaussées, Vol.127, pp. 357-377.

Ménard, L. 1963. Calcul de la force portante des fondations sur la base des résultats des essais pressiométriques. Sols-Soils, Paris, Vol.2, No.5, 9-24.

Morrison, J.L.M. 1948. The criterion of yield of gun steels. Proc. Inst. Mech. Engrs, Vol.159, pp. 81-94.

Nádai, A. 1931. Plasticity , Chap. 29 (Theory of flow and fracture of solids, 1950, Chap. 31), McGraw-Hill Book Co., New York.

Odquist, F.K.G. 1966. Mathematical theory of creep and creep rupture. Oxford Math. Mono. , Clarendon Press, Oxford.

Pressiomètre type G: Description - utilisation. Société Pressiométrique Ménard, Paris, 1968.

Shepherd, W.H. 1948. Plastic stress-strain relations. Proc. Inst. Mech. Engrs, Vol.159, pp. 95-99.

LIST OF SYMBOLS

a = current radius of borehole. Also: exponent.

a_o = initial radius of borehole.

A = length

b = exponent

B = length

c = Coulomb cohesion

C = length. Also: constant

c_u = undrained cohesion

D = length

E = modulus of elasticity

E_p = pressuremeter modulus

f = function

g = function

G = function

h = difference in elevation from the pressure gage to the top of the borehole. Also: function

h_o = height of probe center during calibration

H = difference in elevation from the center of the probe to the ground surface.

K = constant

K_o = at rest earth pressure coefficient

m = creep exponent

M = magnitude defined by Eq. (55)

n = $m/(1+\mu)$

N = magnitude defined by Eq. (57)

p = pressure

p_o = total lateral ground pressure at the test level

p_c = corrected (applied) pressure

p_m = pressure reading at the gage

q = $(\sigma_1 - \sigma_3)$, principal stress difference

q_i = extension resistance of the probe, read from the calibration curve

q_{pz} = piezometric pressure

r = radius

t = time

T = temperature

T_o = tensile strength

u_r = radial displacement at r

V = $V_o + \Delta V$

V_m = total volume of liquid injected from the start of test to p_c

V_{mo} = total volume of liquid injected from the start of test to p_o

V_o = $V_{empty} + V_{mo}$ = volume of the measuring section of the probe at p_o

V_{empty} = volume of the measuring section of empty probe

ΔV = $V_m - V_{mo}$

γ = $\epsilon_1 - \epsilon_3$ = engineering shear strain

ϵ = total normal strain

ϵ_1, ϵ_3 = principal normal strains

$\epsilon^{(c)}$ = creep strain

$\epsilon^{(i)}$ = instantaneous strain

ϵ_e = equivalent strain = $(\sqrt{2}/3)\{(\epsilon_1-\epsilon_2)^2+(\epsilon_2-\epsilon_3)^2+(\epsilon_3-\epsilon_1)^2\}^{\frac{1}{2}}$

ϵ_{ef} = equivalent failure strain

μ = creep exponent

ν = Poisson's ratio

σ = total normal stress

σ_c = creep modulus (proof stress in creep equation)

σ_e = equivalent stress = $(1/\sqrt{2})\{(\sigma_1-\sigma_2)^2+(\sigma_2-\sigma_3)^2+(\sigma_3-\sigma_1)^2\}^{\frac{1}{2}}$

σ_1, σ_3 = major and minor principal stress

σ_r, σ_θ = radial and circumferential principal stress

τ = shear stress. Also: tranformed time

Φ = angle of friction in Coulomb equation. Also: function

Ψ = function

TABLE 1

Test No.	Depth ft (cm)	Thickness of soil and ice layers (mm)			Min. soil temp. deg F	p_o kg/cm^2	Short term parameters				Creep parameters			Predicted σ_{ef}, kg/cm^2 after		Figs. No.
		silt	clay	ice			E_p	T_o kg/cm^2	c	ø (assum)	1+μ	m	σ_c kg/cm^2	30 min	1 year	
1	2	3			4	5	6	7	8	9	10	11	12	13	14	15
DBRII-1	19.0 (580)	0	all	0	>32	0.30	90	1.55	1.90	0						4, 12 13, 15 16
1-1	5.42 (165)	20 to 50	20	3 to 10	31.5	0.33	500	5.22	6.40	15						19, 20
1-2	8.92 (272)	150 to 200	12 to 20	1 to 3	31.8	0.54	372	7.86	8.00	15	1.80					21, 22 23, 58
2-1	5.17 (158)	20	20	1 to 10	31.9	0.32	378	5.00	5.70	15						24, 25 26
2-2	8.33 (254)	150 to 200	12 to 25	1 to 3	31.7	0.51	415	5.80	7.20	15						27, 28
2-3	11.17 (340)	150 to 180	12 to 25	1 to 6	31.8	0.68	380	4.87	9.45	15	1.68					29, 30 59
3-1	6.33 (193)	130 to 180	12 to 25	1 to 6	31.7	0.39	298	4.60	9.20	15	1.79	2.72	5.13	17.9	1.14	31, 32 33, 60
3-2	8.83 (270)	150	12	0	31.8	0.54	268	11.66	11.90	15	1.93	3.93	10.93	23.8	3.57	34, 35 61
4-1	6.83 (208)	150	25	1 to 12	31.8	0.42	448	7.23	12.90	15	1.74	2.03	4.44	25.9	0.67	36, 37 62
4-2	10.83 (330)	200	25	0	31.7	0.66	565	11.74	13.65	15	1.97	2.12	24.00	94.5	2.81	38, 39 63

Test No.	Depth ft (cm)	Thickness of soil and ice layers (mm)			Min. soil temp. deg F	p_o kg/cm^2	Short term parameters				Creep parameters			Predicted σ_{ef}, kg/cm^2 after		Figs. No.
		silt	clay	ice			E_p	T_o kg/cm^2	c	ø (assum)	1+μ	m	σ_c kg/cm^2	30 min	1 year	
1	2	3			4	5	6	7	8	9	10	11	12	13	14	15
5-1	7.92 (242)	250	0	0	31.7	0.48	651	5.72	9.10	15	2.04					40,41 64
6-1	6.25 (190)	50 to 150	12 to 32	1 to 1.5	31.8	0.38	795	3.65	5.05	15	2.02					42,43 65
7-1	7.42 (226)	50 to 150	12 to 38	1 to 1.5	31.3	0.45					2.66					66
8-1	8.00 (244)	25 to 50	25 to 50	0	35.2	0.49	66	1.18	2.08	15						44,45 46
8-2	11.08 (340)	25 to 75	25 to 50	0	35.4	0.68	77	4.85	5.26	15						47,48
9-1	6.42 (196)	25 to 75	12 to 25	1 to 5	31.5	0.40	466	3.20	6.50	15	1.59	3.34	5.00	16.6	1.77	49,50 67
10-1	6.33 (193)	75 to 200	25	1 to 6	31.9	0.39	615	1.61	6.40	15	1.57	3.28	4.71	15.8	1.62	51,52 68
11-1	6.83 (208)	75 to 150	12 to 25	1 to 6	31.8	0.42					3.33					69
12-1	11.08 (338)	0	12 to 38	1 to 12	31.8	0.68	232	3.70	4.70	0						53,54 55
12-2	13.67 (416)	0	25 to 50	12 to 50	31.8	0.83	360	2.63	5.00	0	1.88					56,57 70

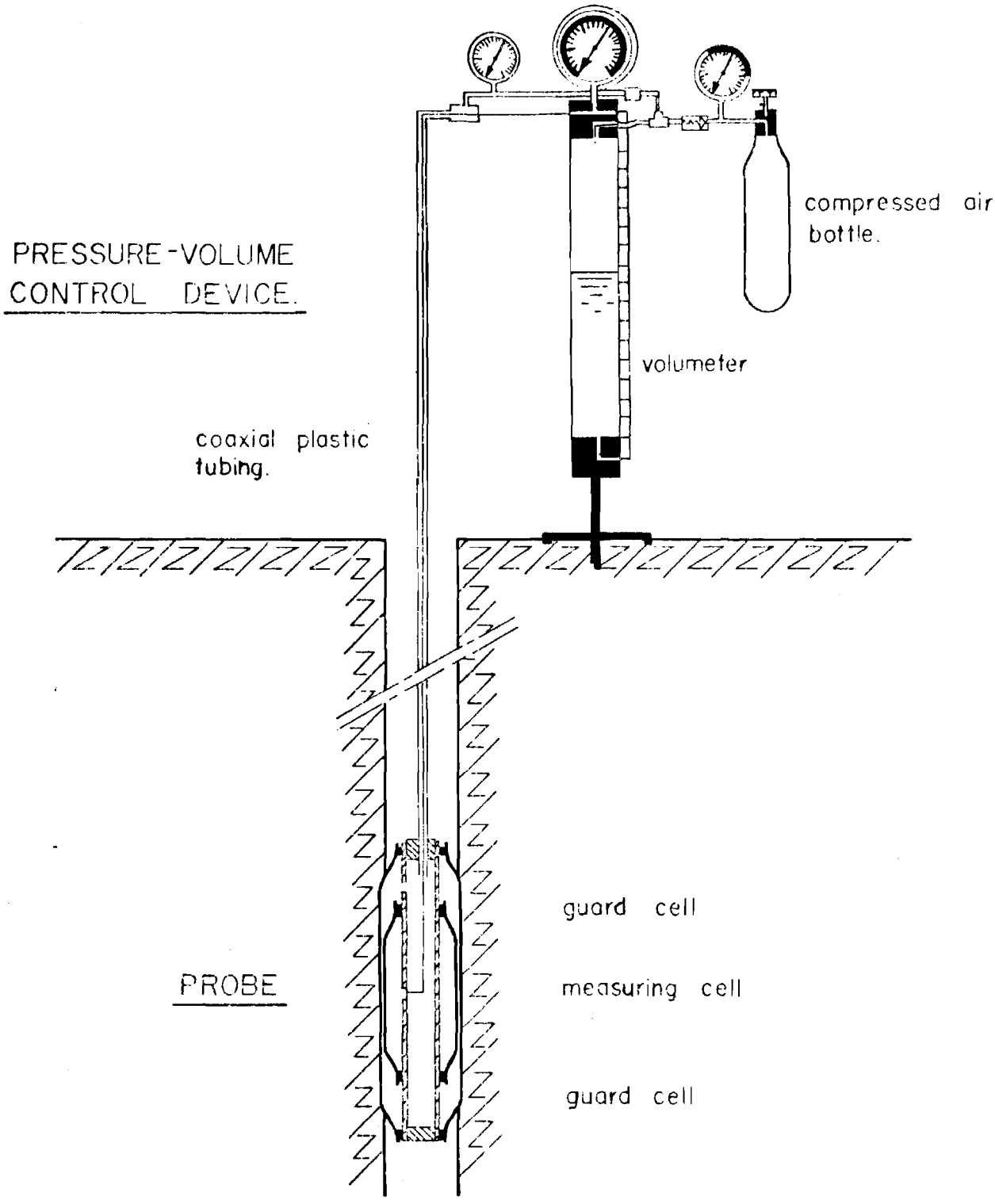

Fig. 1 . Pressuremeter Type G - Test Set-up.

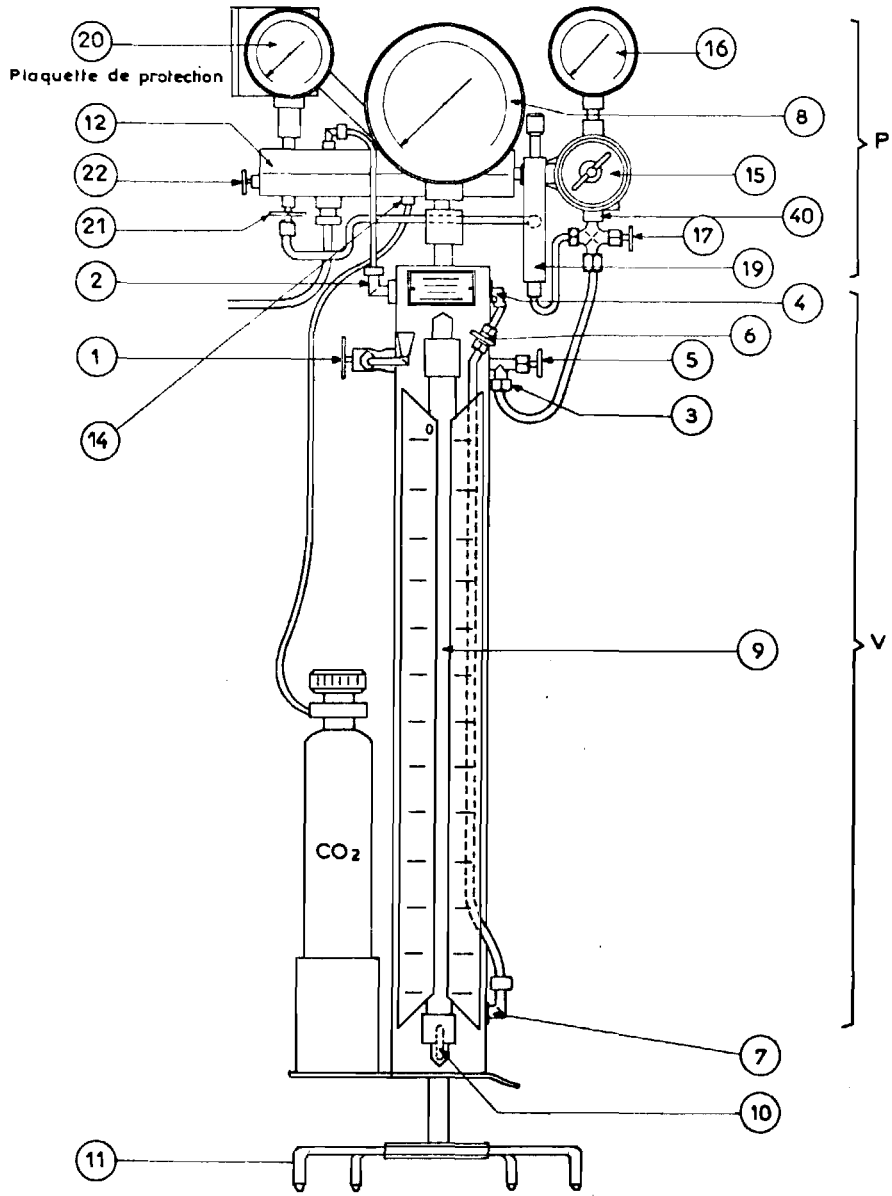

(a) Pressiomètre type G - Ensemble du CPV.

(b) . Pressiomètre type G - Sonde de 60 mm de diamètre.

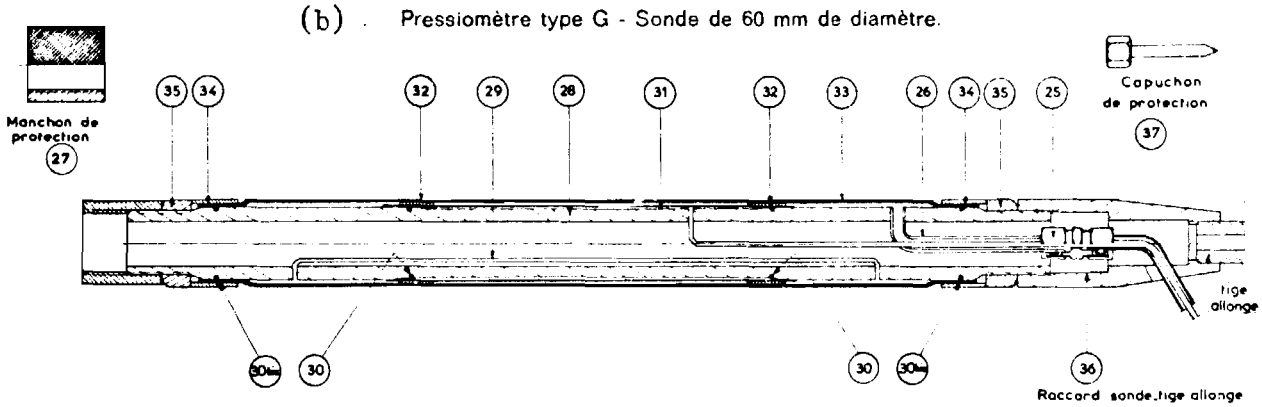

Fig. 2 . Pressuremeter Type G - (a) Pressure-Volume Control (CPV); (b) 60 mm diametre probe.

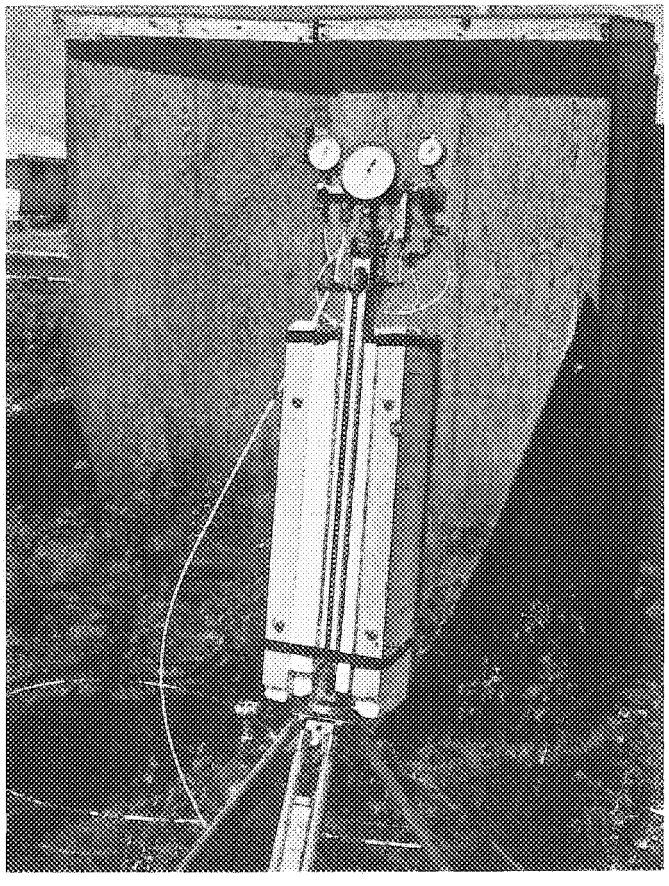

Fig. 3. Pressuremeter equipment used in the tests.

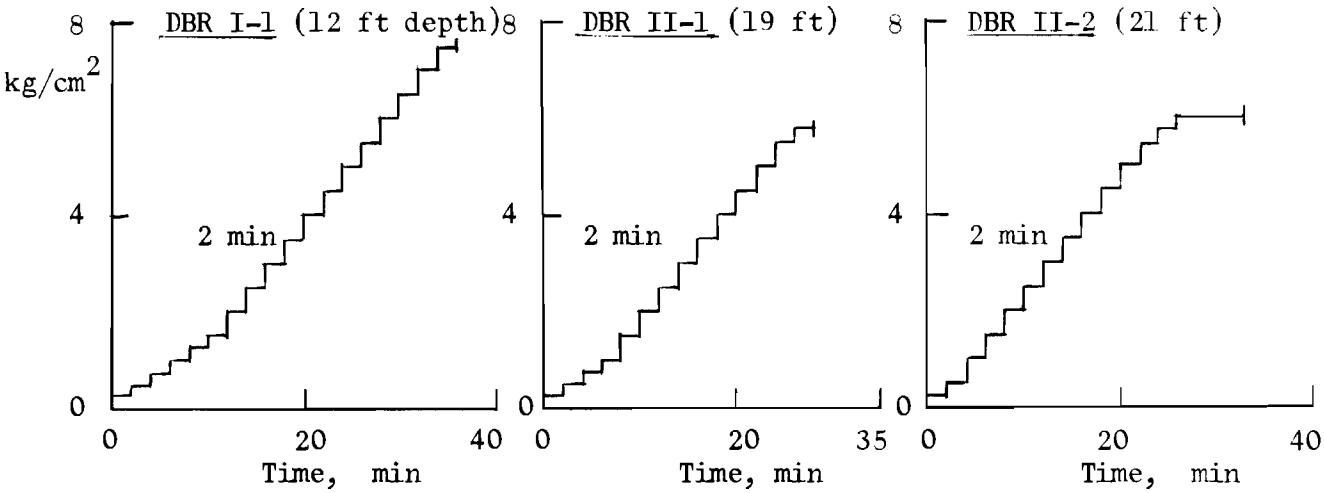

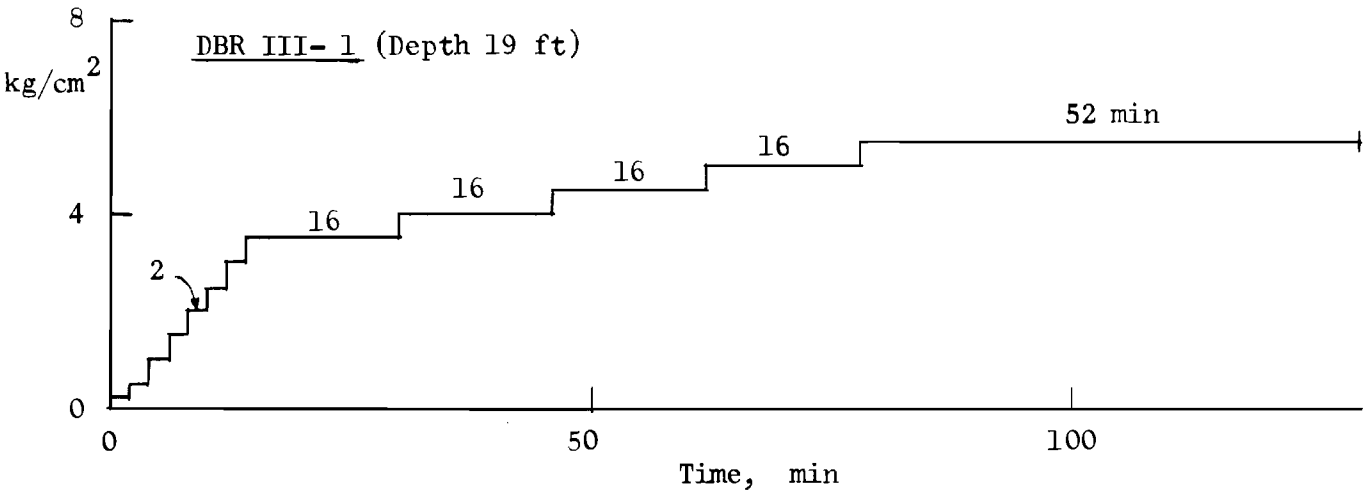

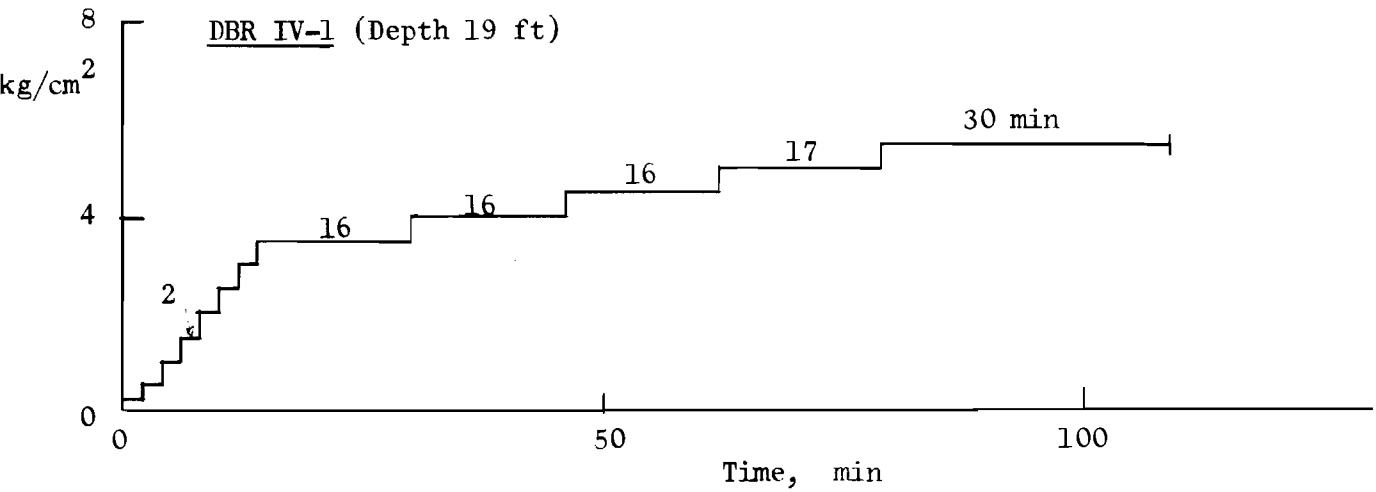

Fig. 4. Applied pressure vs time diagrams for pressure-meter tests in Leda clay at the DBR - NRCC site in Ottawa.

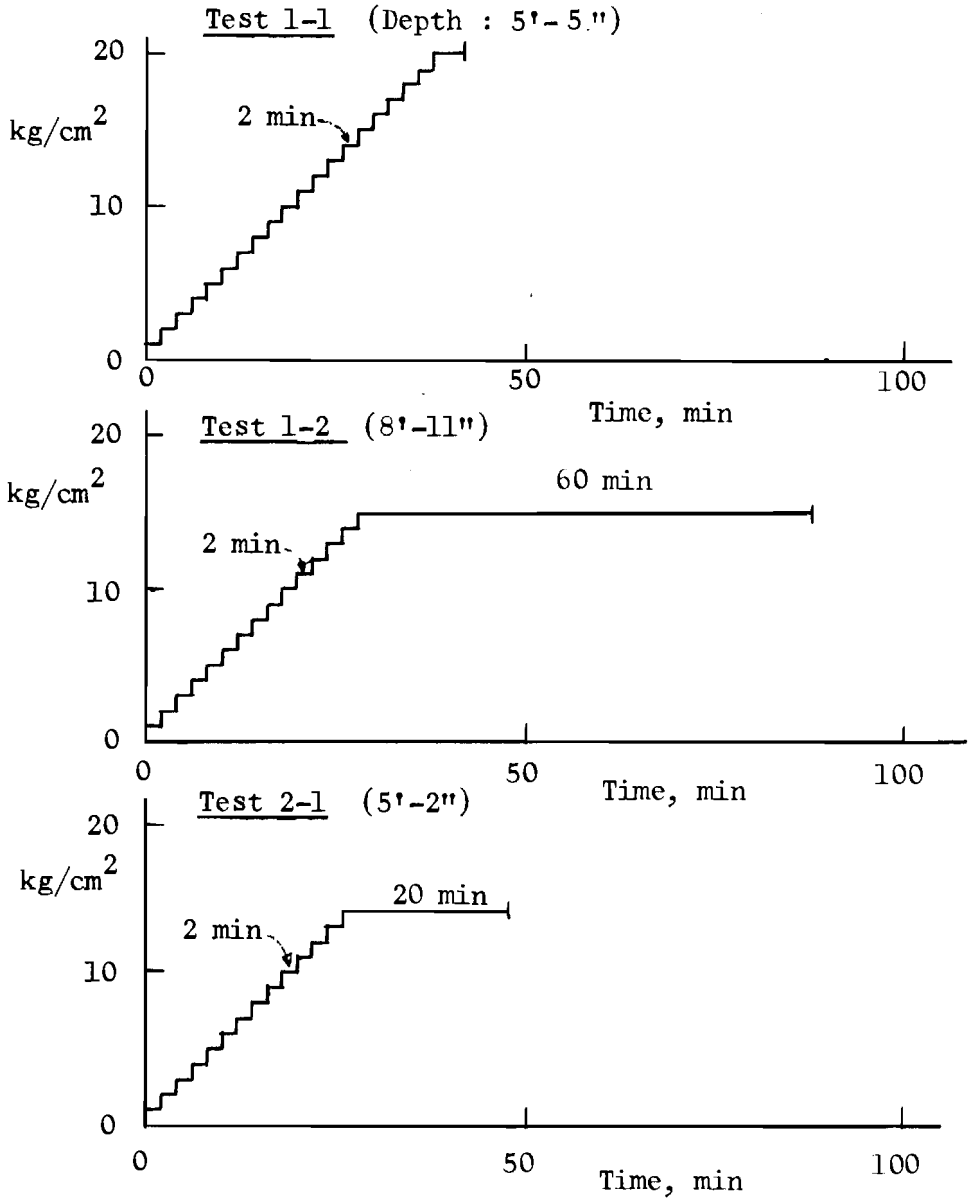

Fig. 5. Applied pressure vs time diagrams for pressuremeter tests in frozen varved soil at Thompson.

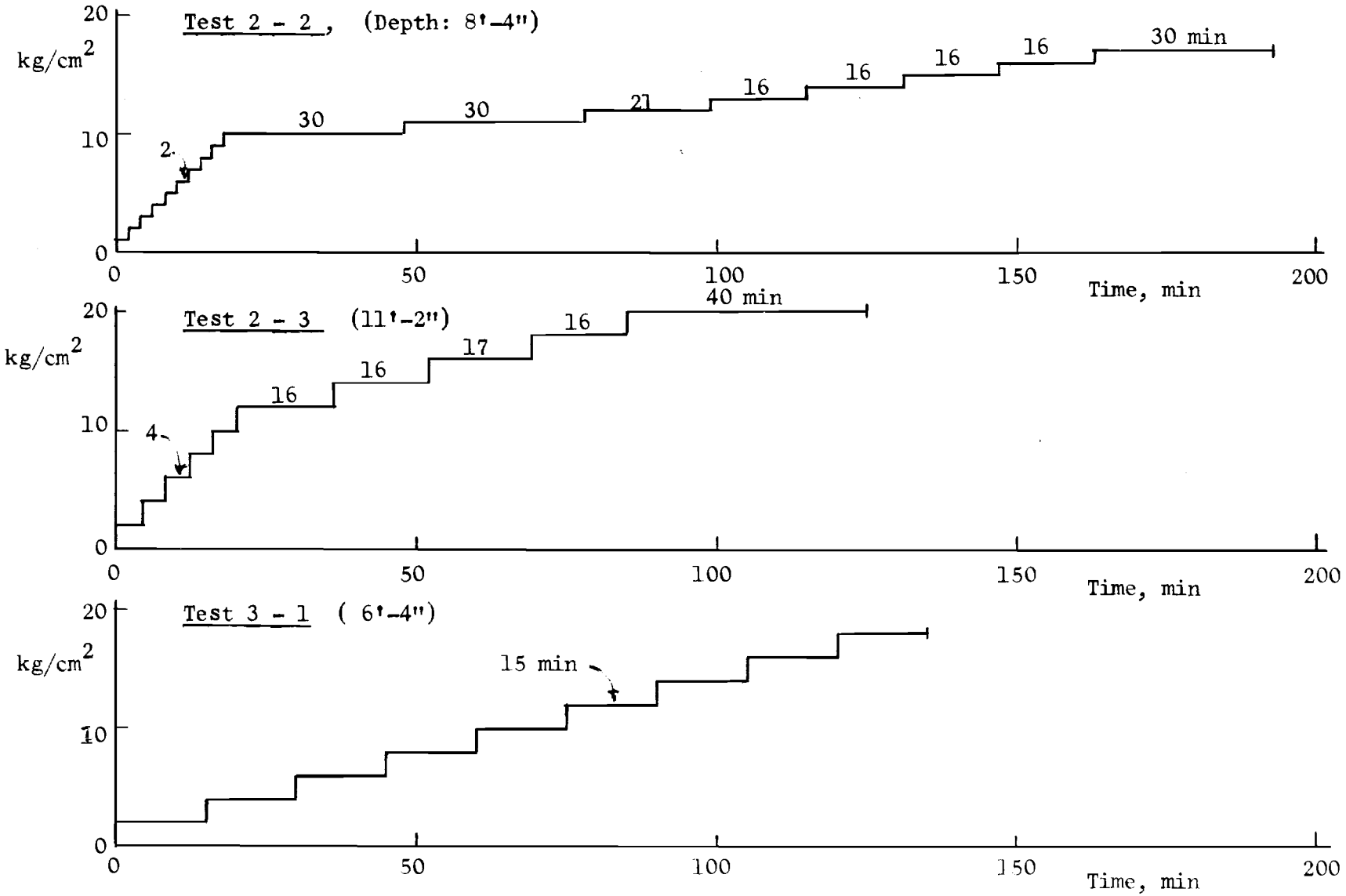

Fig. 6. Applied pressure vs time diagrams. Frozen varved soil, Thompson.

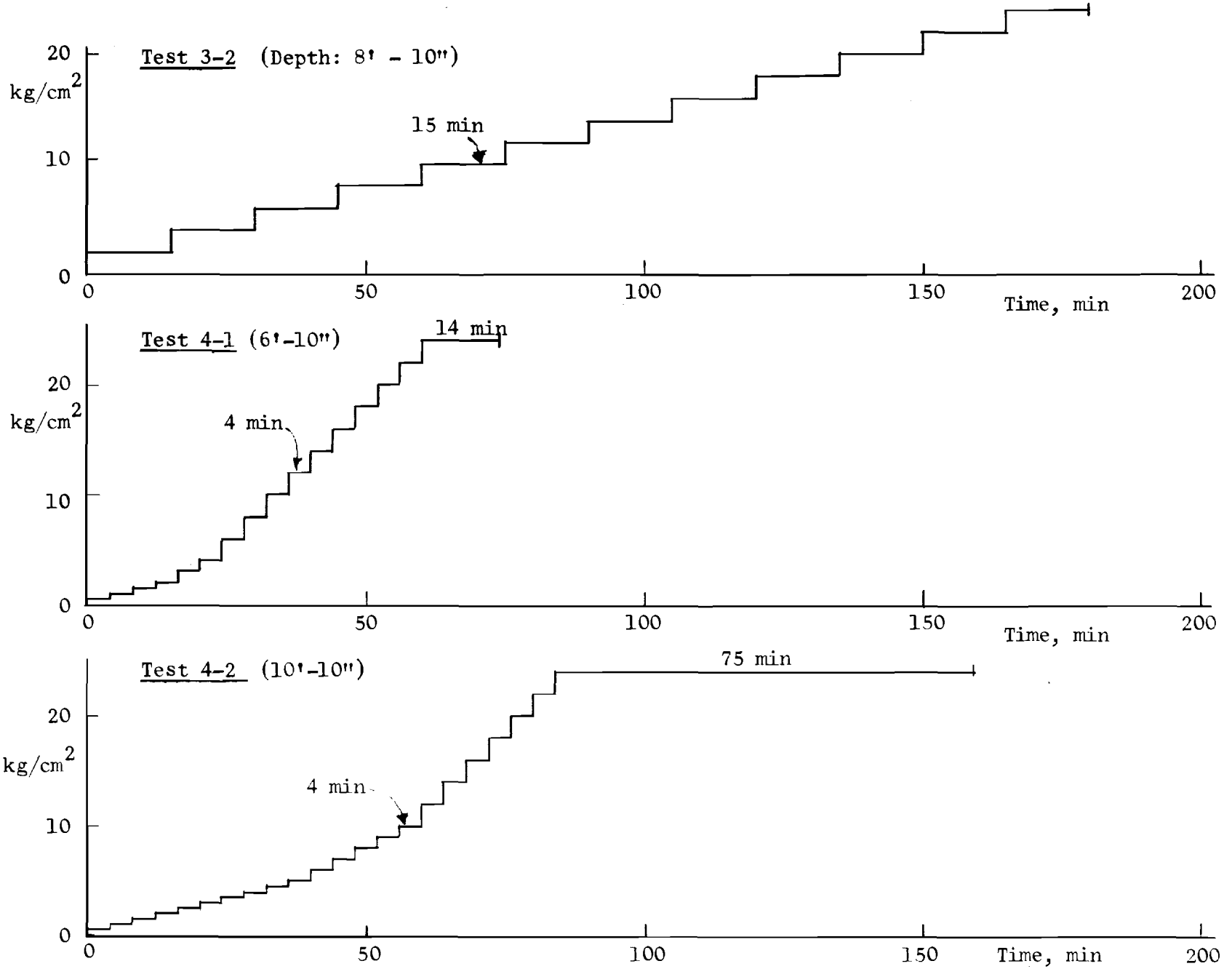

Fig. 7. Applied pressure vs time diagrams. Frozen varved soil, Thompson.

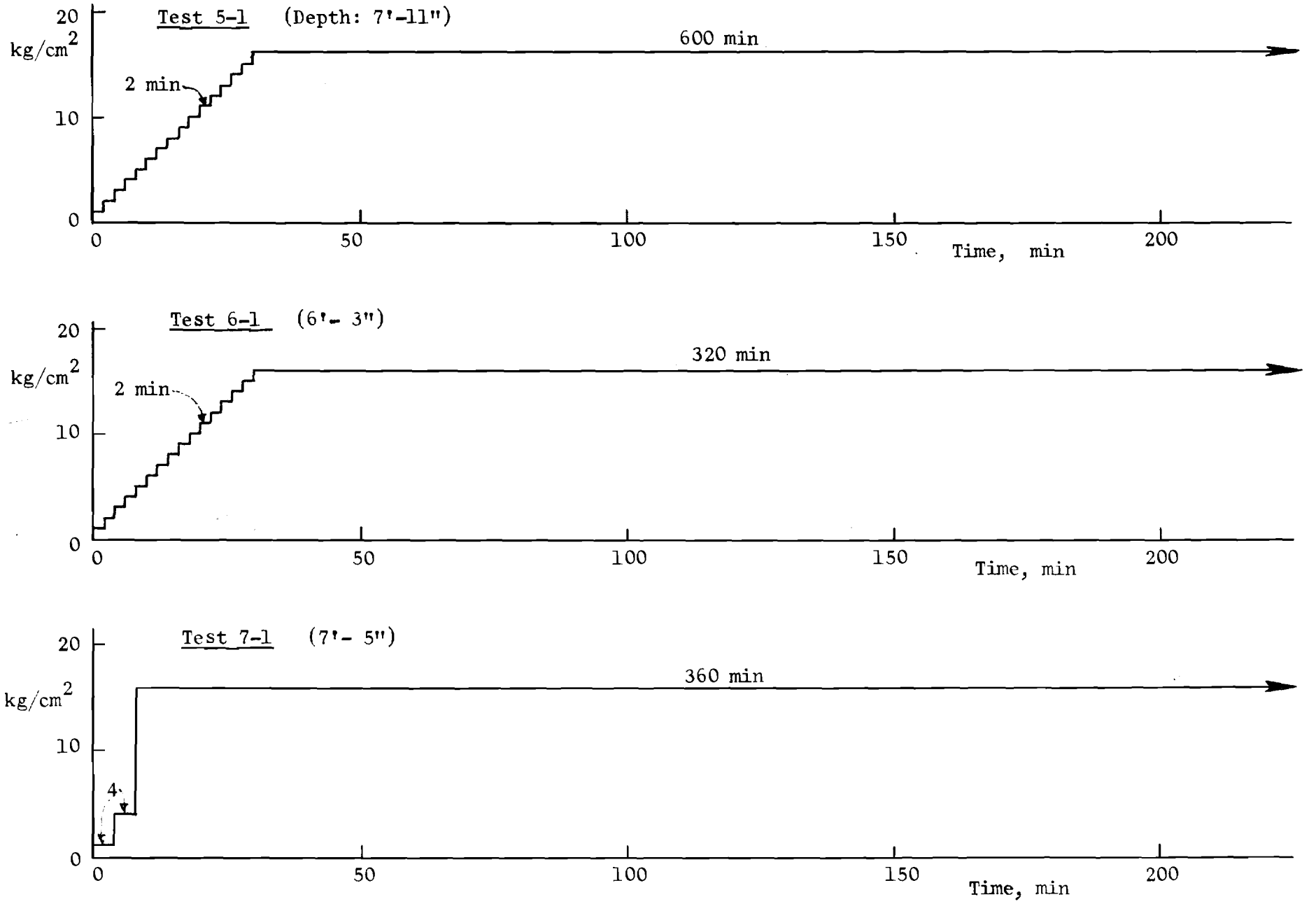

Fig. 5. Applied pressure vs time diagrams. Frozen varved soil, Thompson.

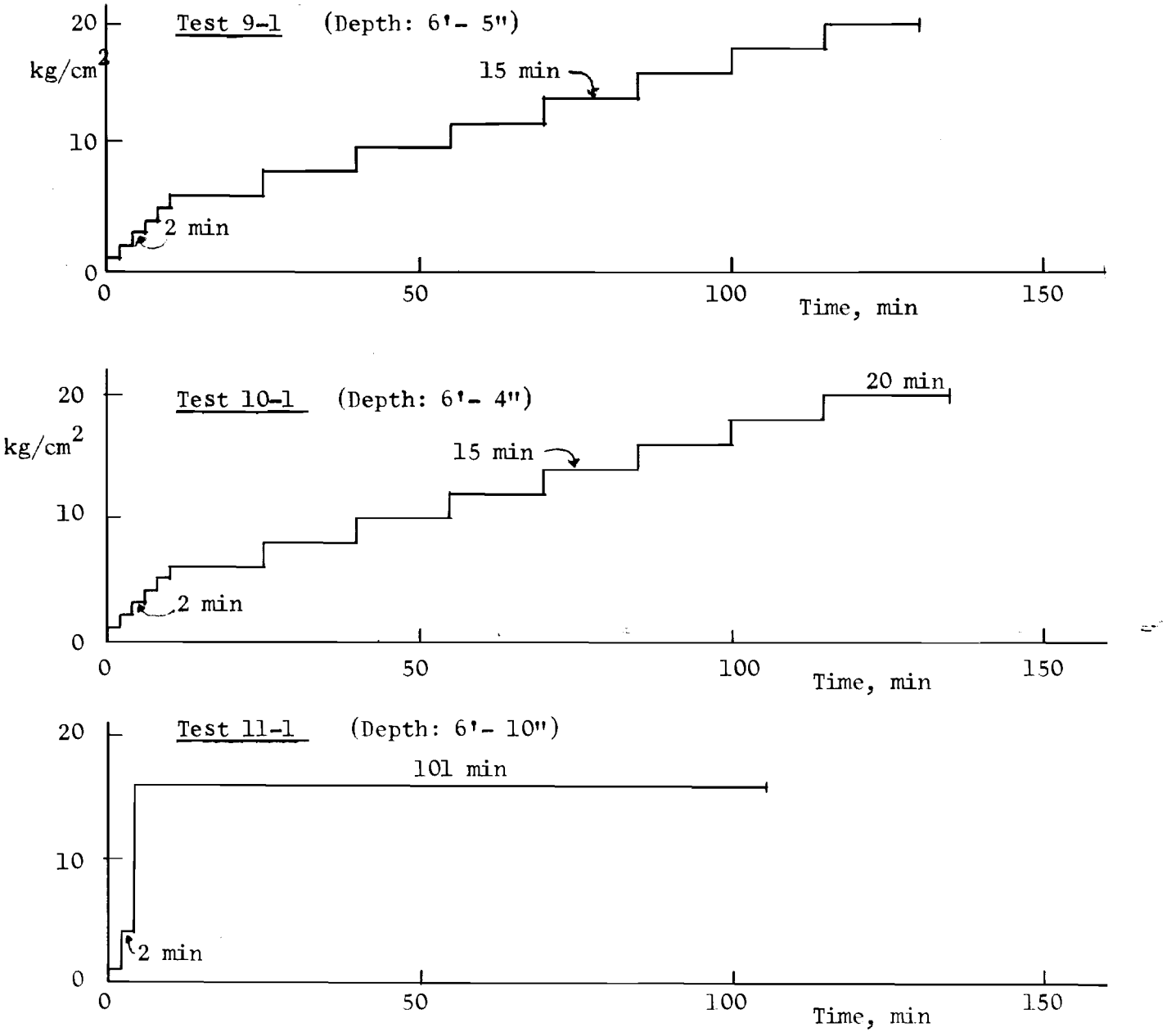

Fig. 10. Applied pressure vs time diagrams. Pressuremeter tests in frozen varved soil at Thompson.

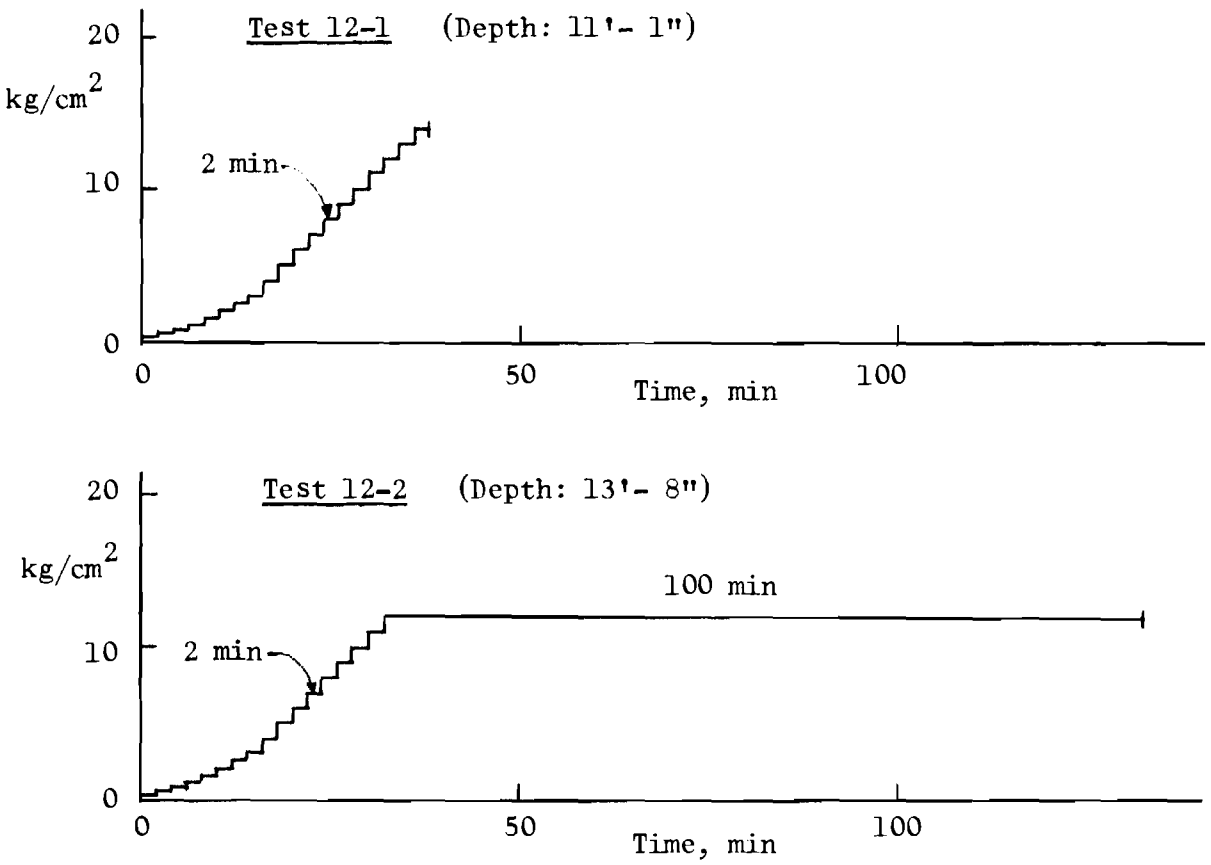

Fig. 11. Applied pressure vs time diagrams. Pressuremeter tests in frozen clay at Thompson 2 site.

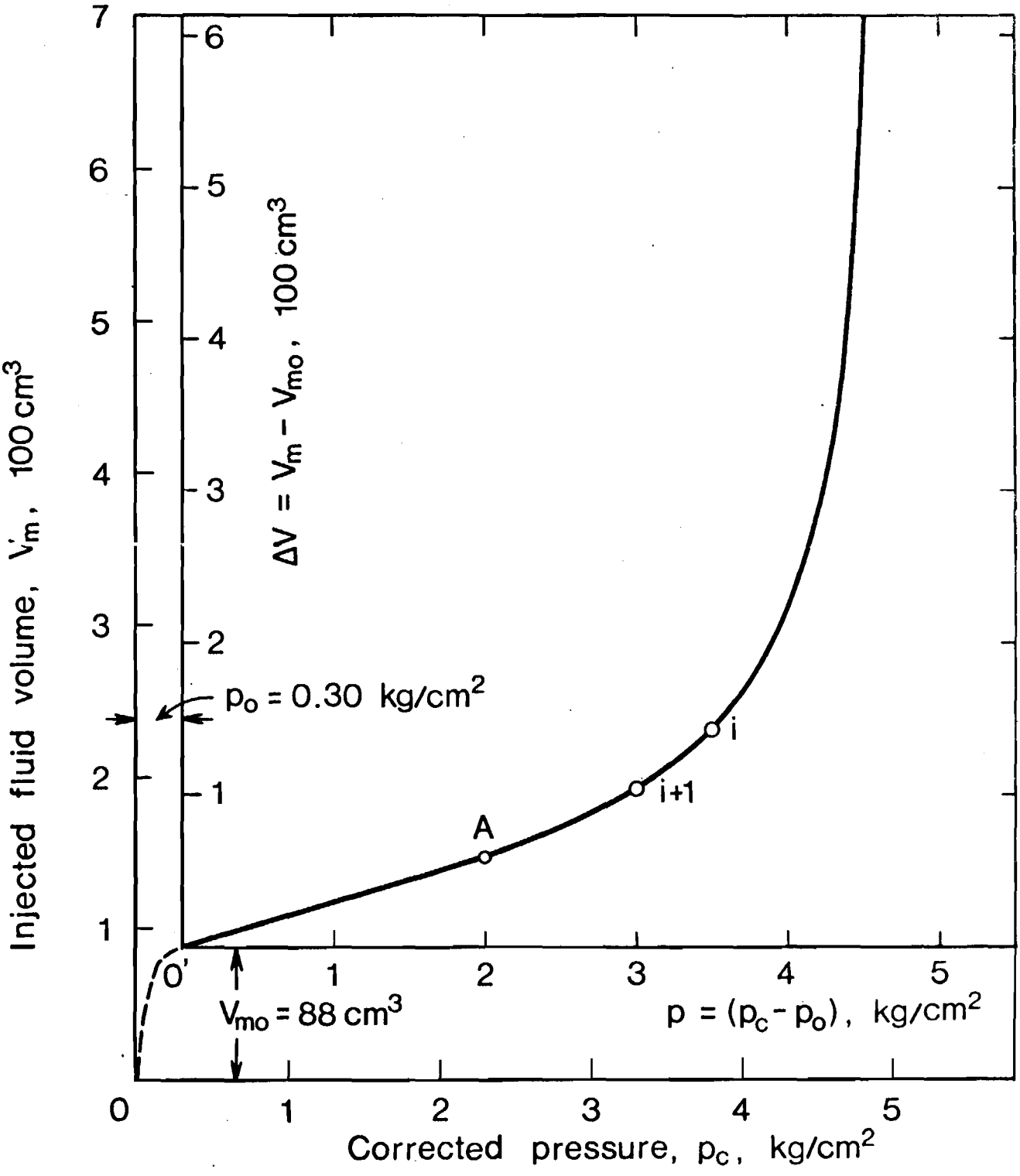

Fig. 12. Standard plot of pressuremeter curve.

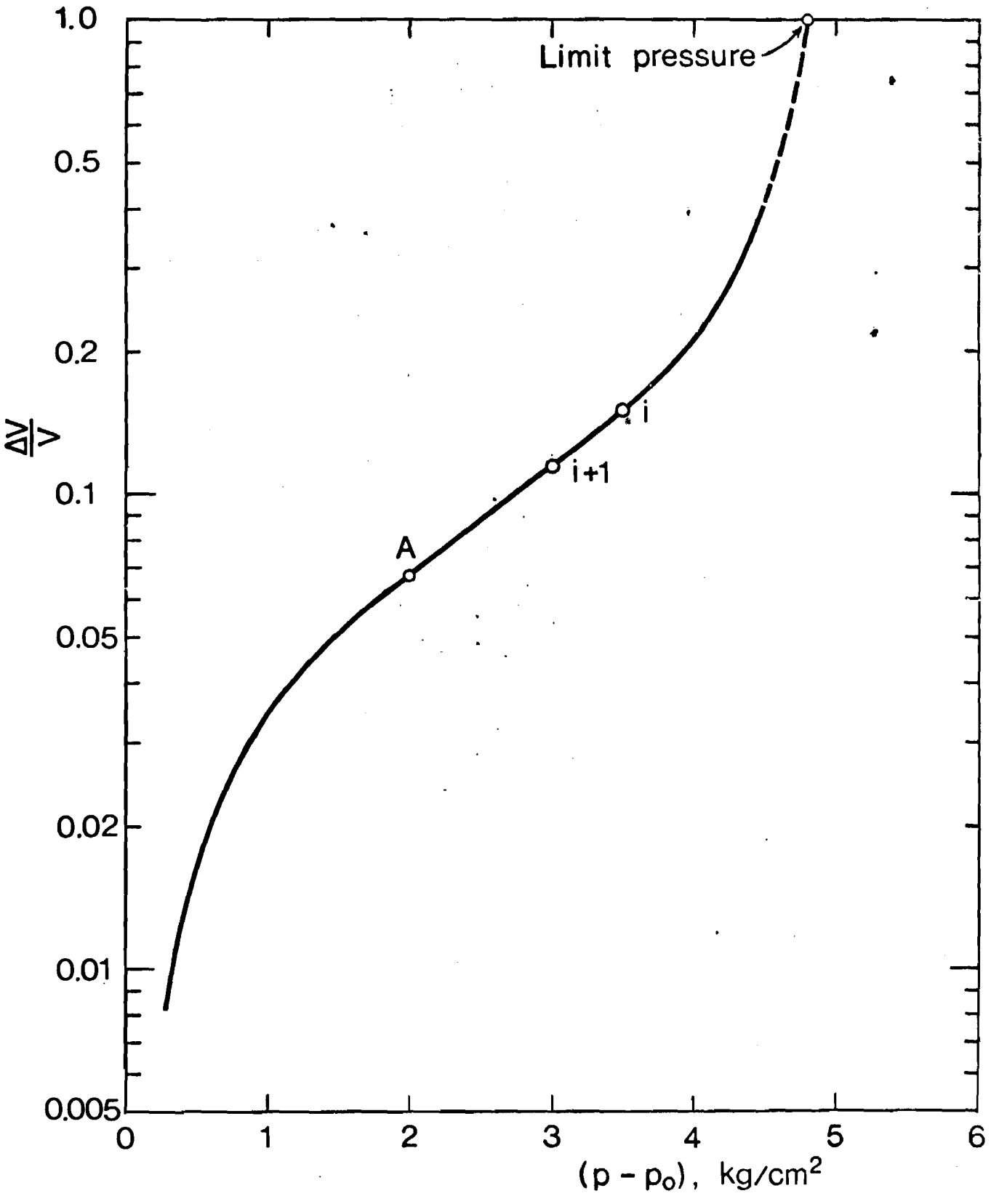

Fig. 13. Semi-log plot of pressuremeter curve from Fig. 12.

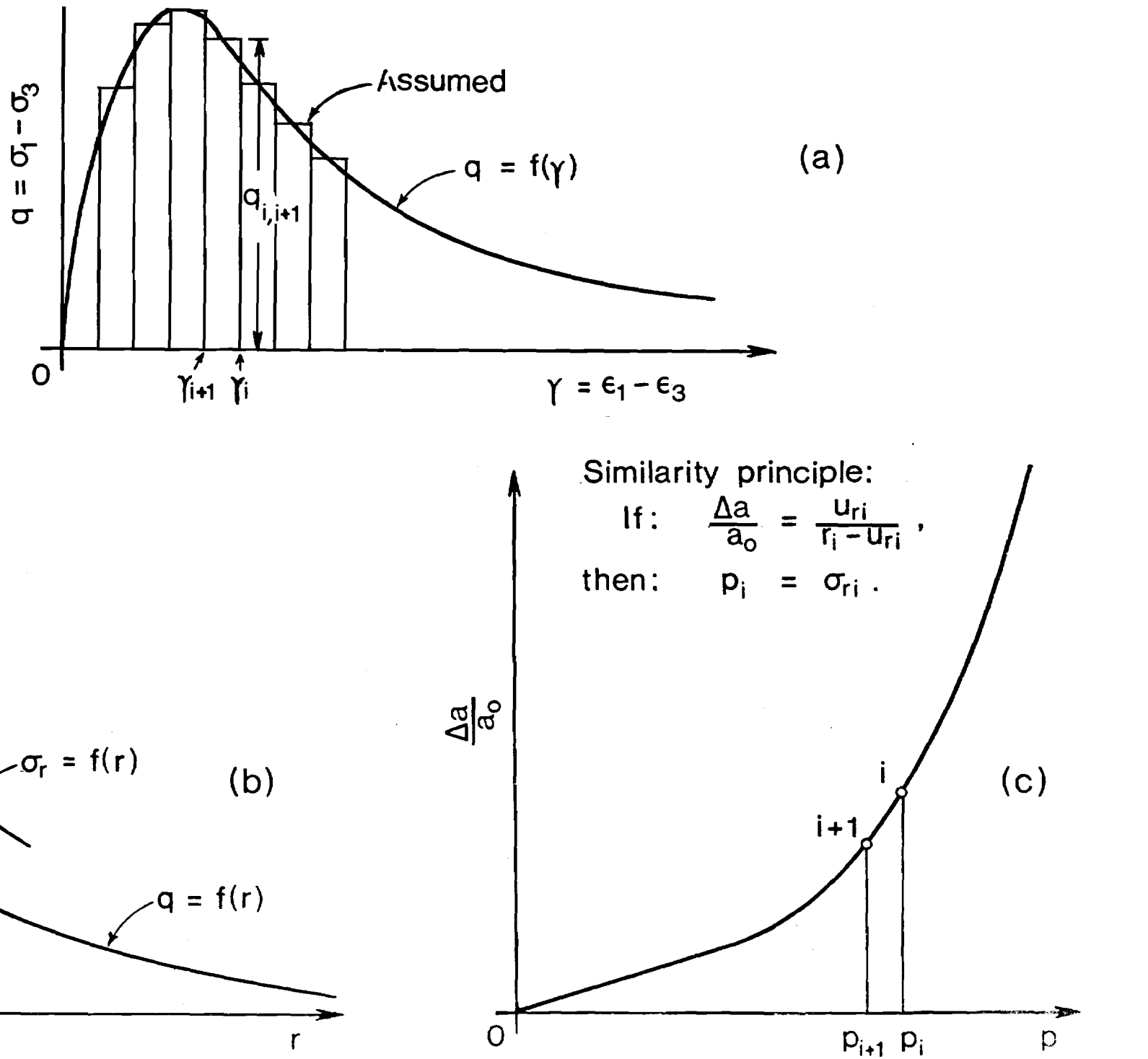

Fig. 14. Relationship between the pressuremeter curve and the stress-strain curve.

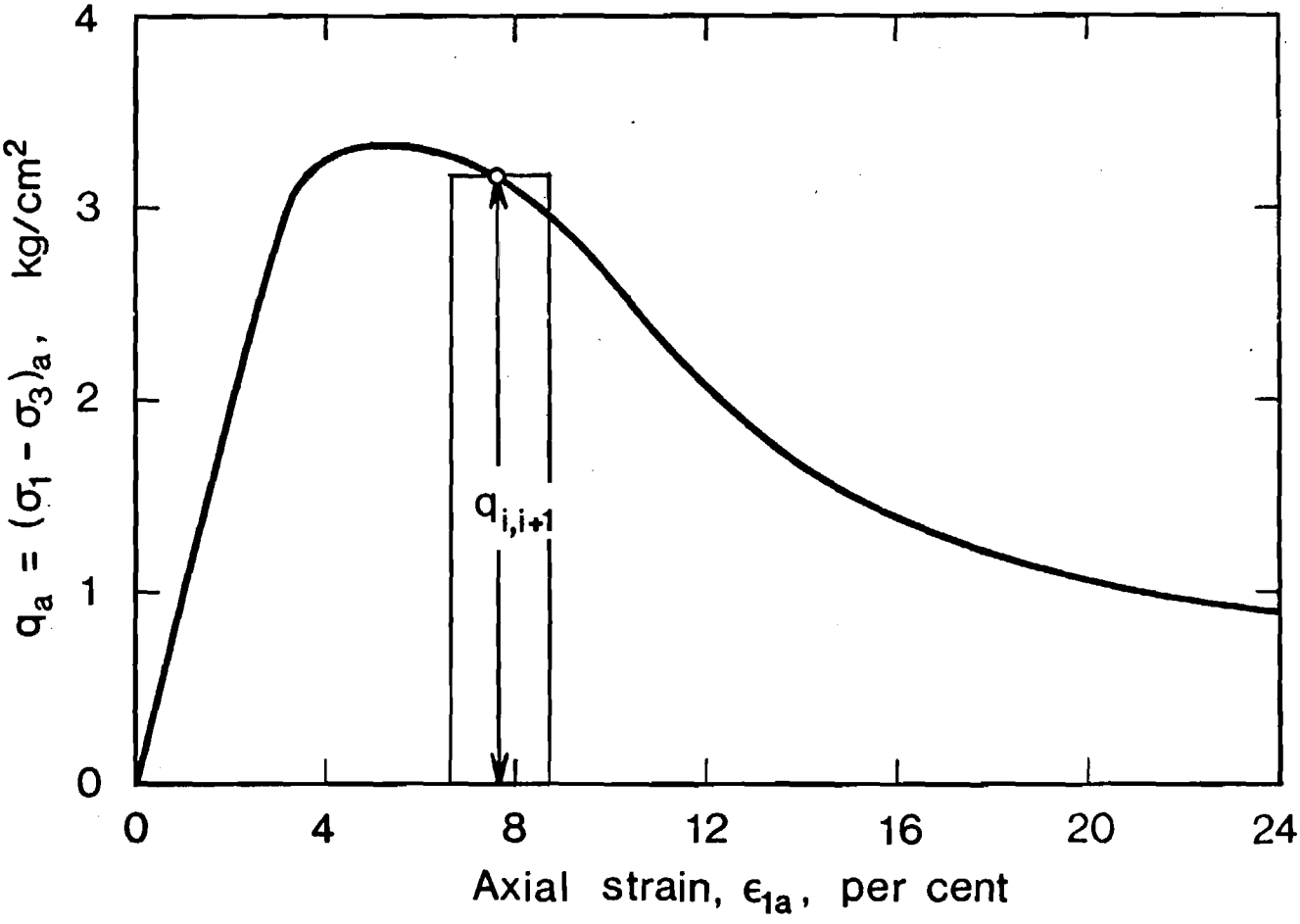

Fig. 15. Stress-strain curve deduced from the pressuremeter curve in Fig. 12.

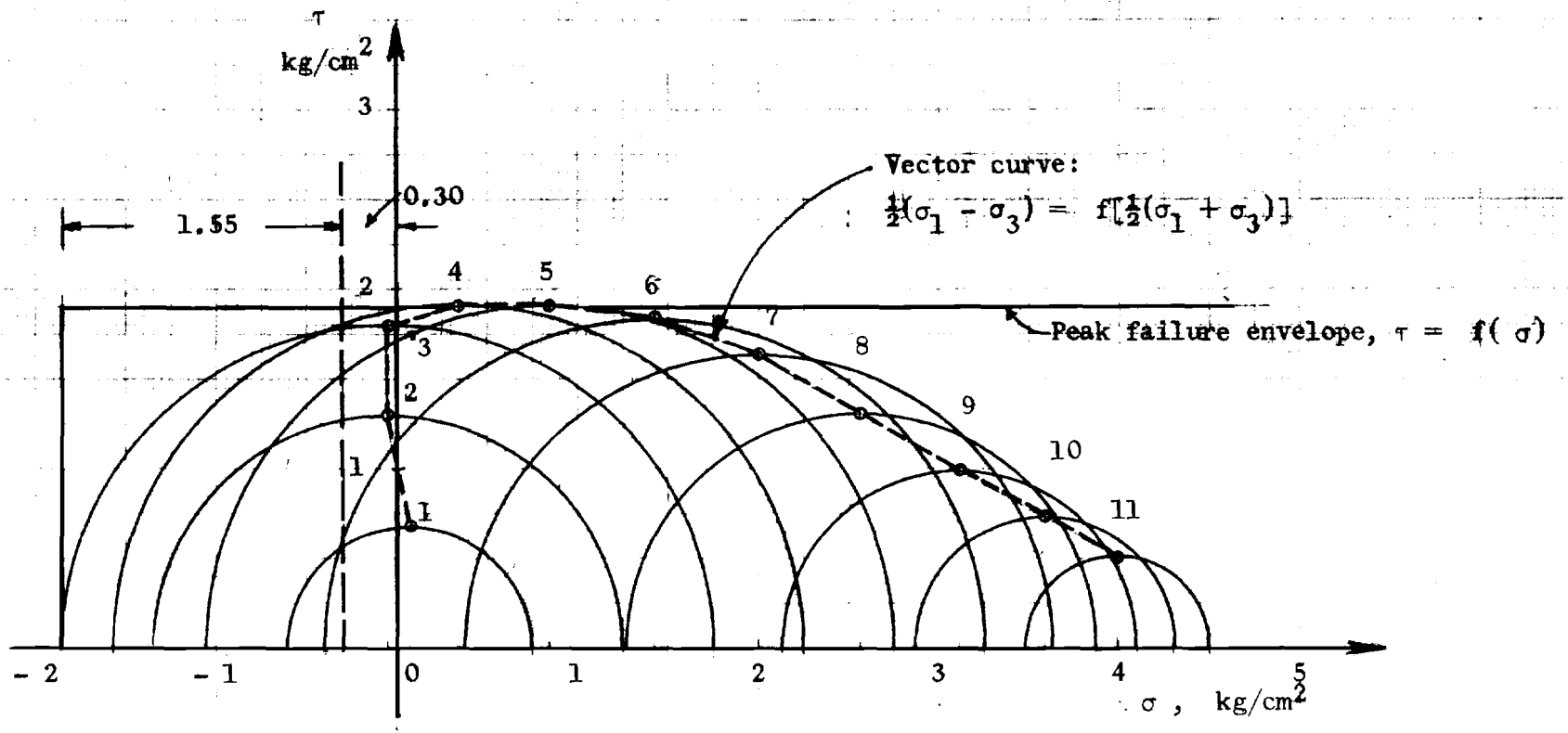

Fig. 16. Mohr circles and vector curve from the test in Fig. 12 (Leda clay, Montreal Road, Ottawa).

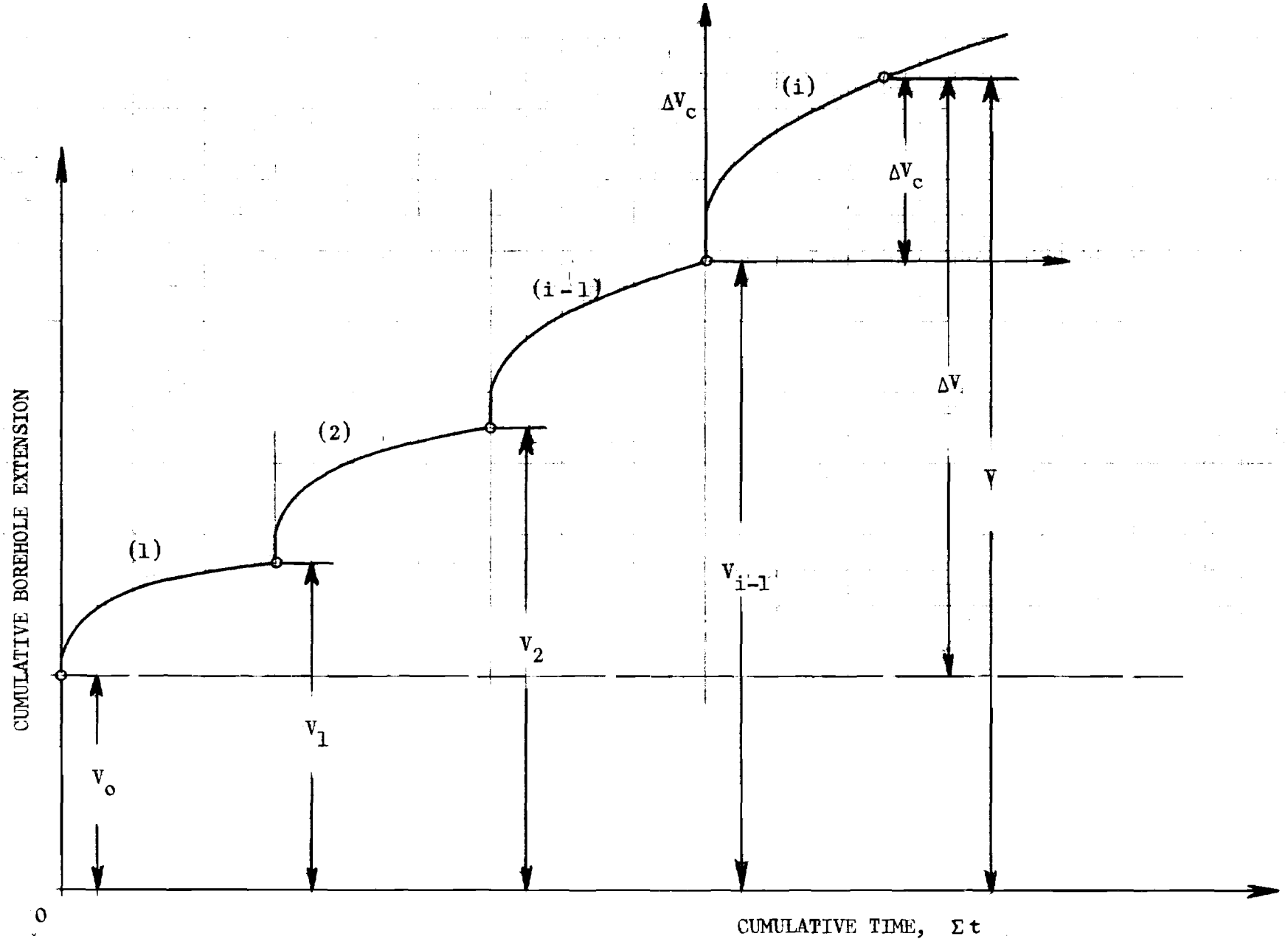

Fig. 17. Notation for interpretation of pressuremeter creep data.

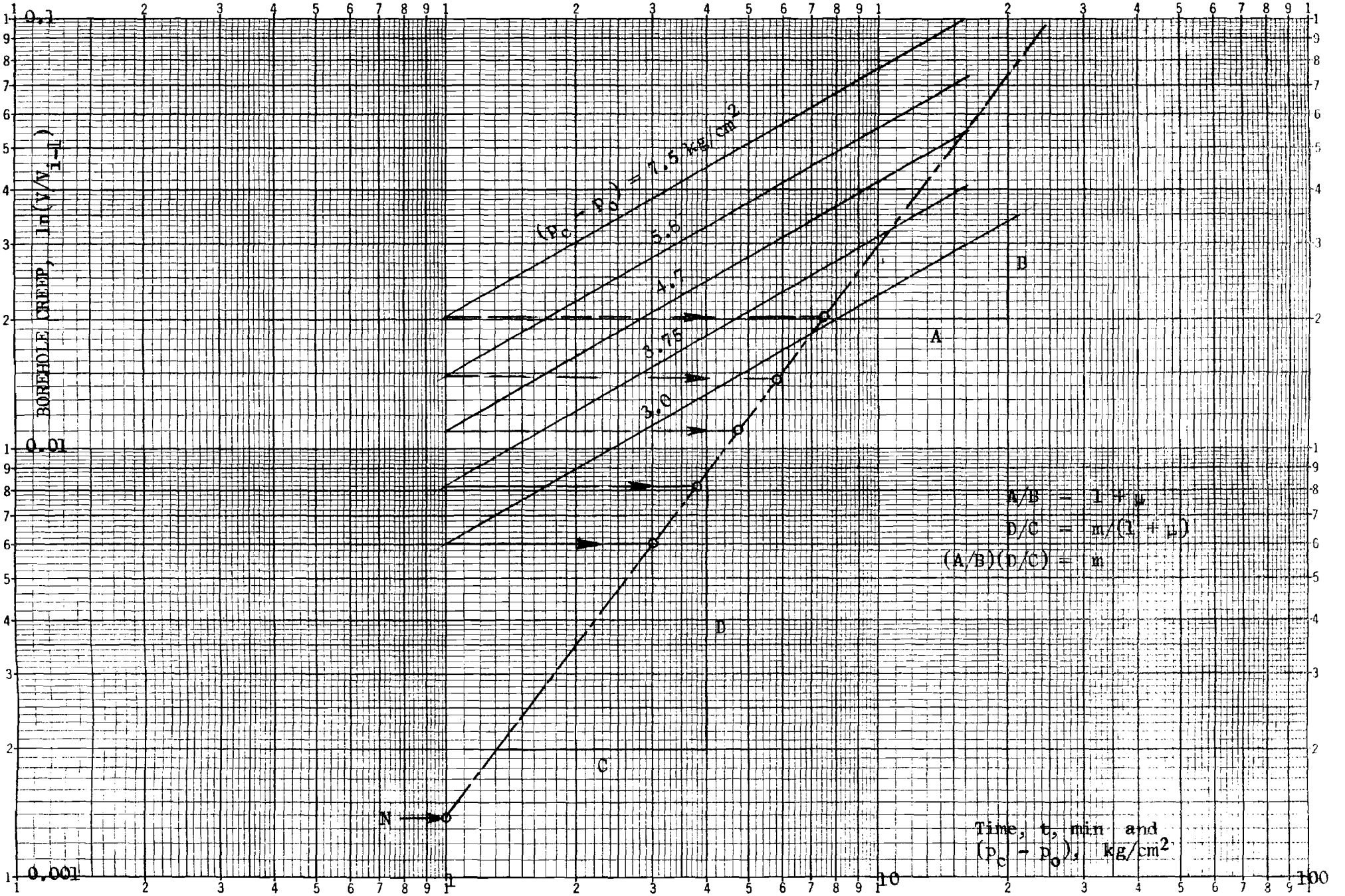

Fig. 18. Semi-graphical determination of creep parameters (schematic).

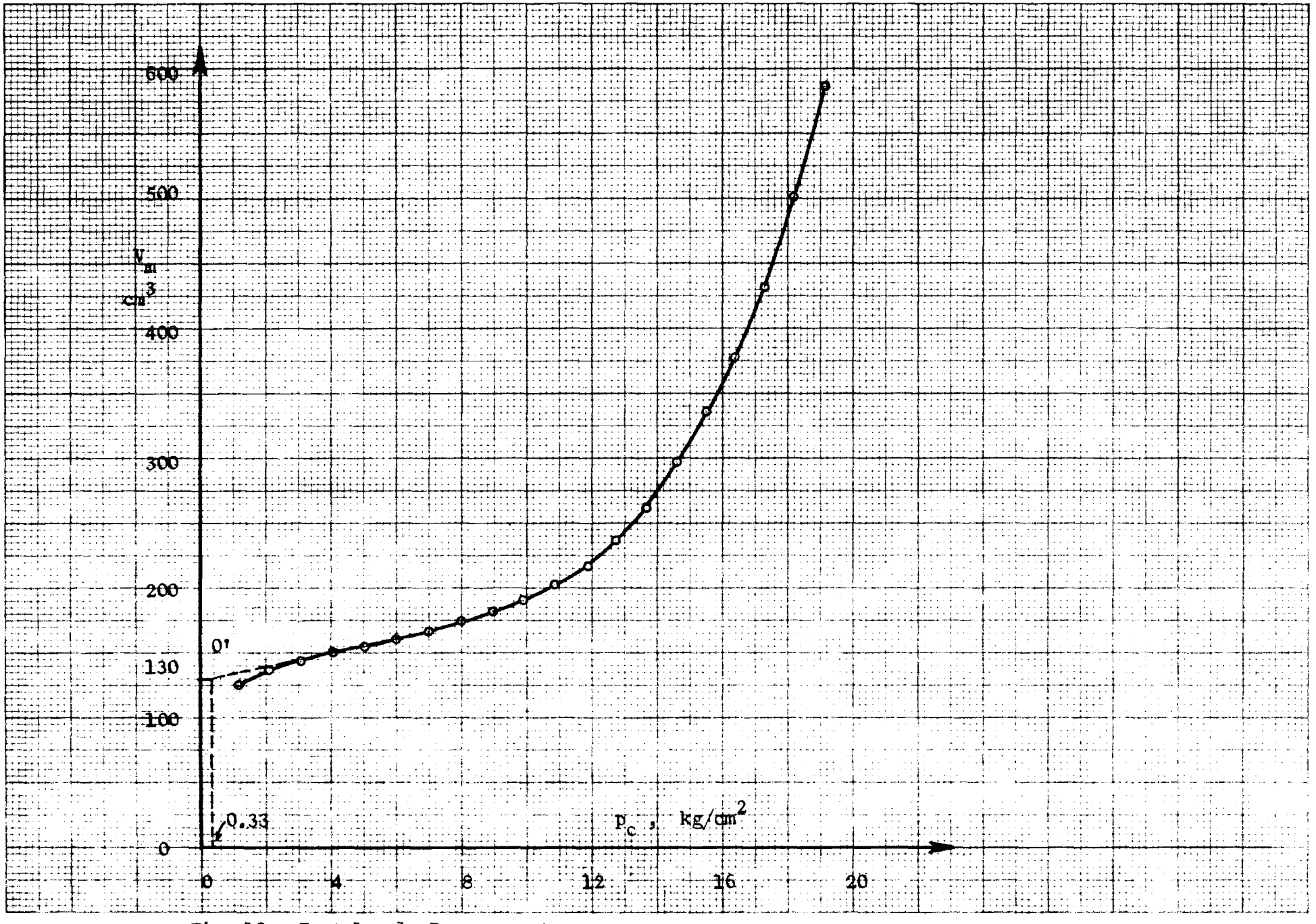

Fig. 19. Test 1 - 1. Pressuremeter curve.

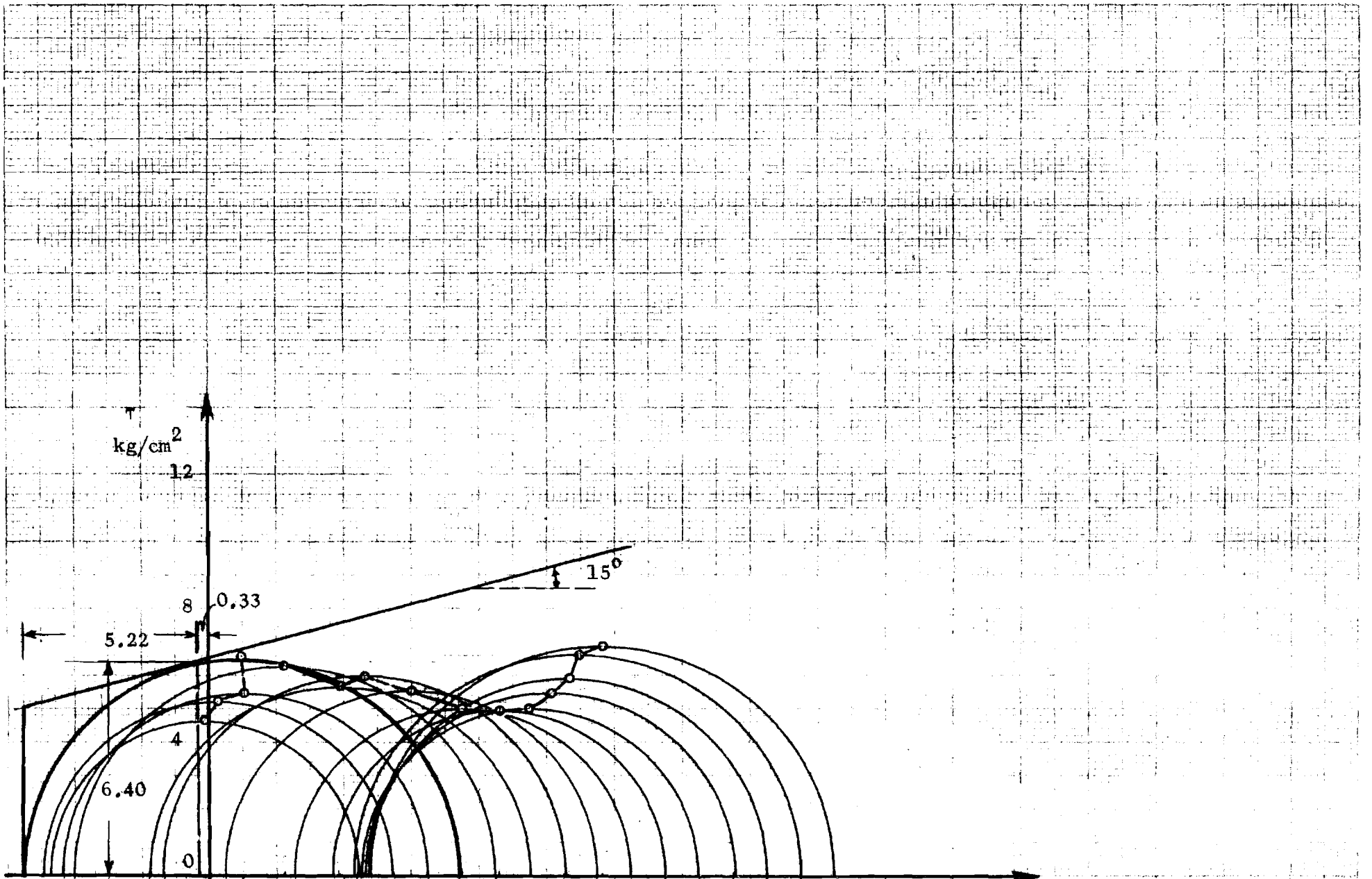

Fig. 20. Test 1 - 1. Vector curve.

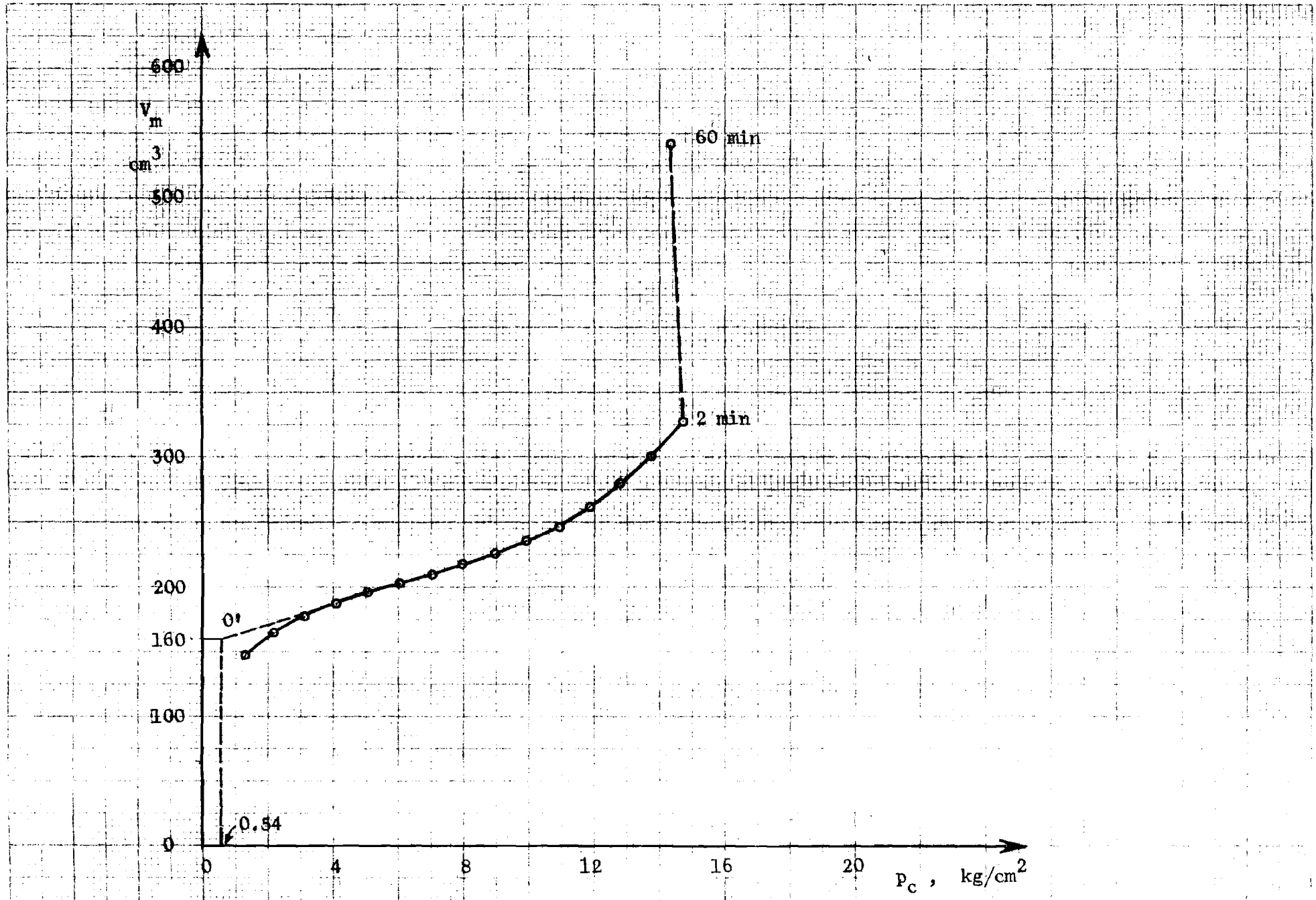

Fig. 21. Test 1 - 2. Pressuremeter curve.

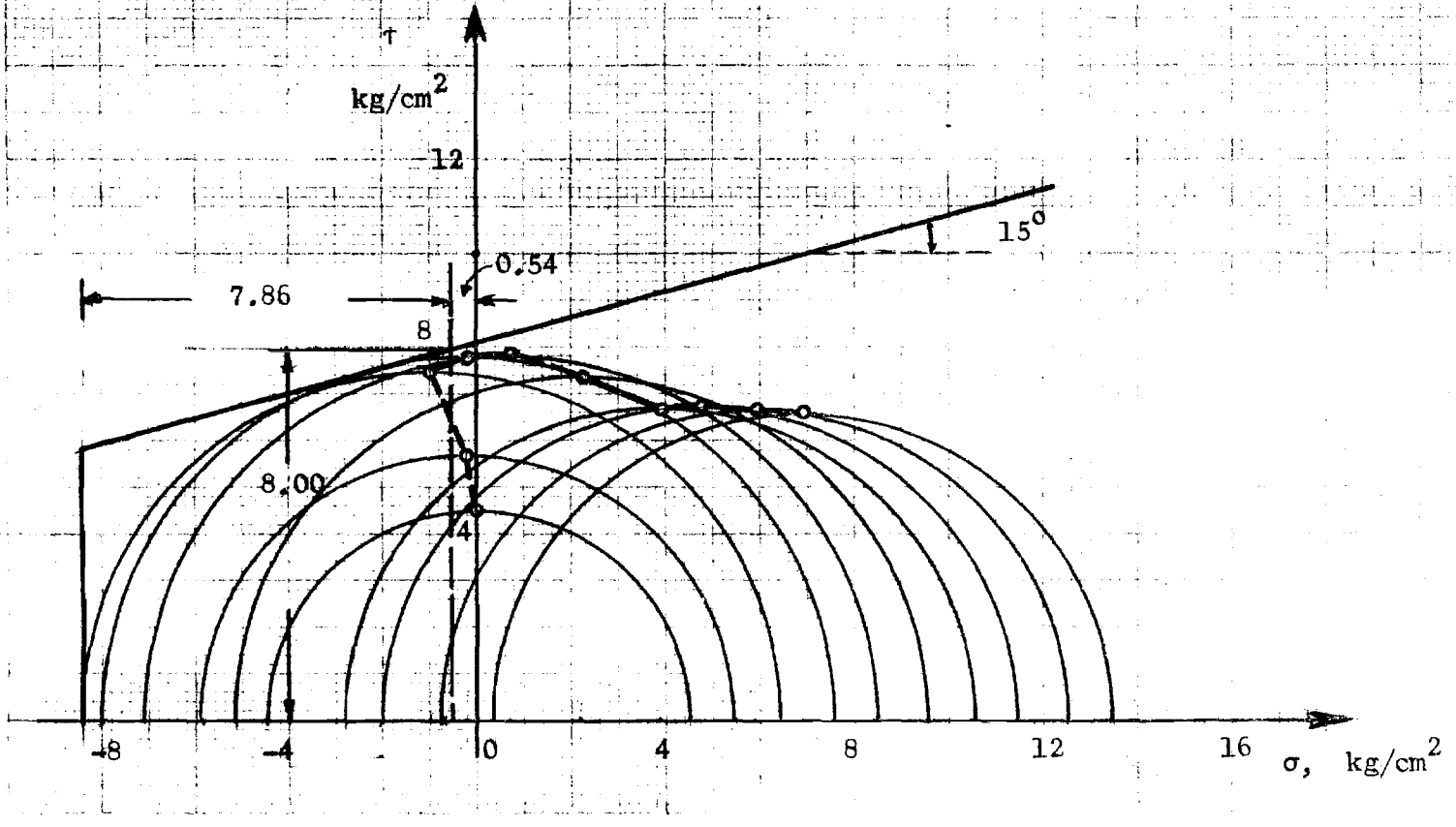

Fig. 22. Test 1 - 2. Vector curve.

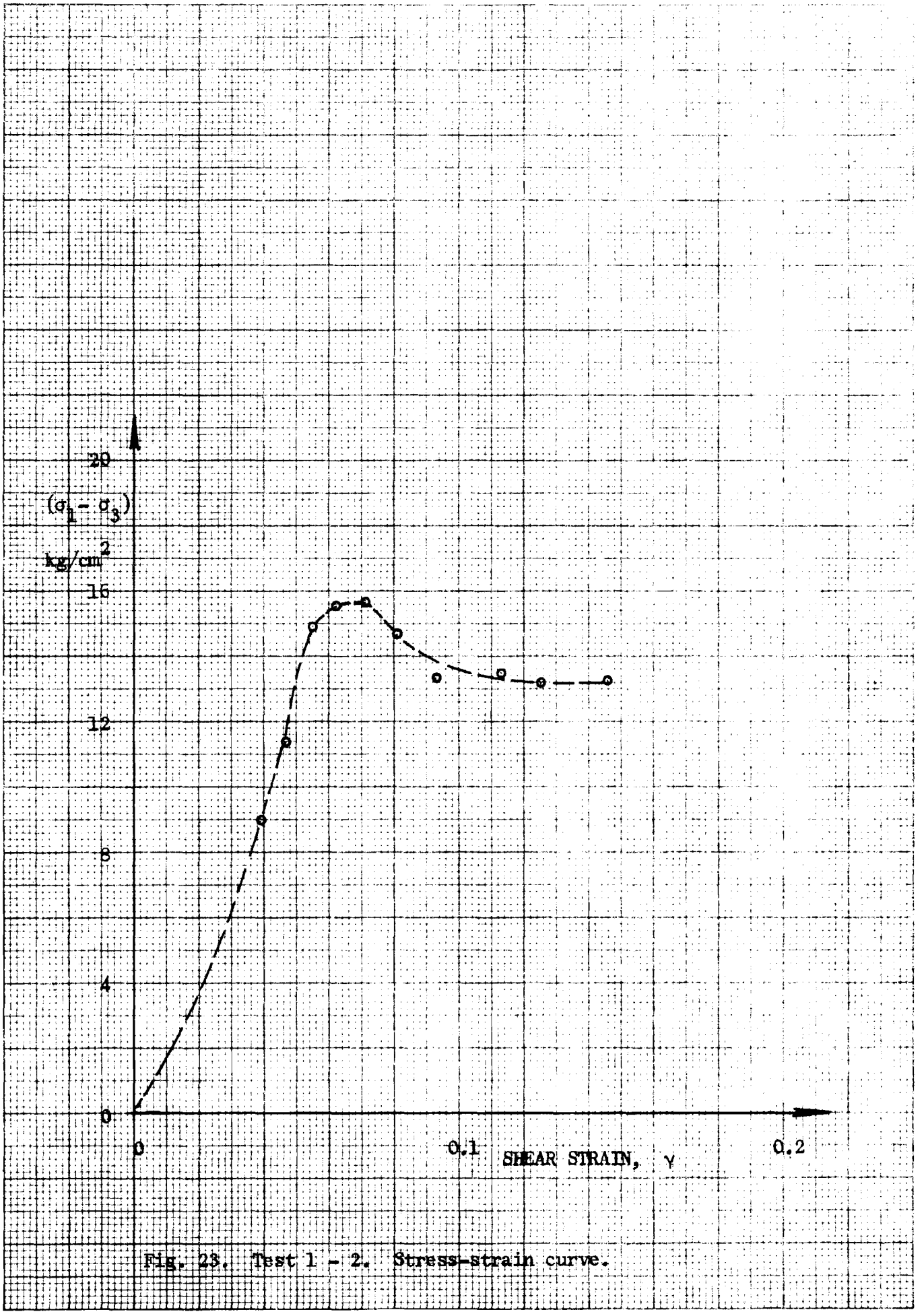

Fig. 23. Test 1 - 2. Stress-strain curve.

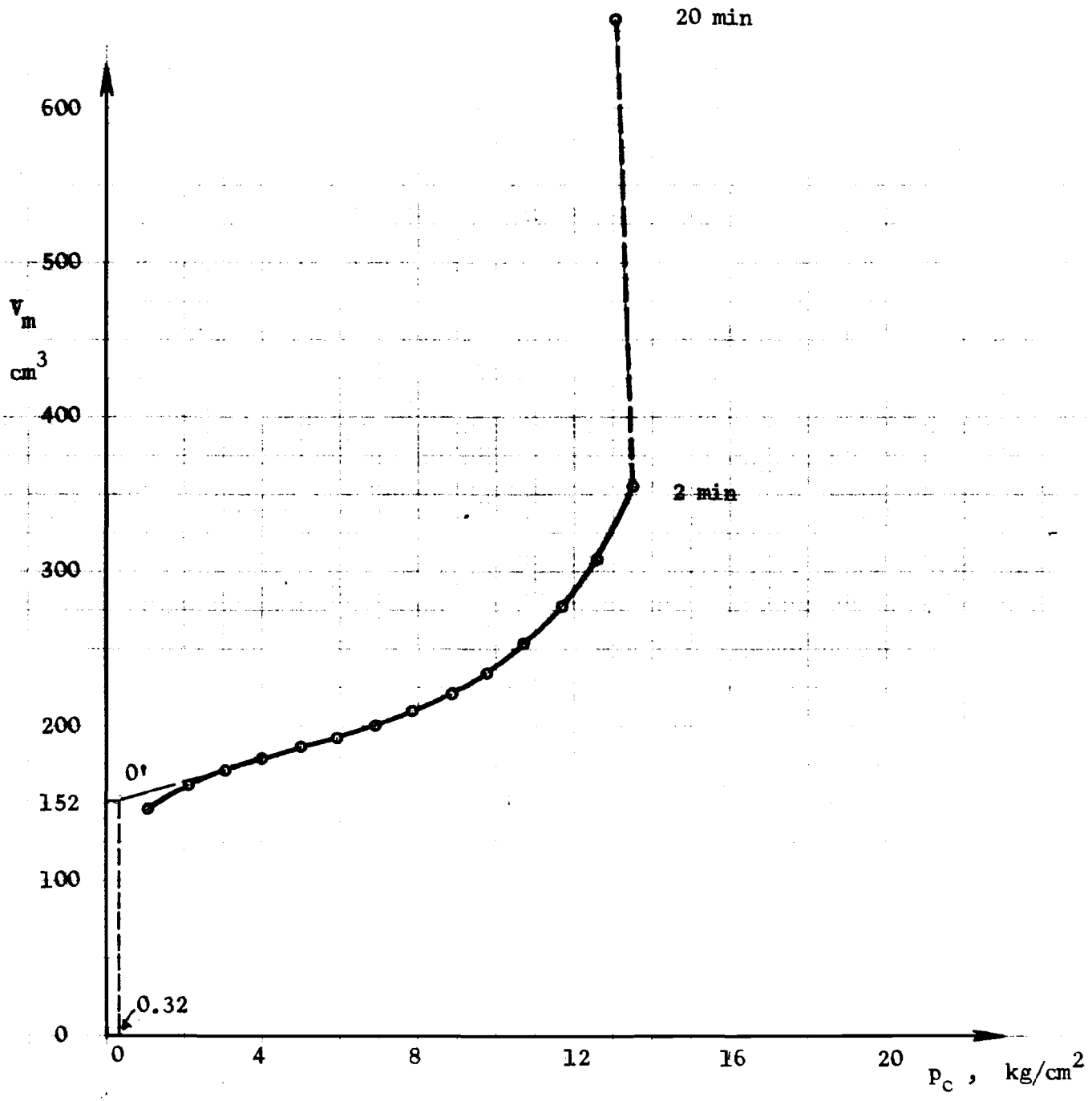

Fig. 24. Test 2 - 1. Pressuremeter curve.

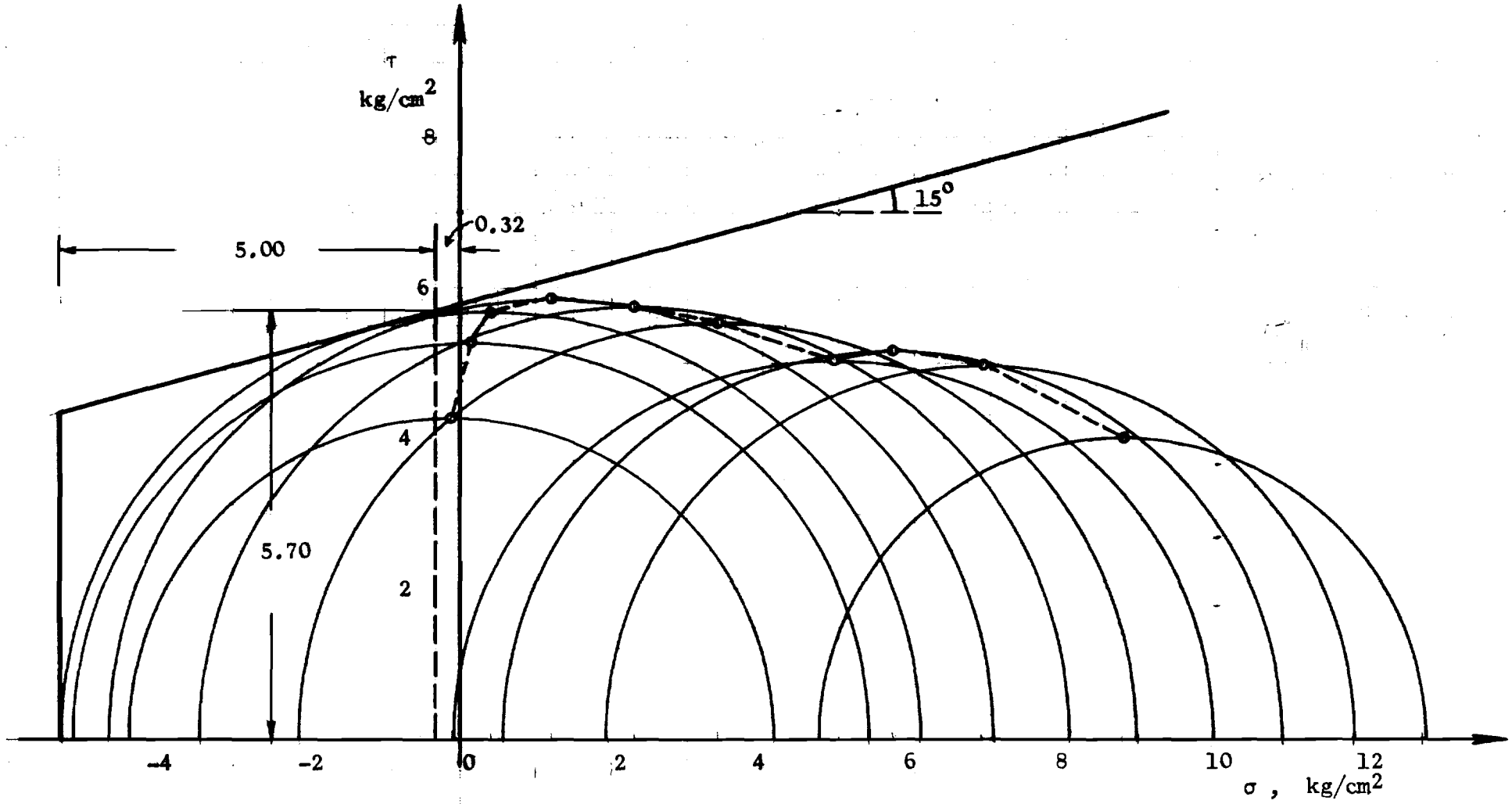

Fig. 25. Test 2 - 1. Vector curve.

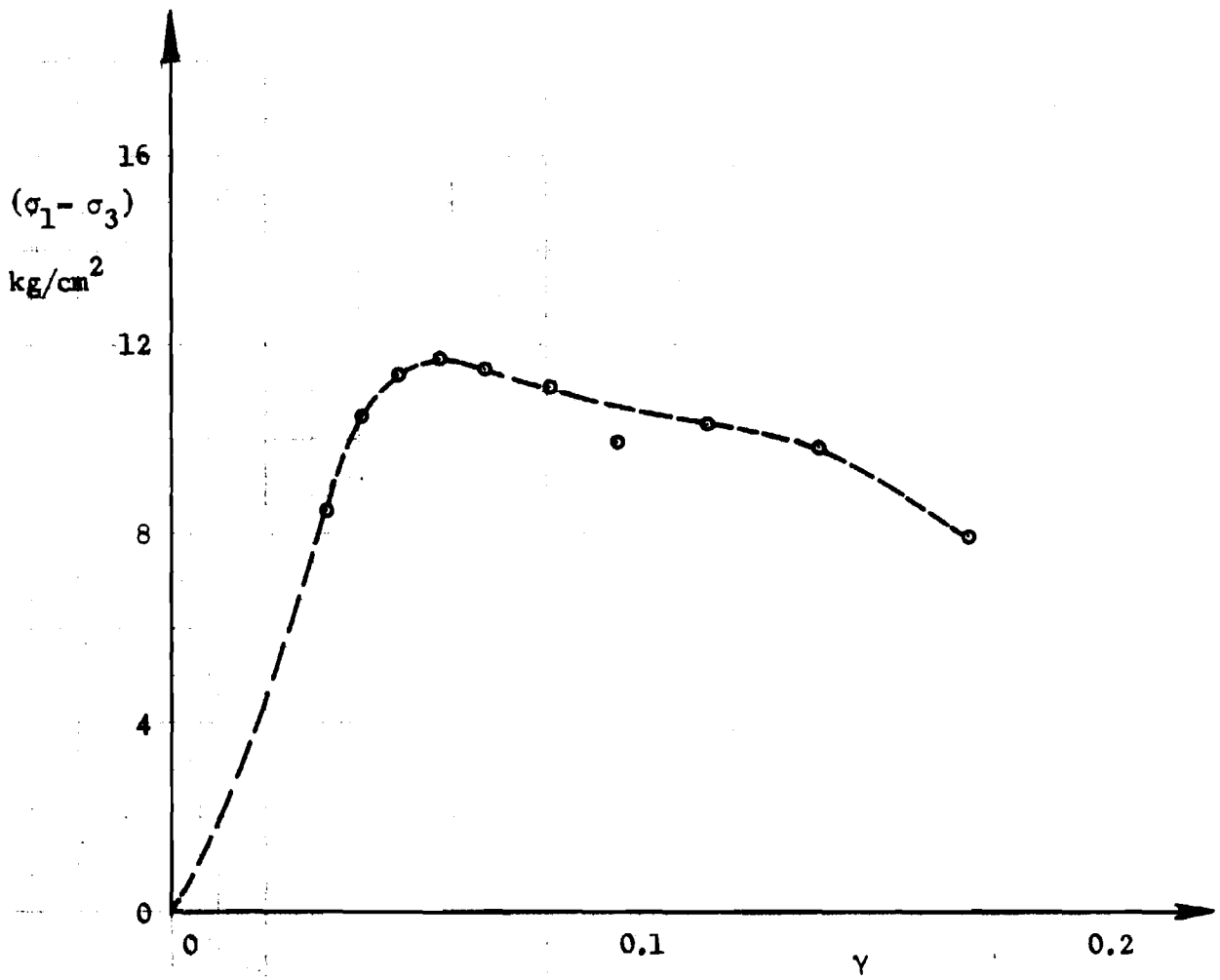

Fig. 26. Test 2 - 1. Stress-strain curve.

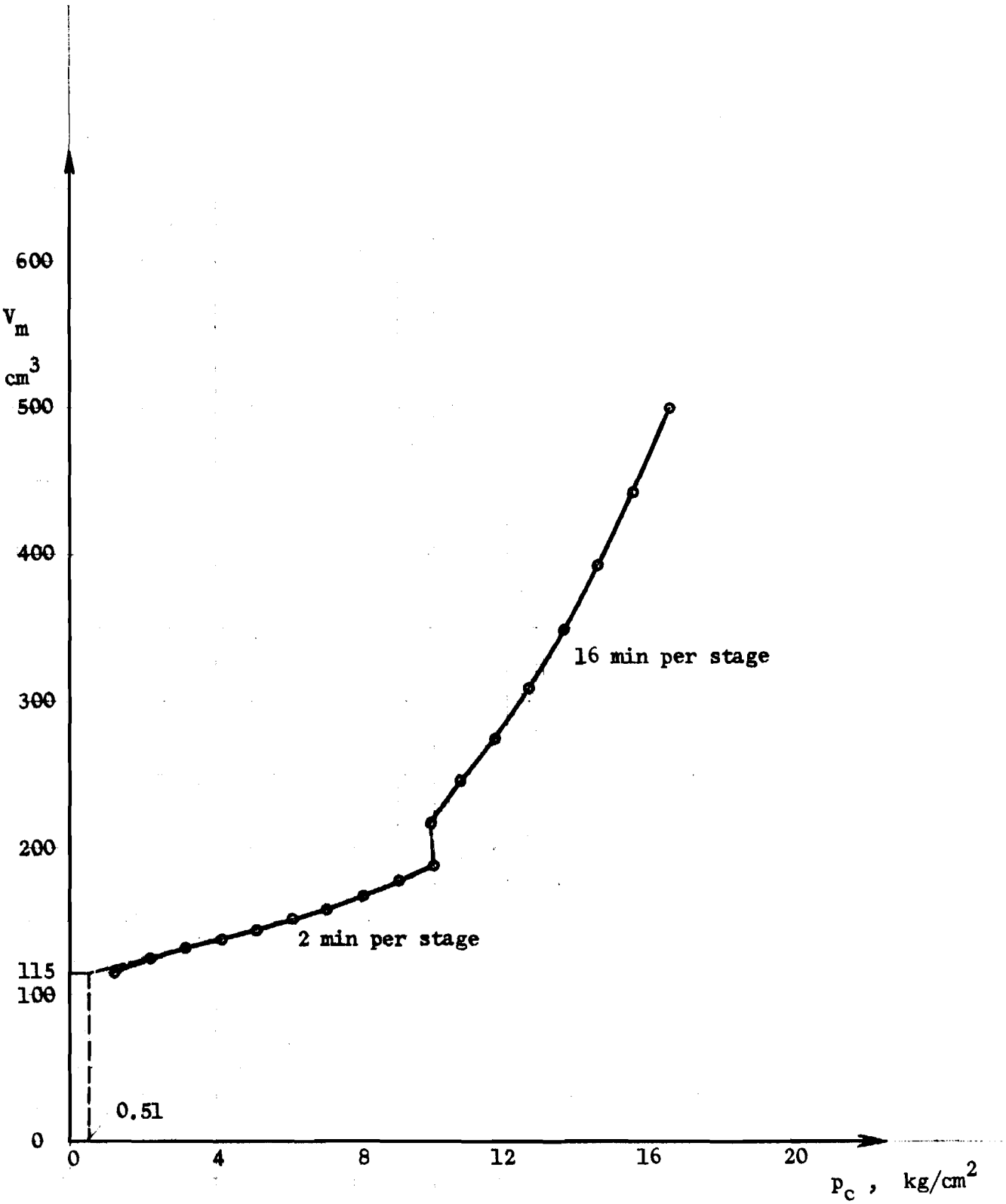

Fig. 27. Test 2 - 2. Pressuremeter curve.

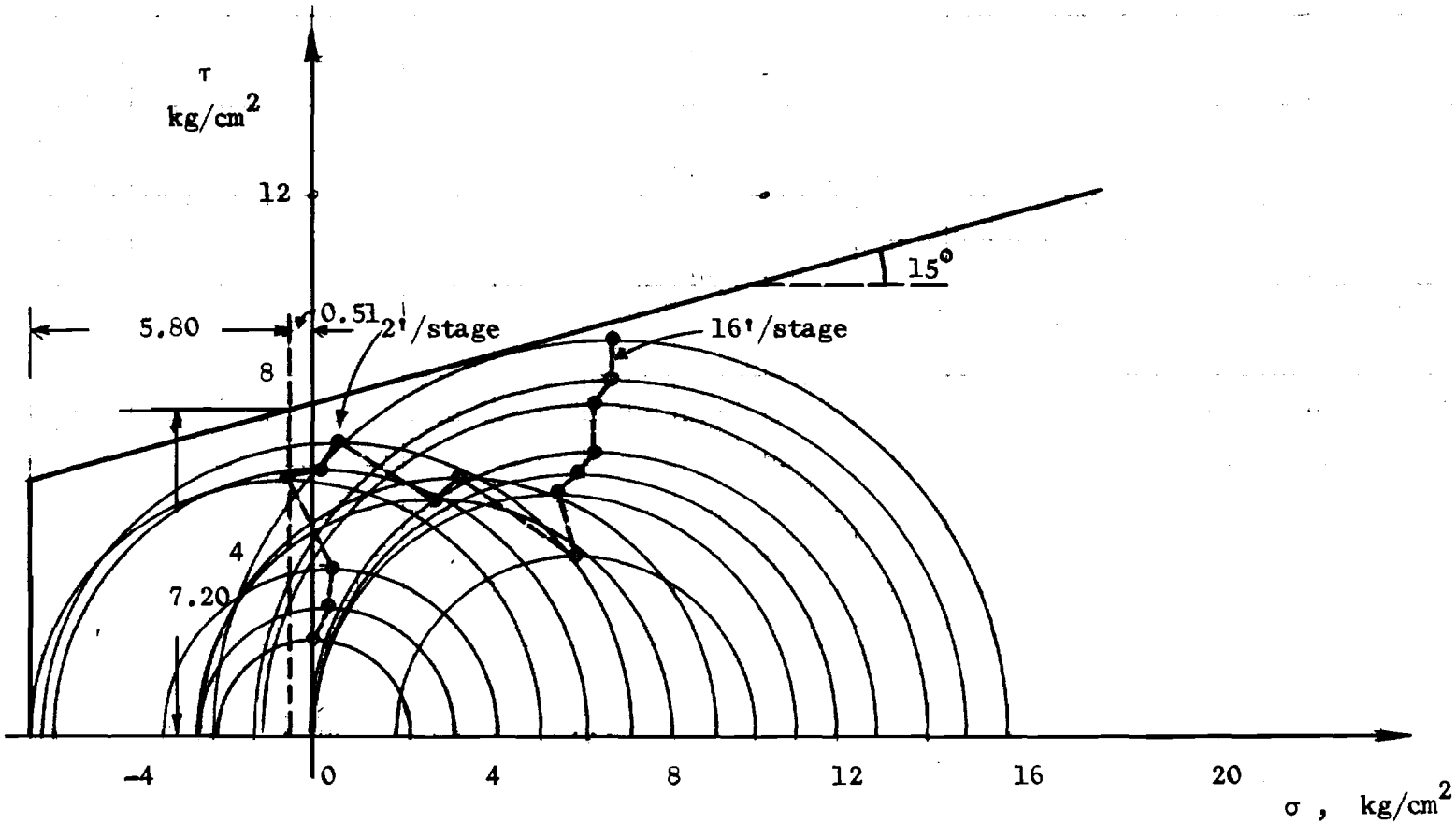

Fig. 28. Test 2 - 2. Vector curve.

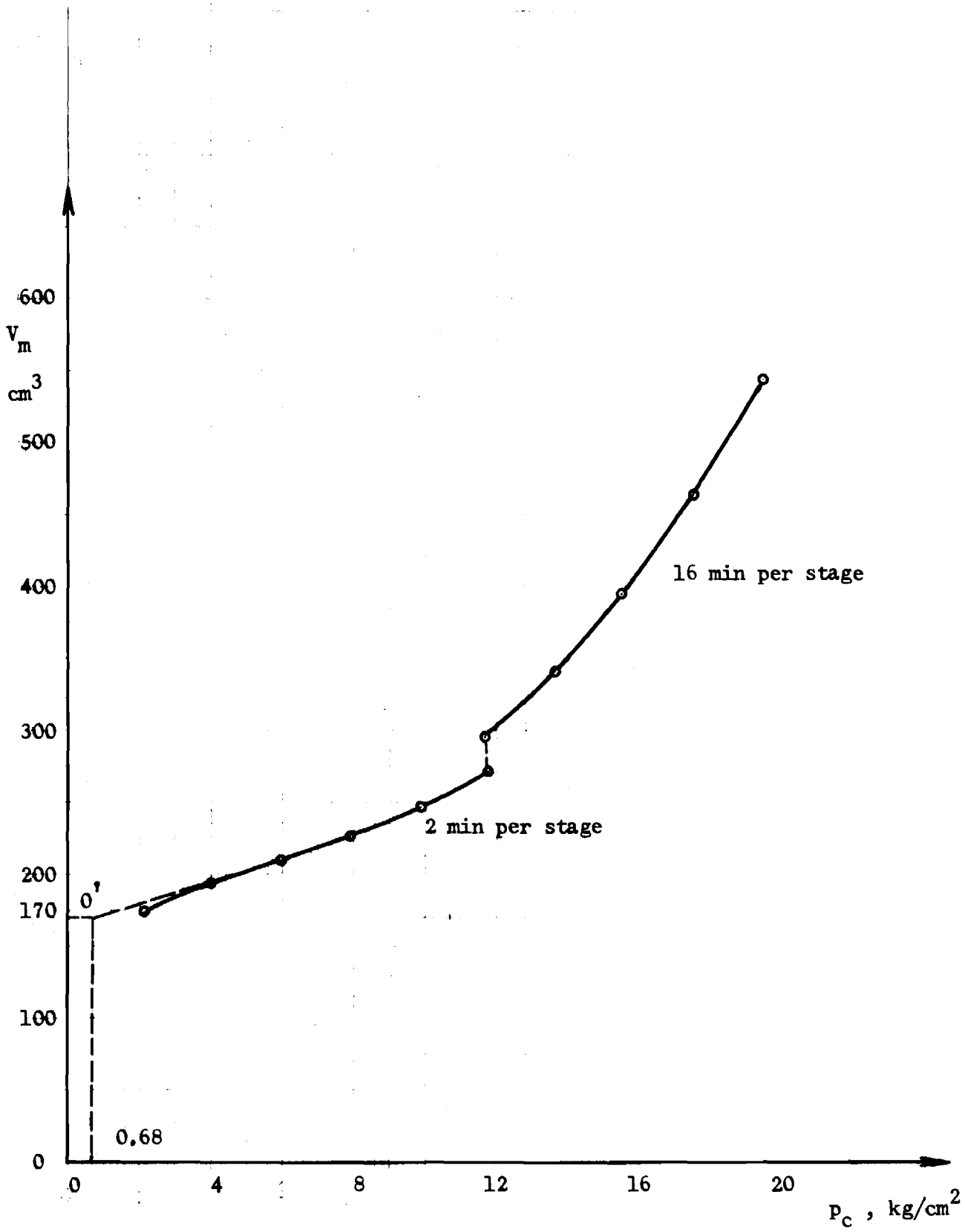

Fig. 29. Test 2 -3. Pressuremeter curve.

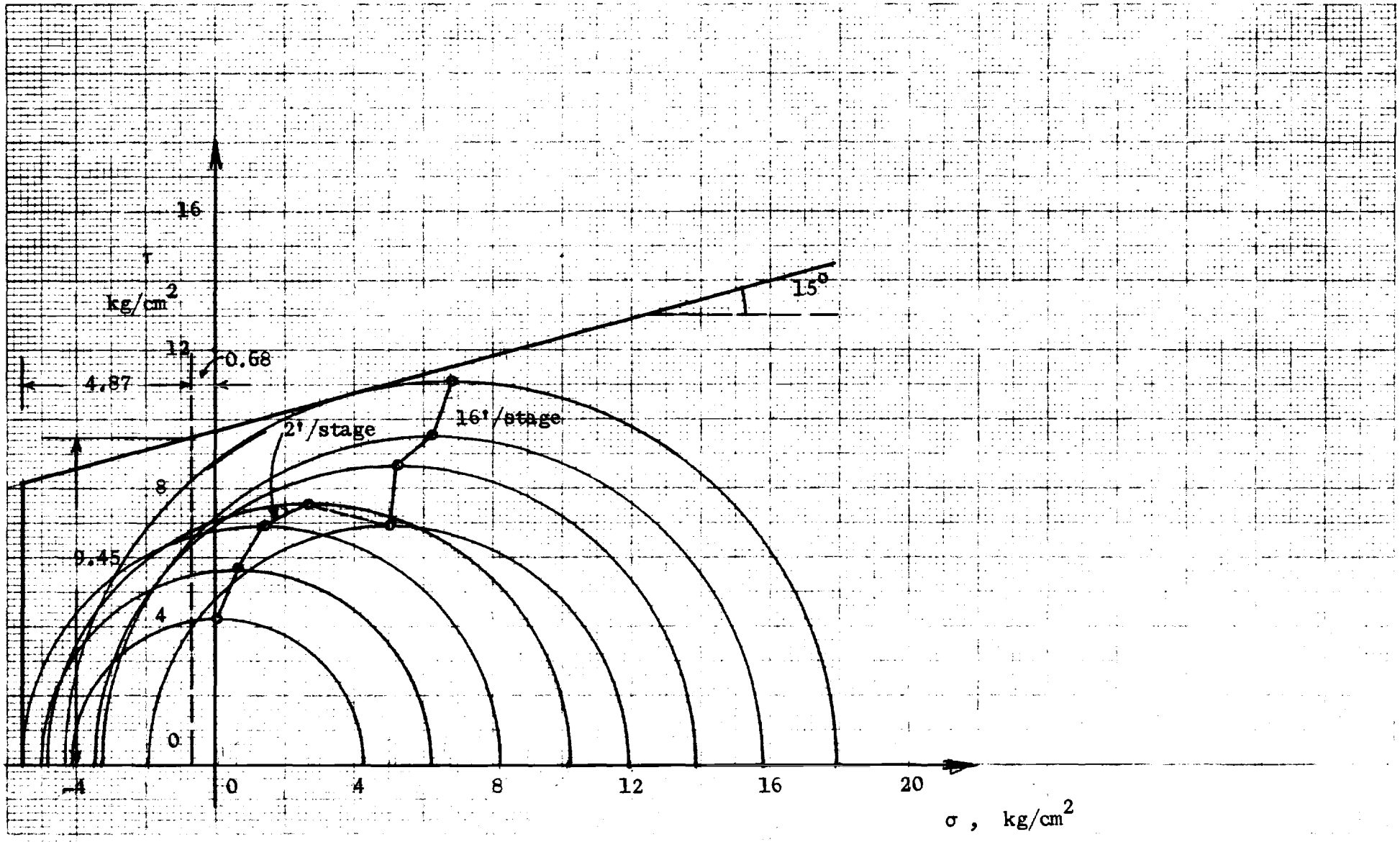

Fig. 30. Test 2 - 3. Vector curve.

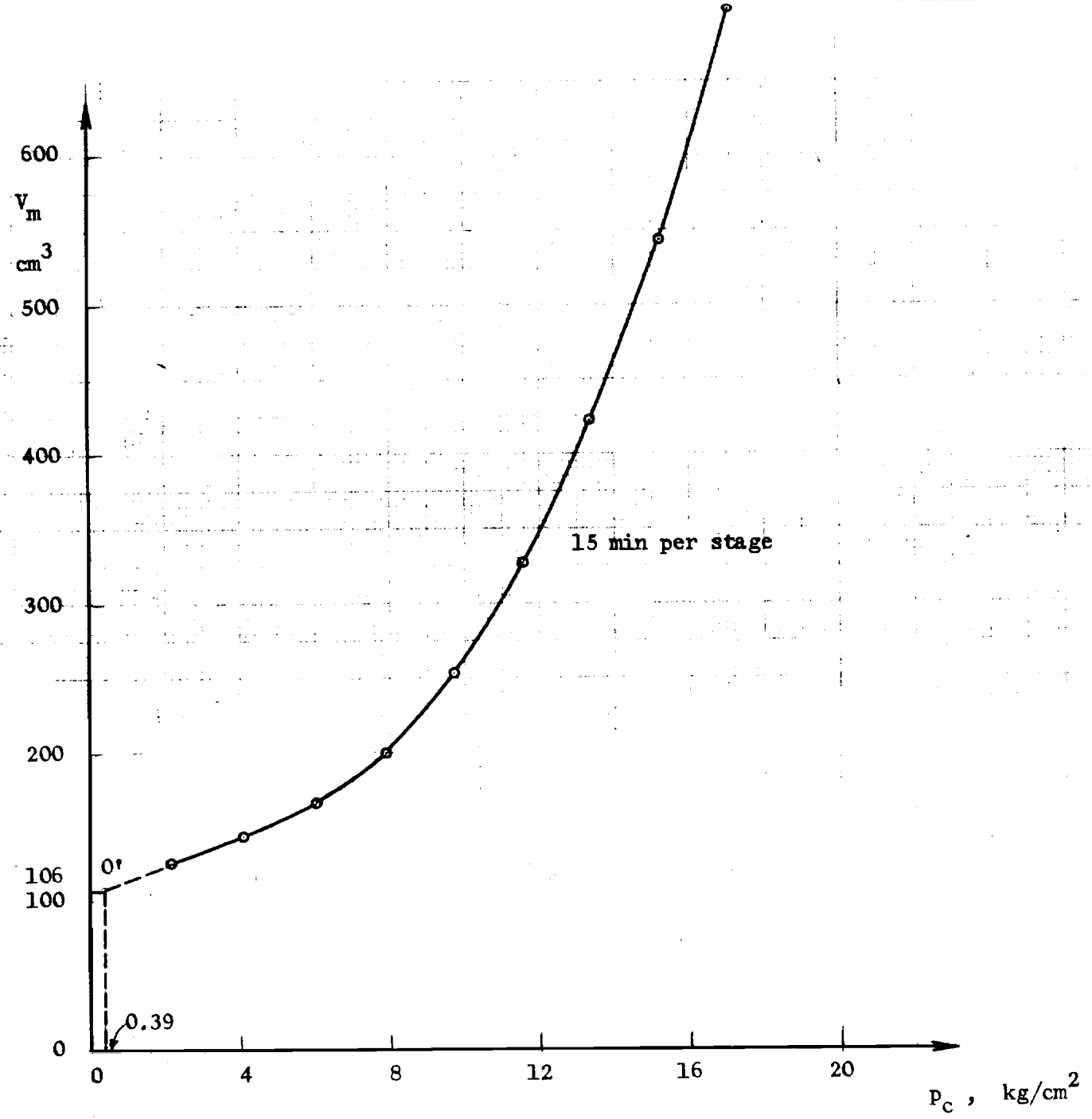

Fig. 31. Test 3 - 1. Pressuremeter curve.

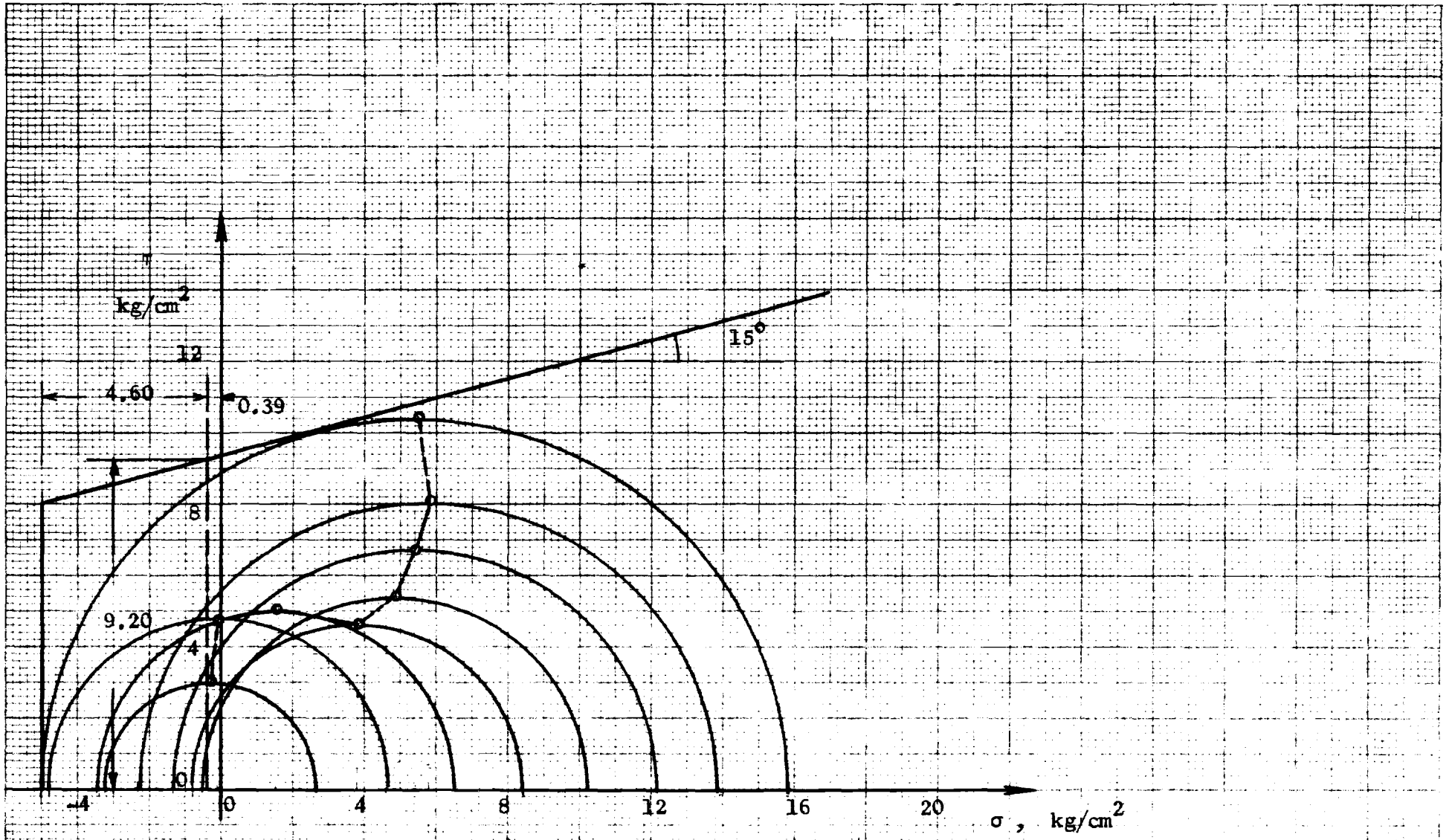

Fig. 32. Test 3 - 1. Vector curve.

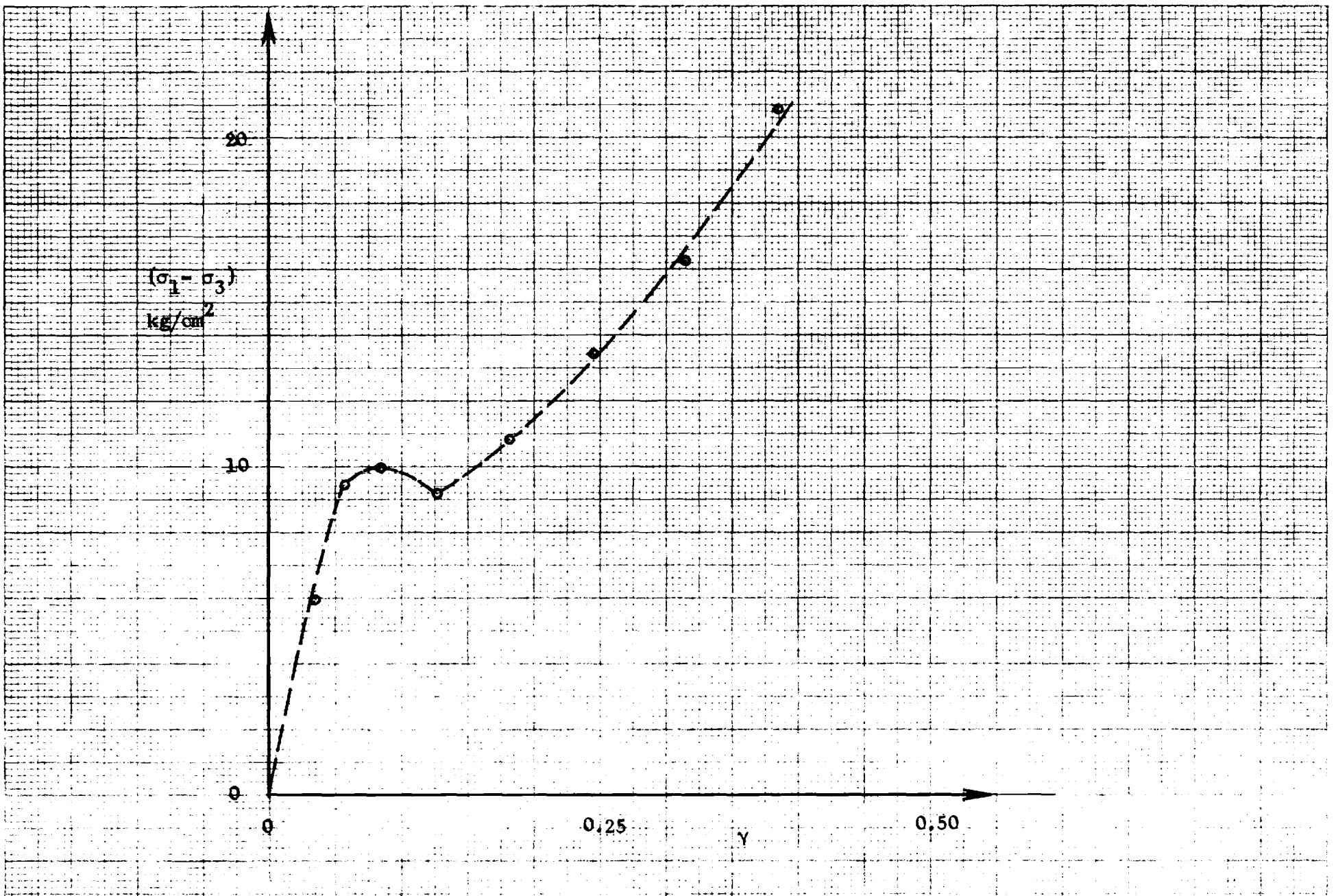

Fig. 33. Test 3 - 1. Stress-strain curve.

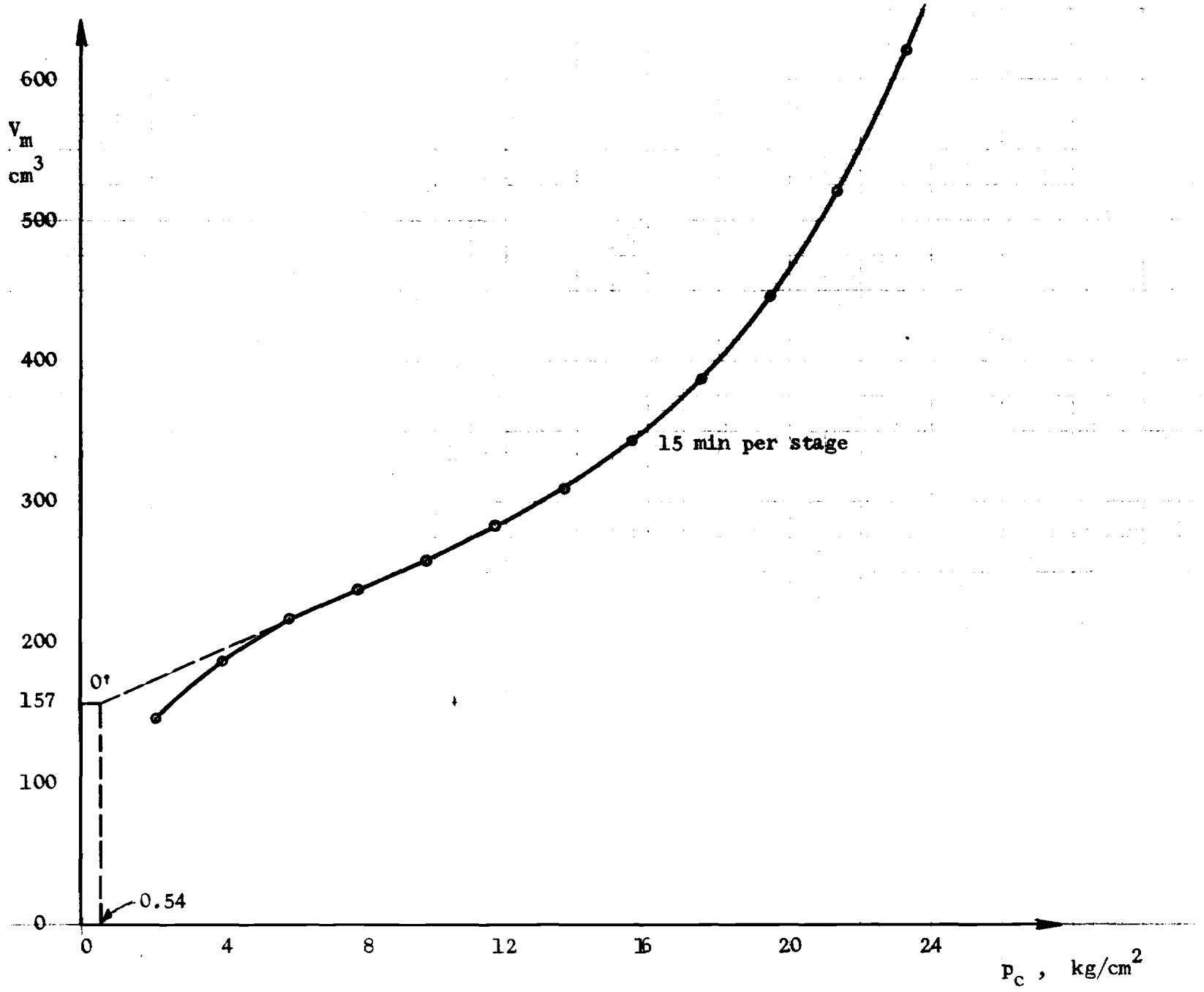

Fig. 34. Test 3 - 2. Pressuremeter curve.

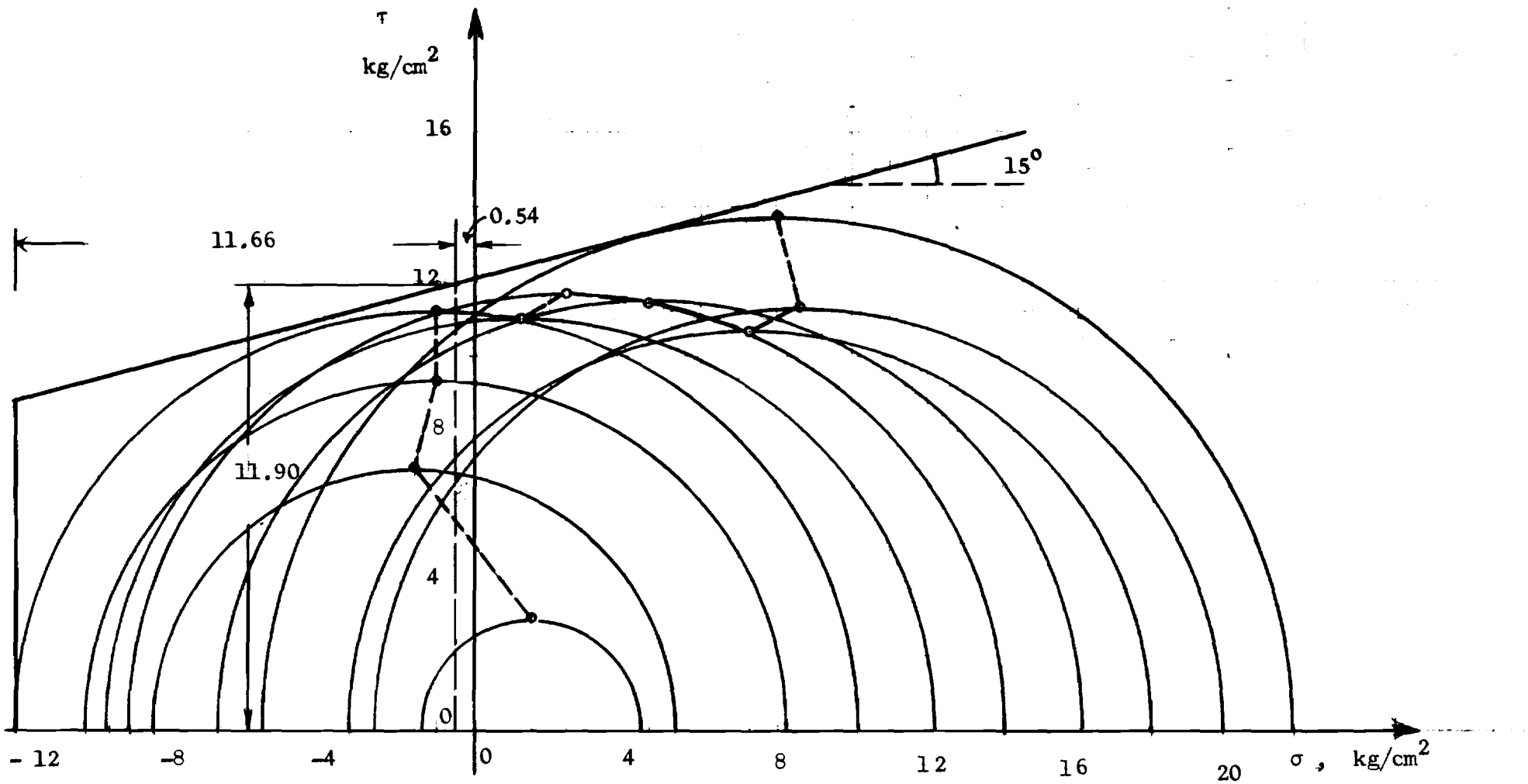

Fig. 35. Test 3 - 2. Vector curve.

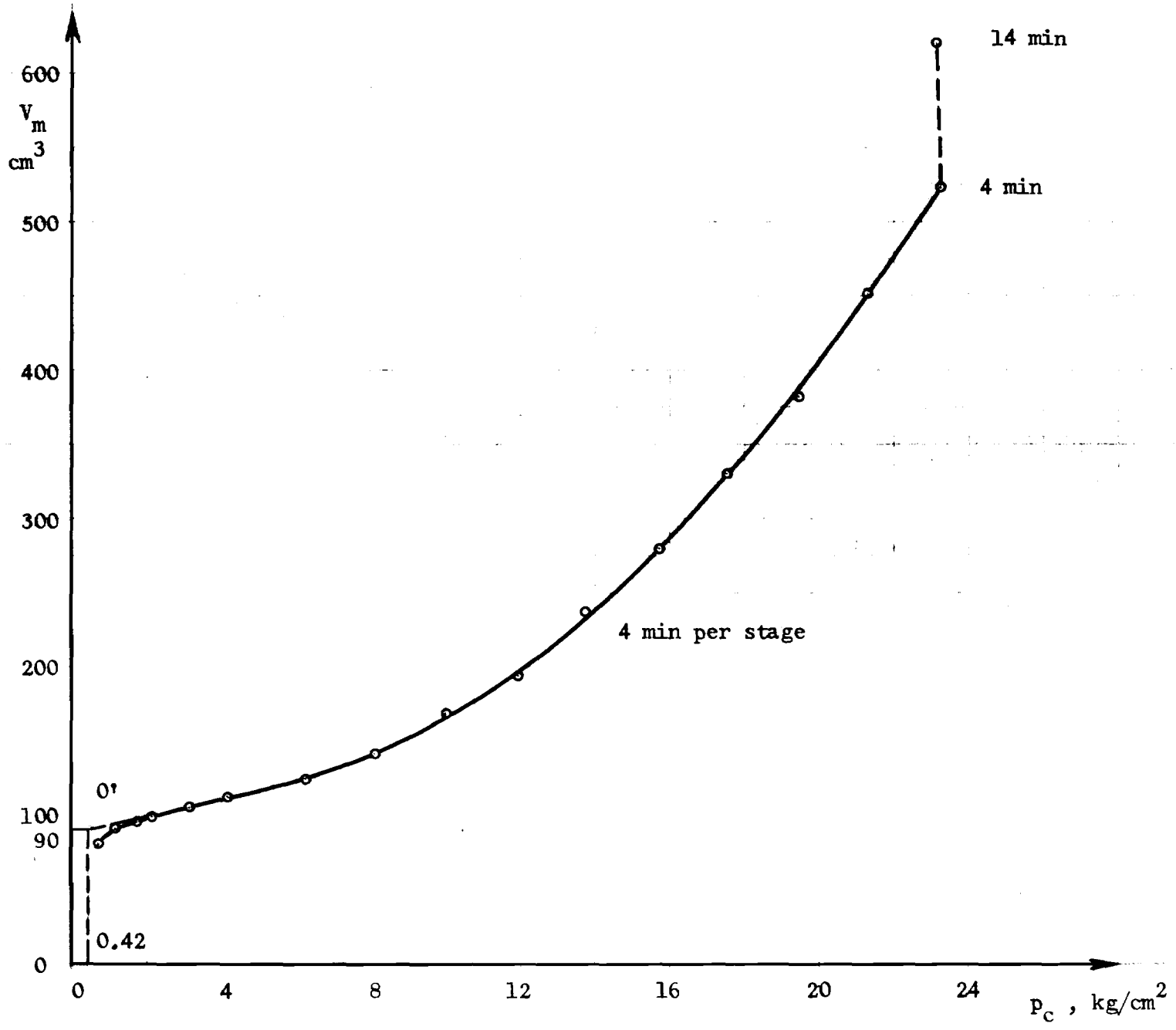

Fig. 36. Test 4 - 1. Pressuremeter curve.

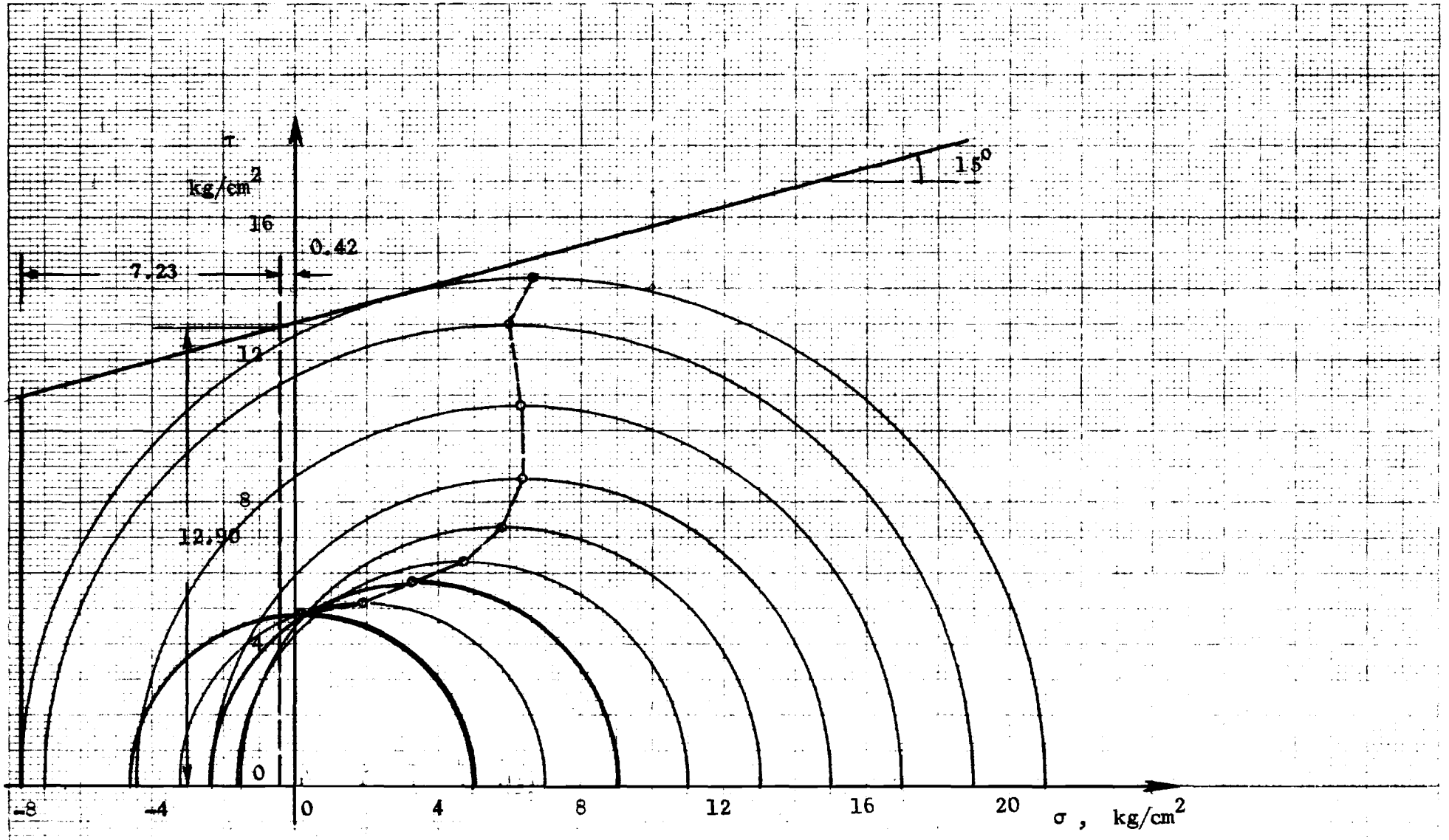

Fig. 37. Test 4 - 1. Vector curve,

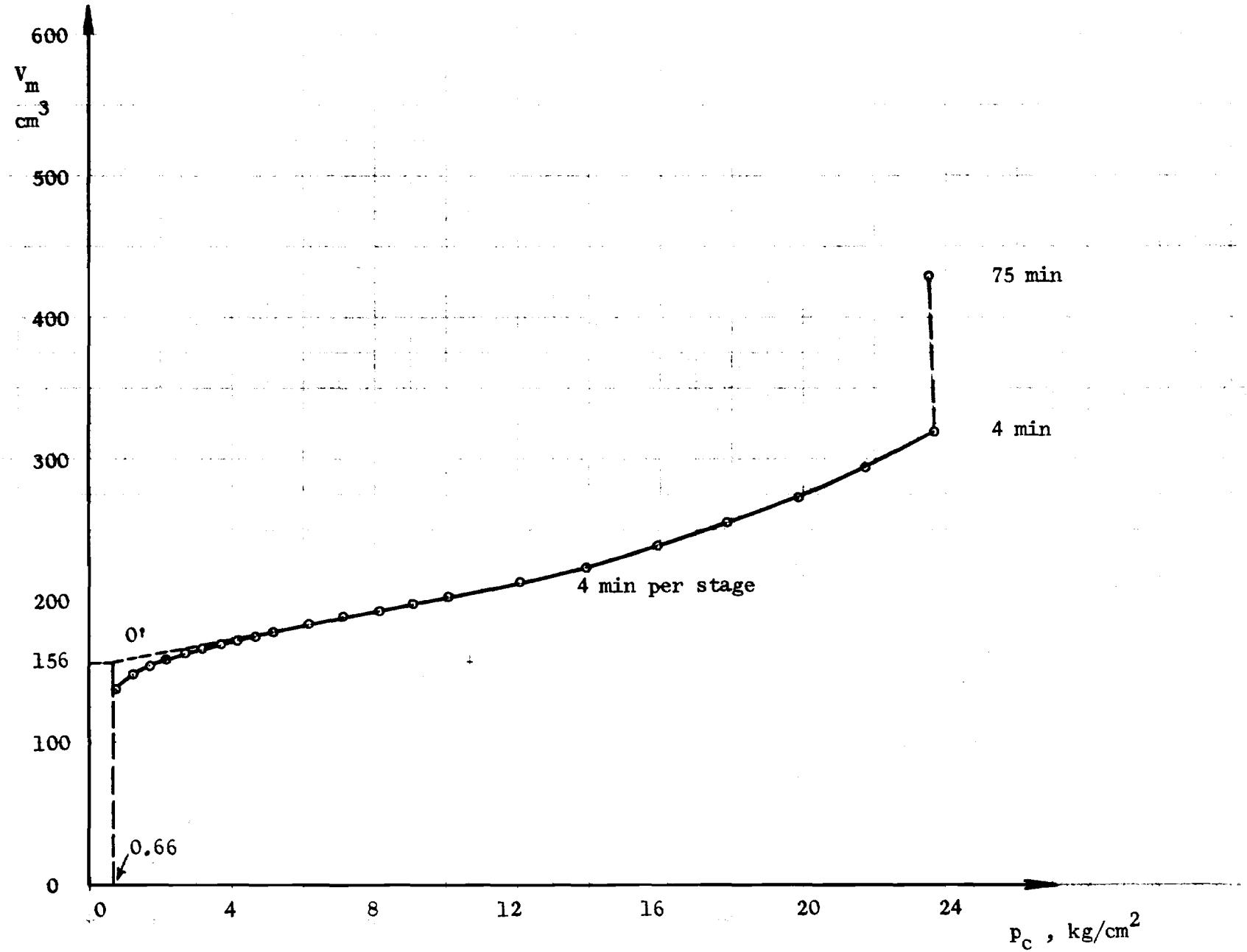

Fig. 38. Test 4 - 2. Pressuremeter curve.

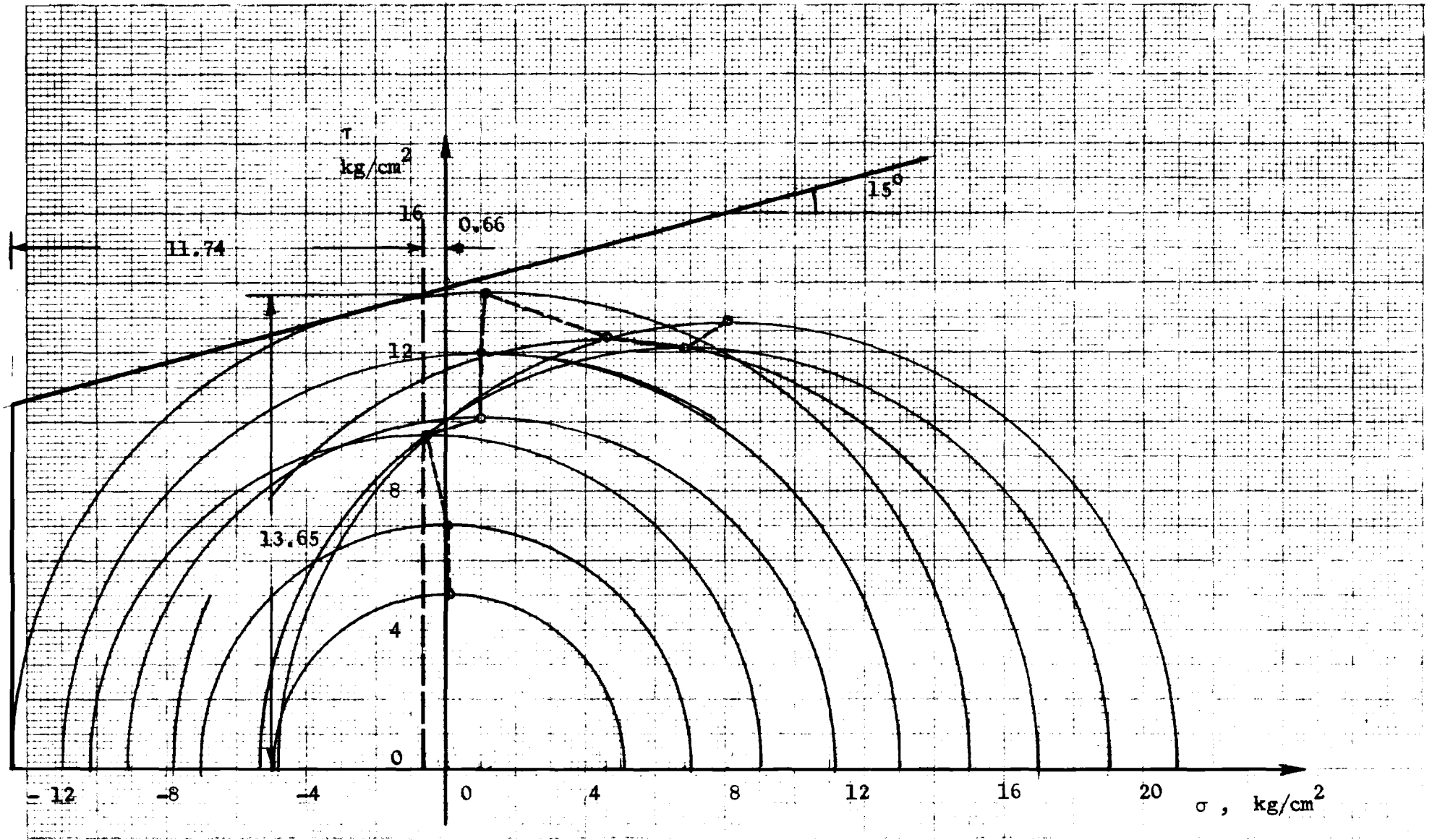

Fig. 39. Test 4 - 2. Vector curve.

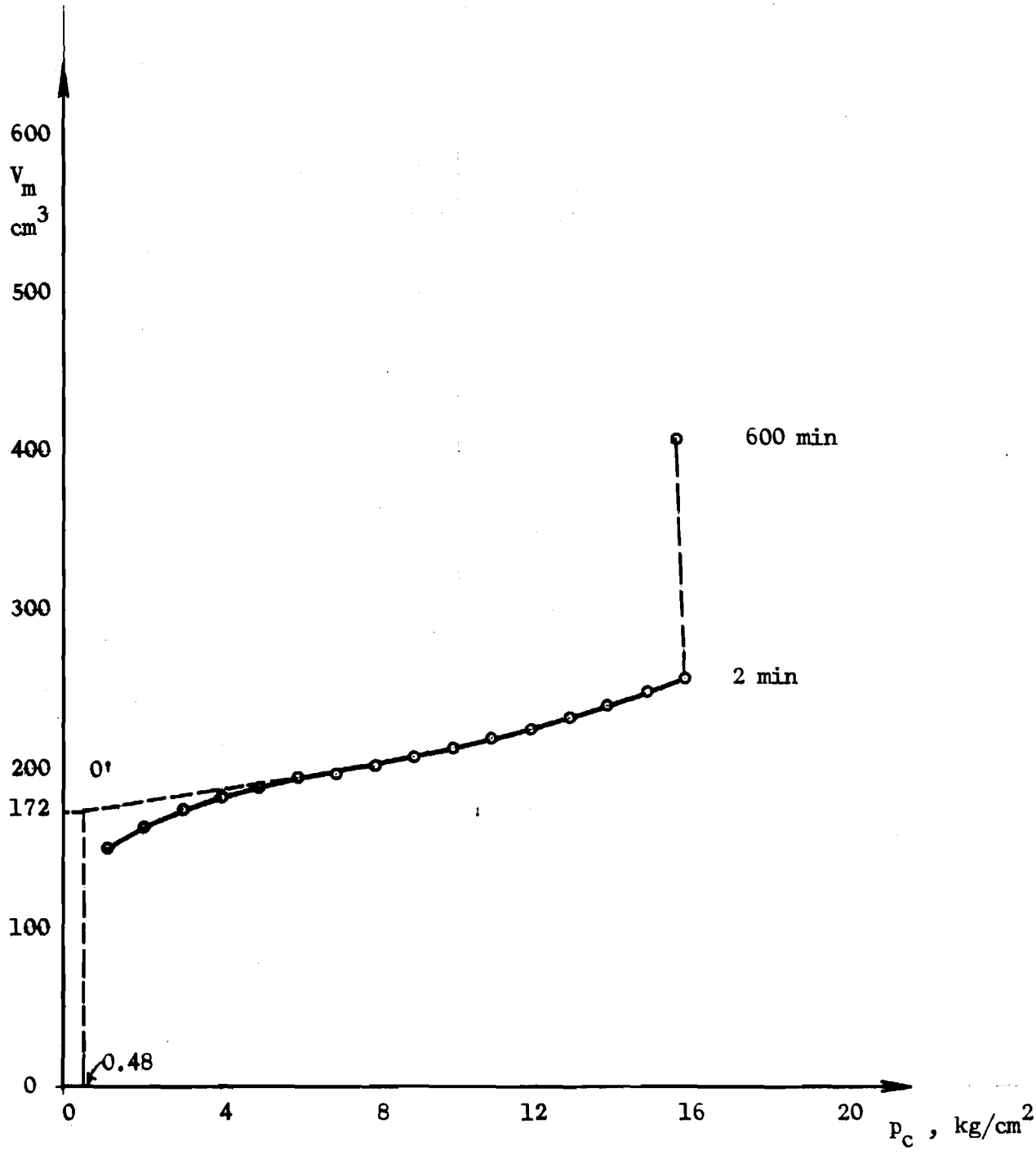

Fig. 40. Test 5 - 1. Pressuremeter curve.

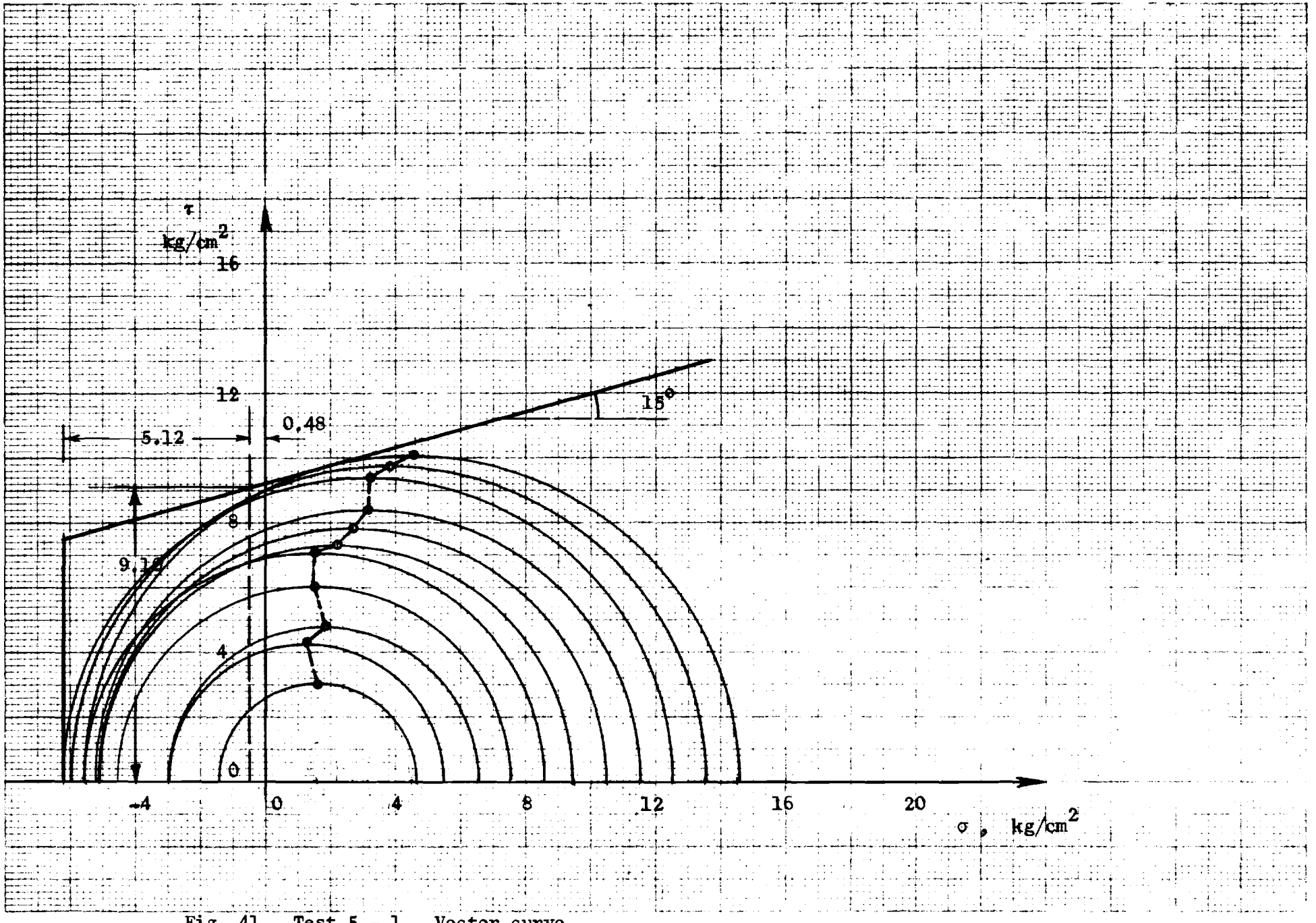

Fig. 41. Test 5 - 1. Vector curve.

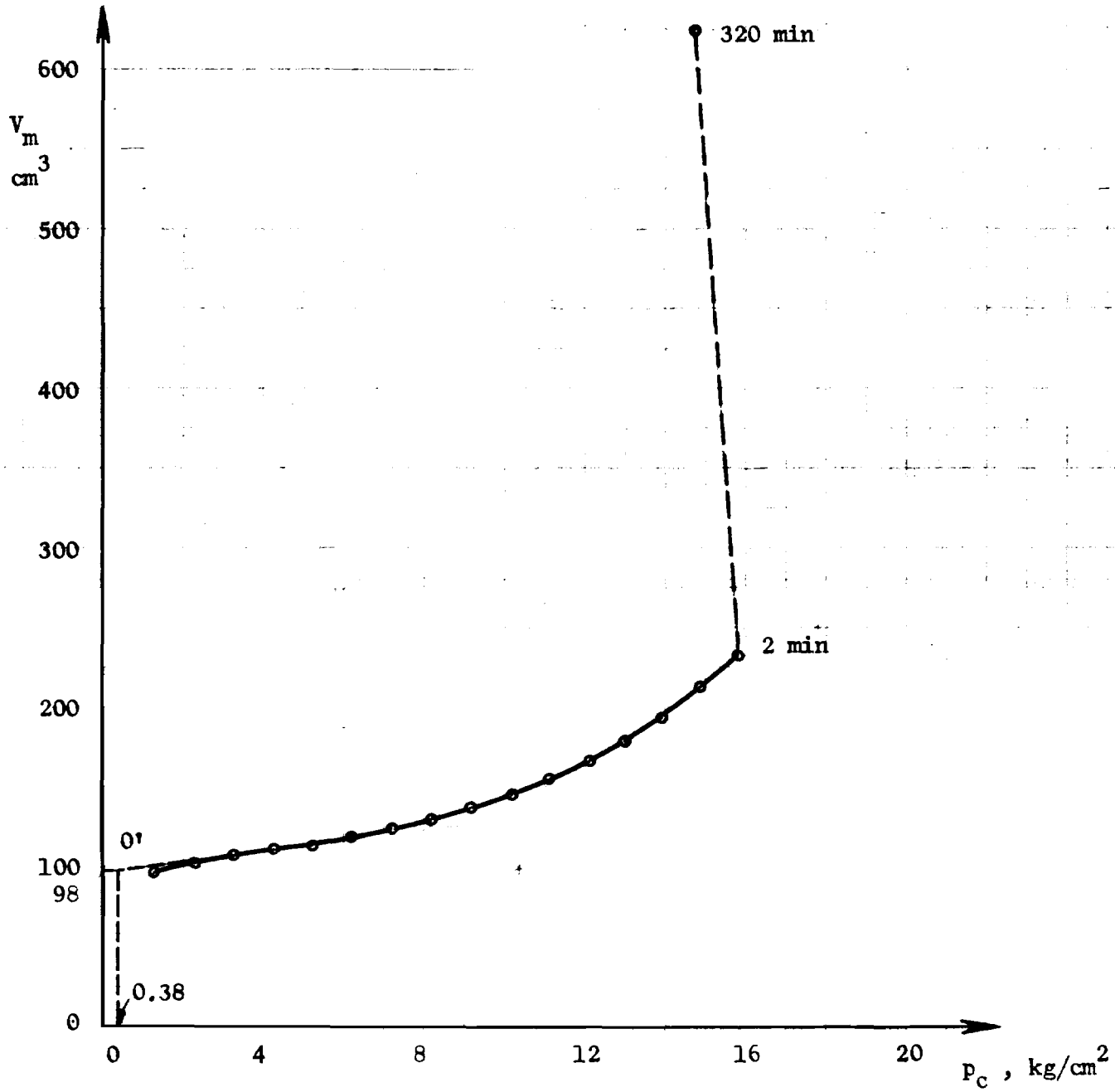

Fig. 42. Test 6 - 1. Pressuremeter curve.

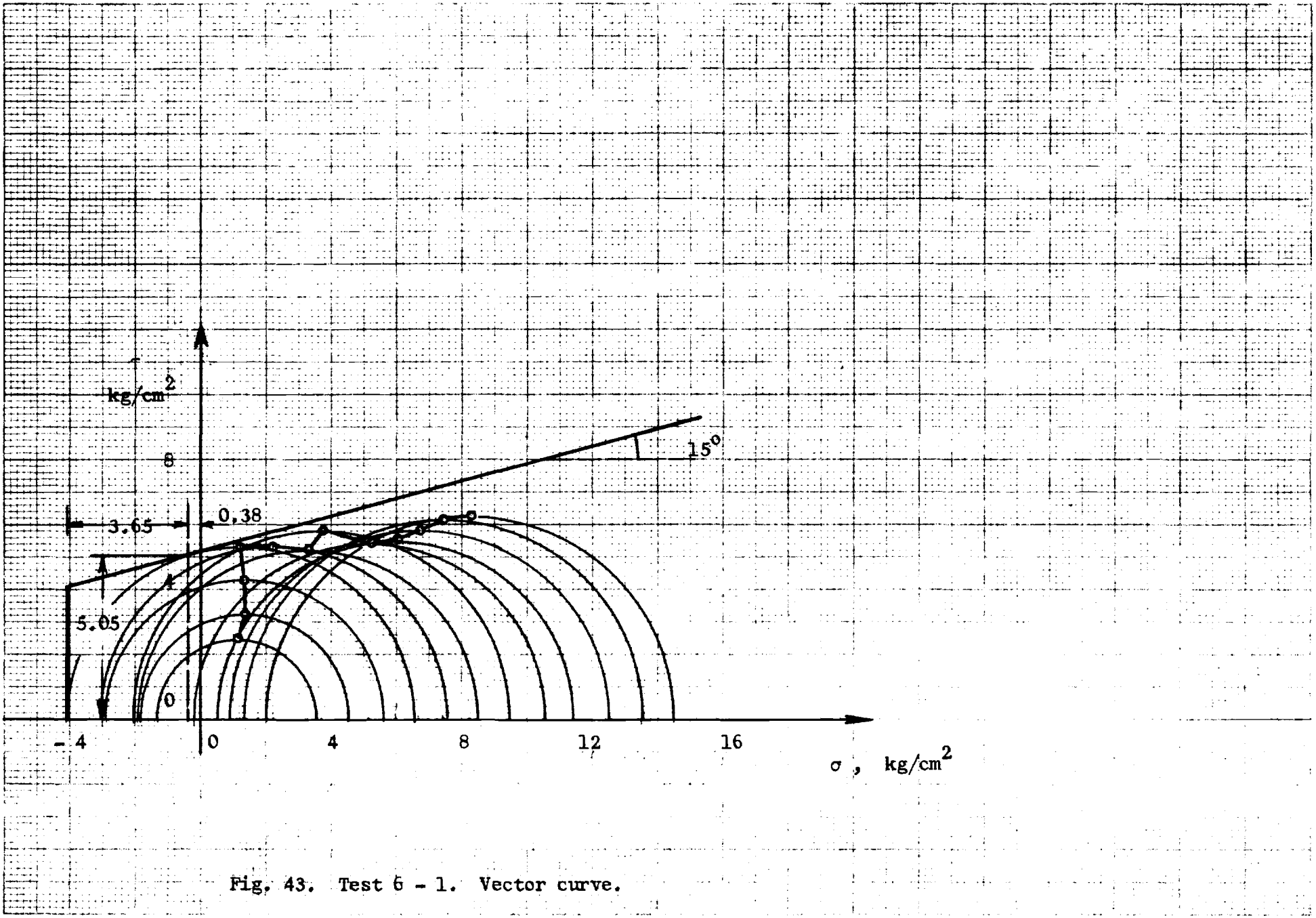

Fig. 43. Test 6 - 1. Vector curve.

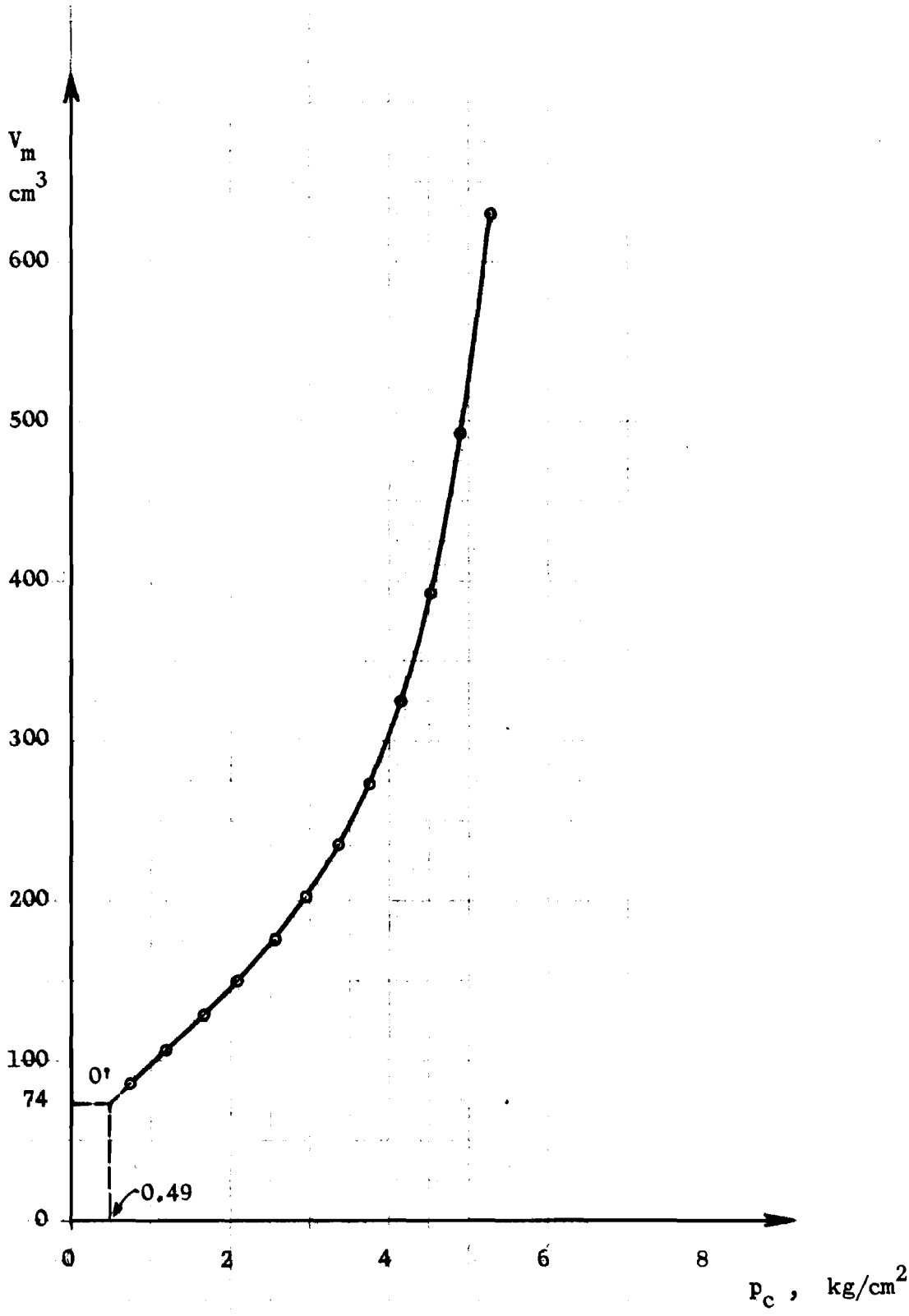

Fig. 44. Test 8 - 1. Pressuremeter curve. (Unfrozen soil).

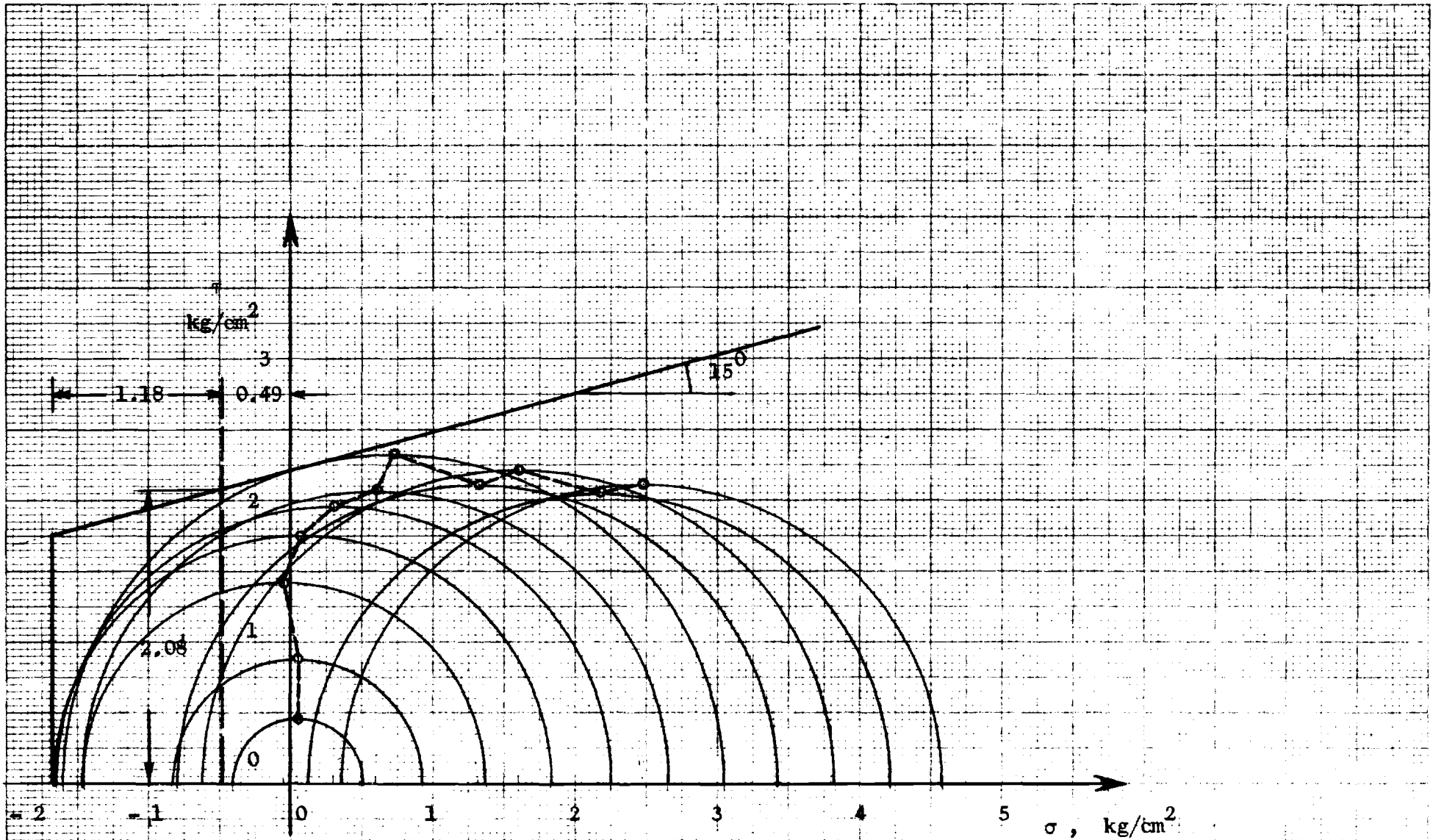

Fig. 45. Test 8 - 1. Vector curve. (Unfrozen soil).

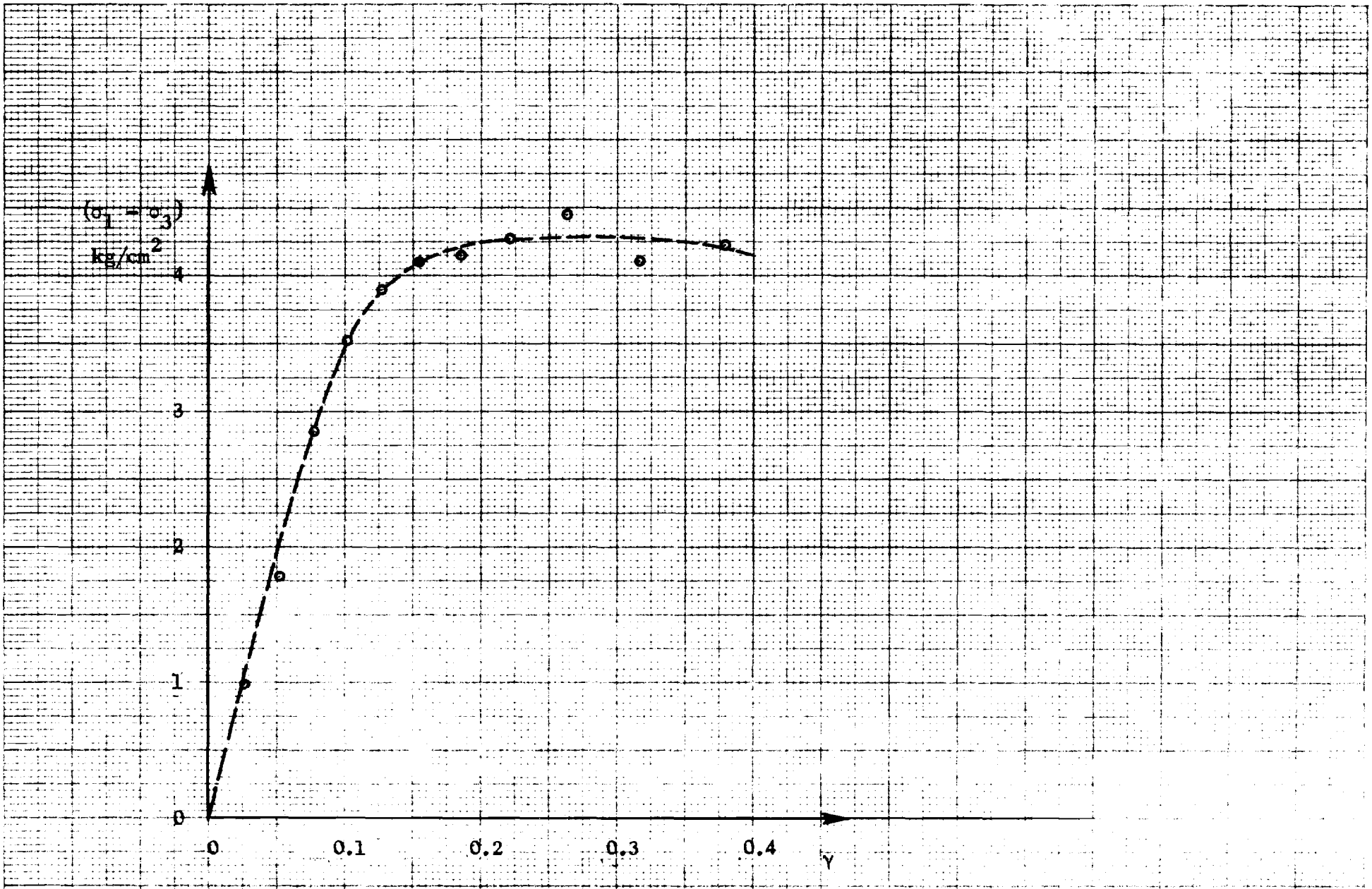

Fig. 46. Test 8 - 1. Stress-strain curve. (Unfrozen soil).

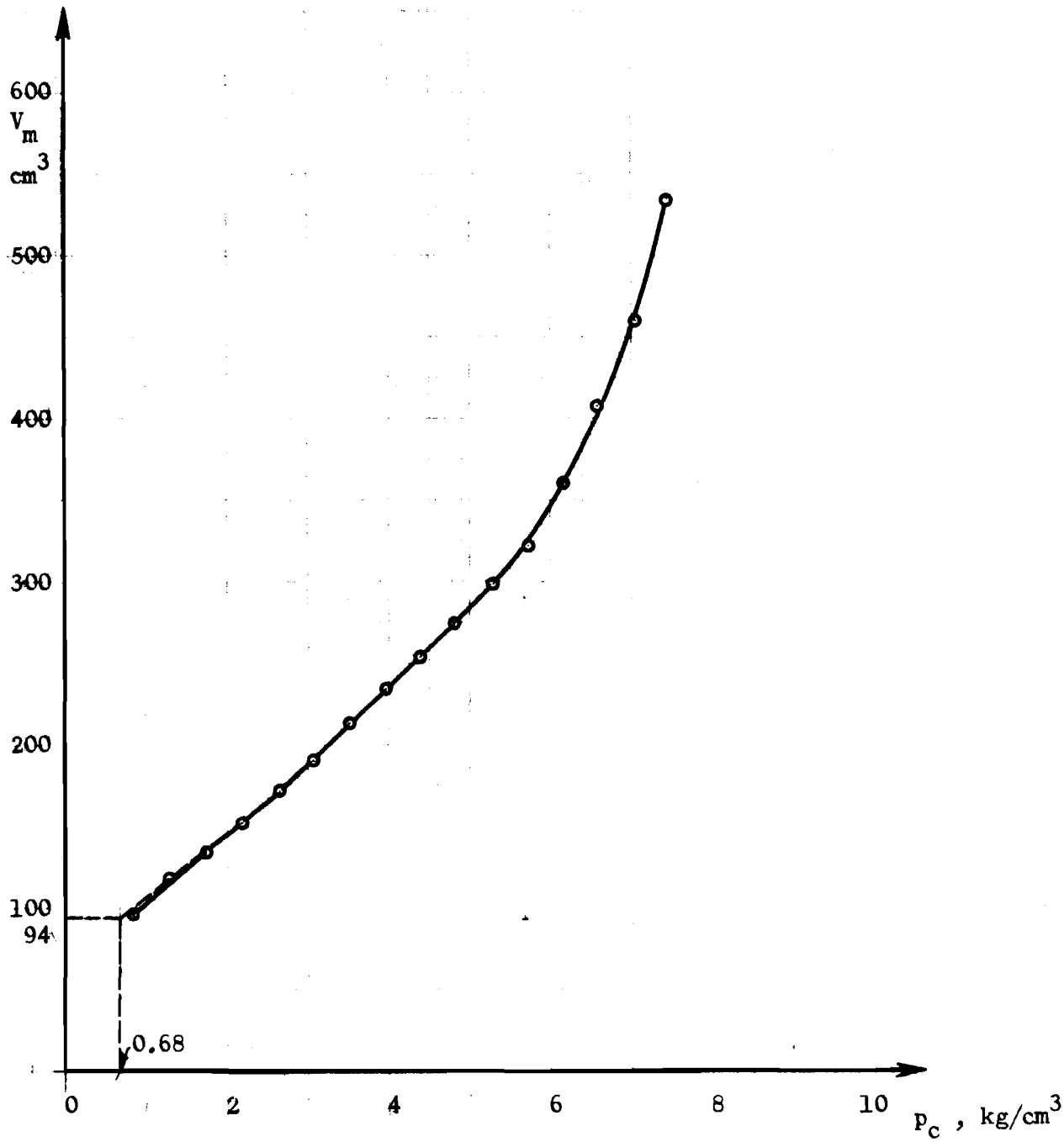

Fig. 47. Test 8 - 2. Pressuremeter curve (Unfrozen soil).

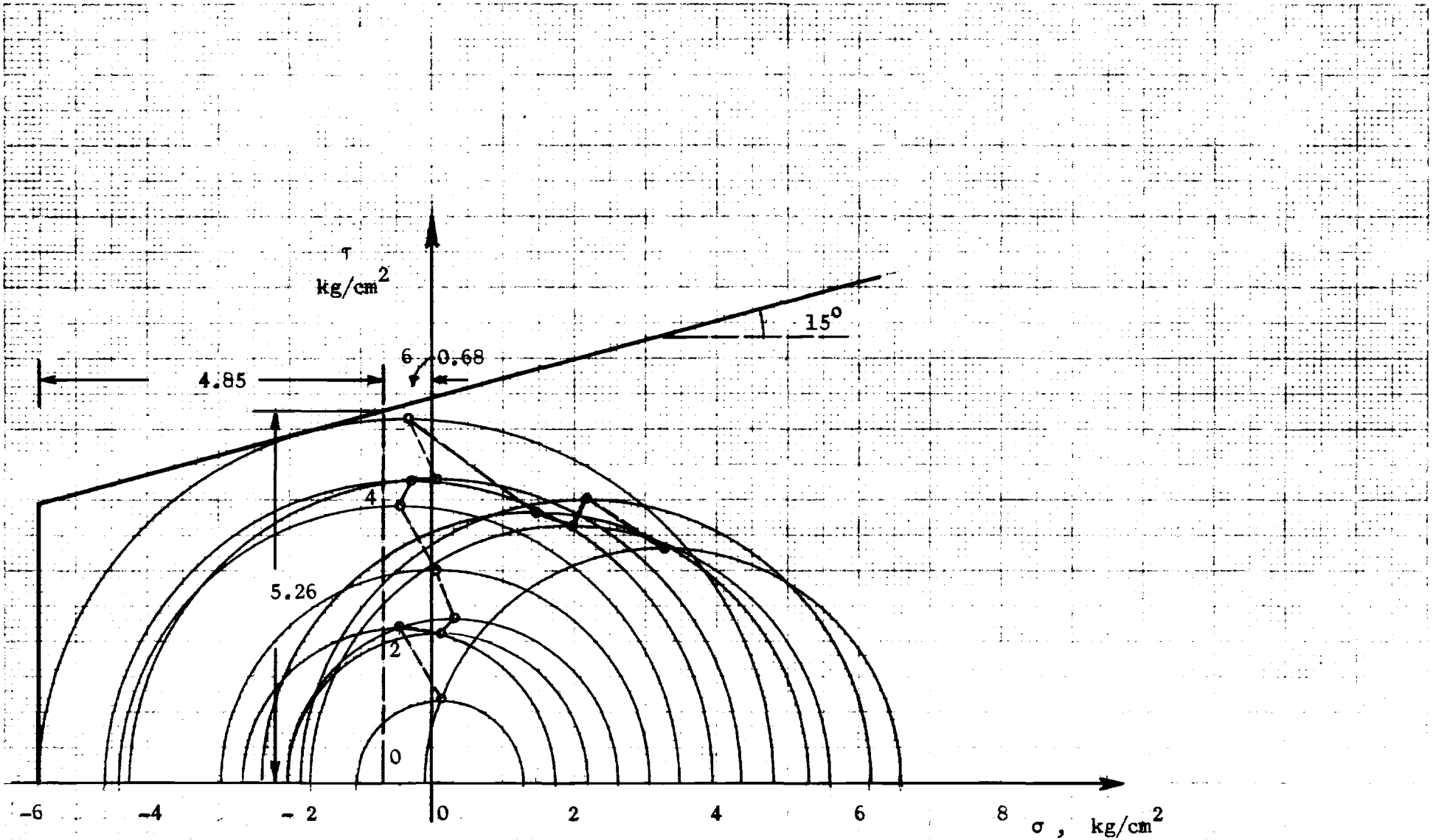

Fig. 48. Test 8 - 2. Vector curve (Unfrozen soil).

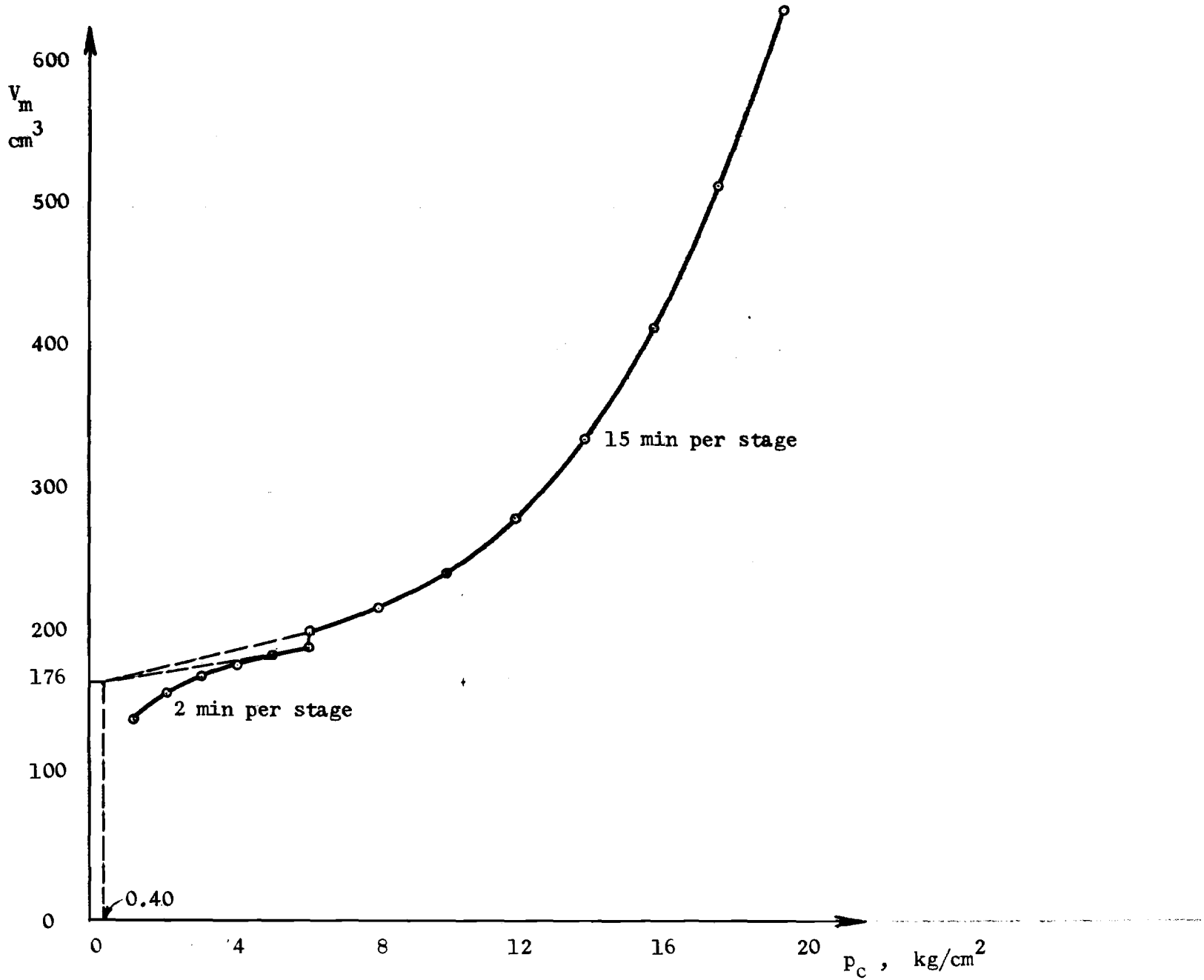

Fig. 49. Test 9 - 1. Pressuremeter curve.

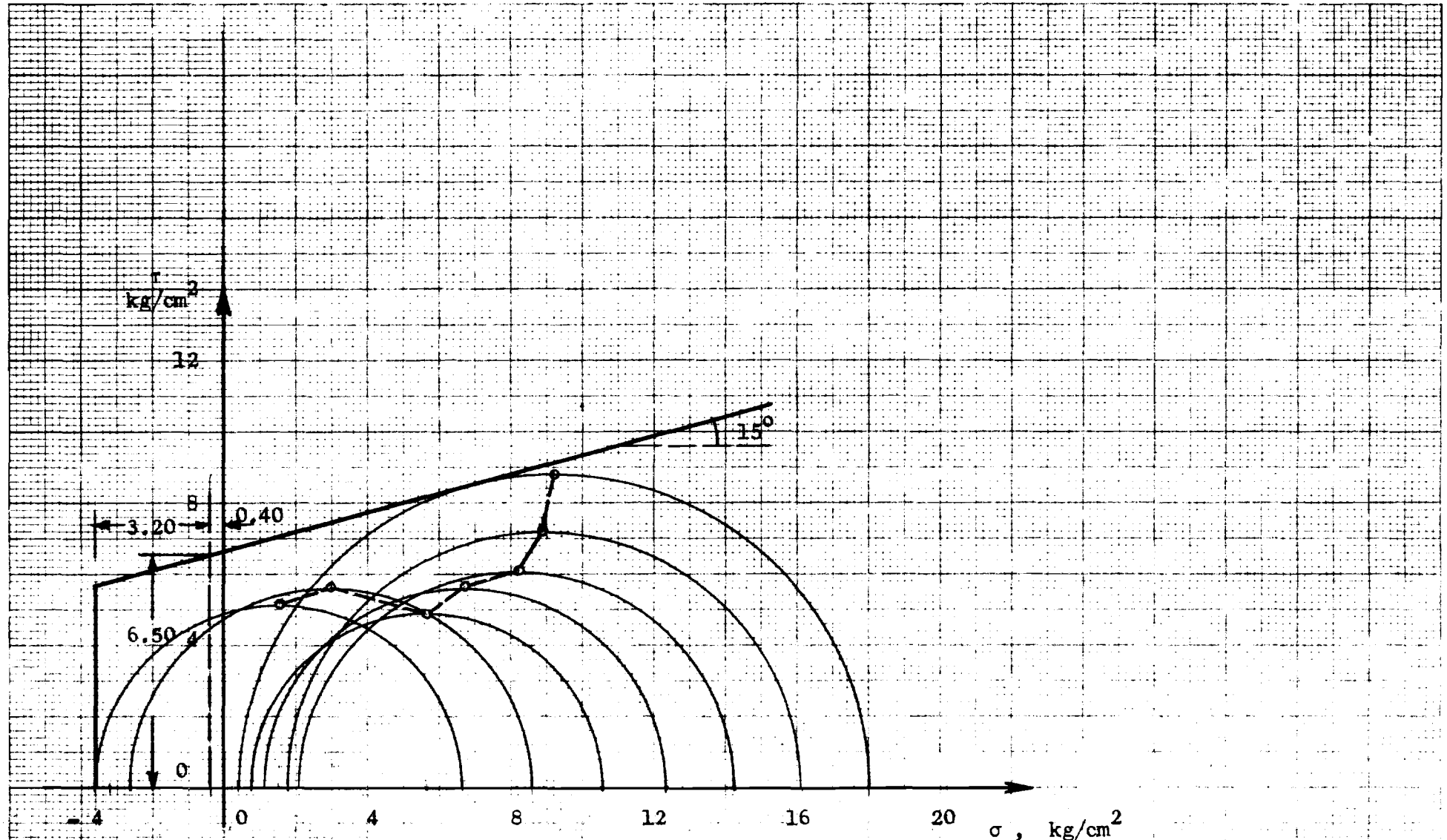

Fig. 50. Test 9 - 1. Vector curve.

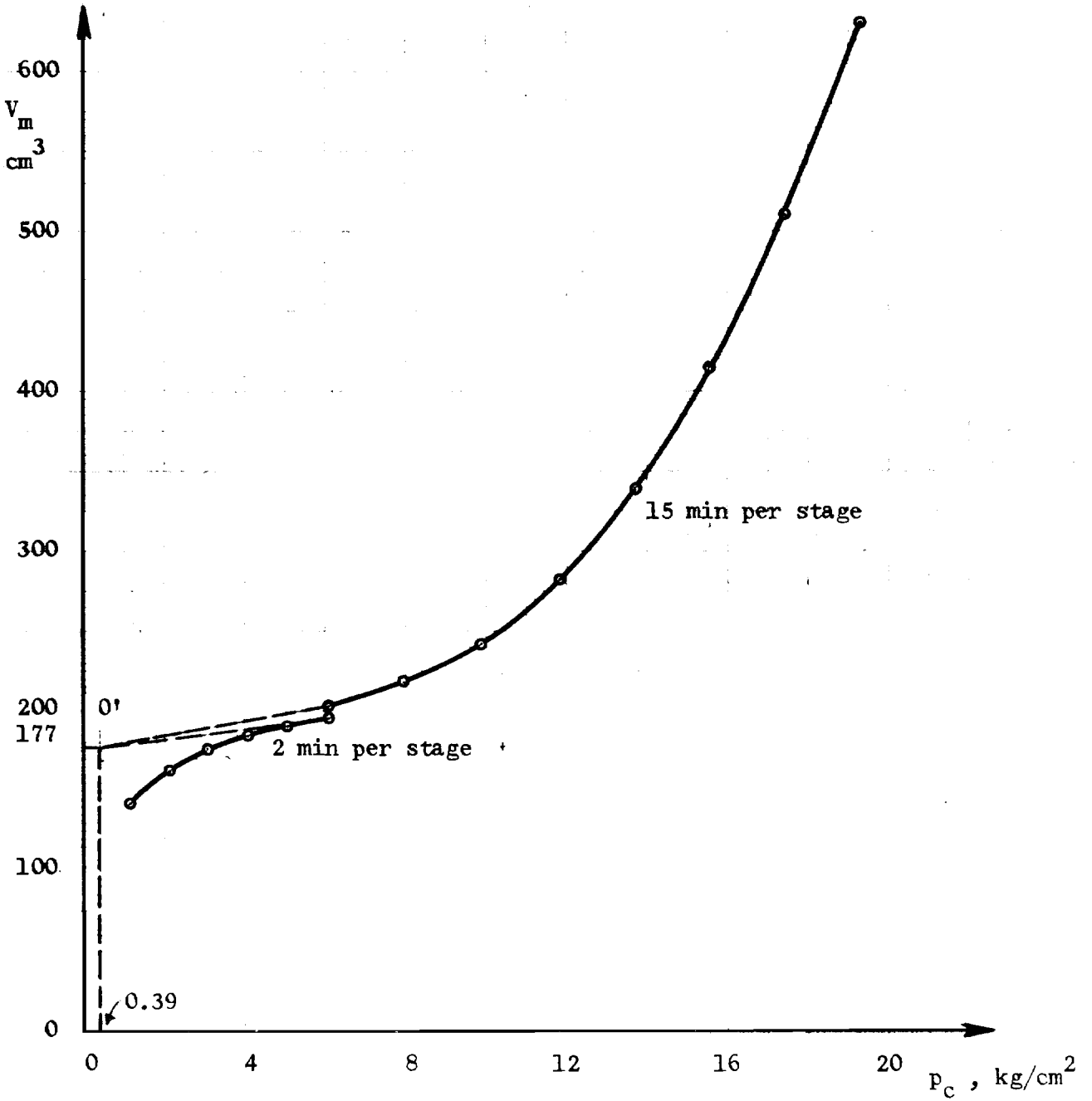

Fig. 51. Test 10 - 1. Pressuremeter curve.

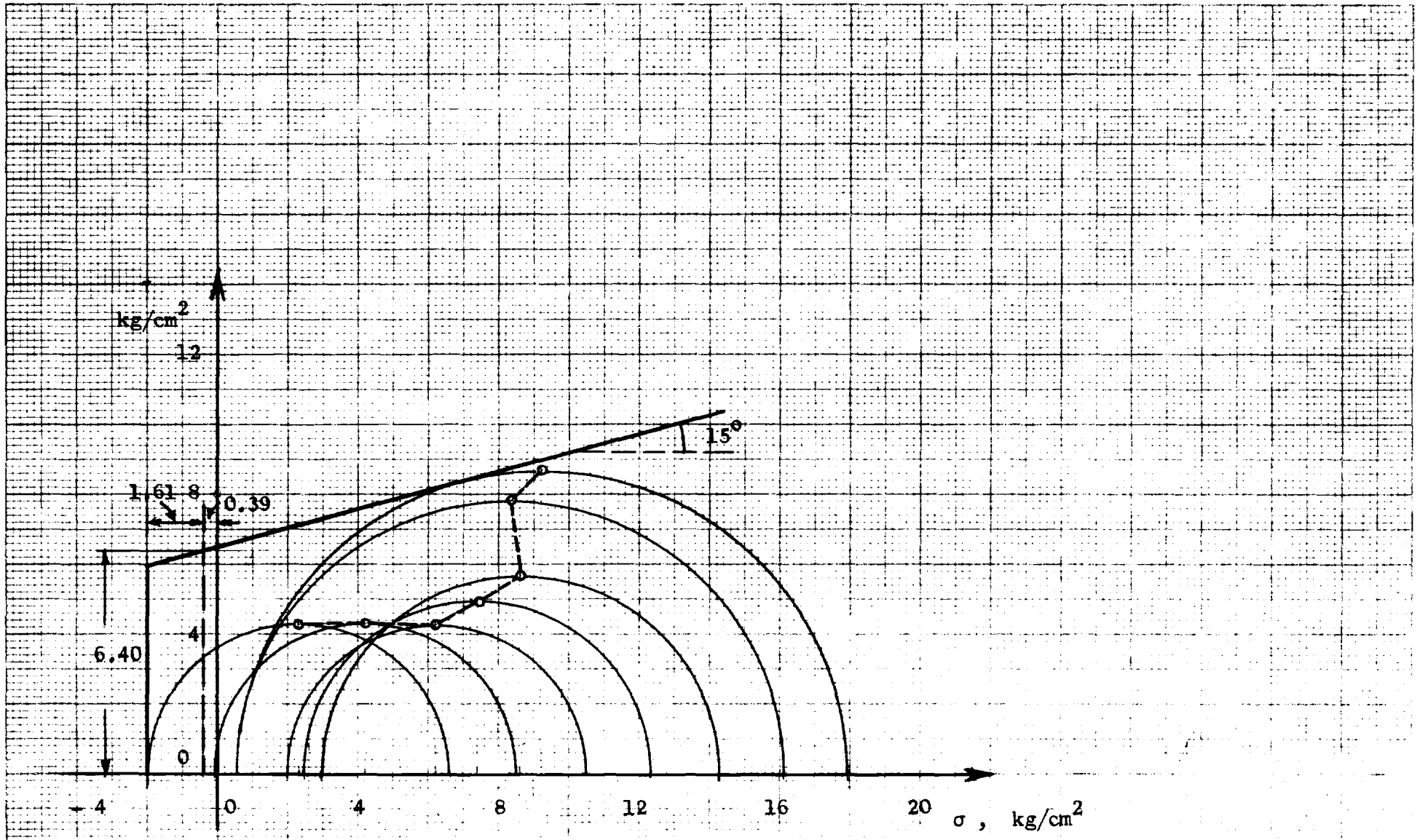

Fig. 52. Test 10 - 1. Vector curve.

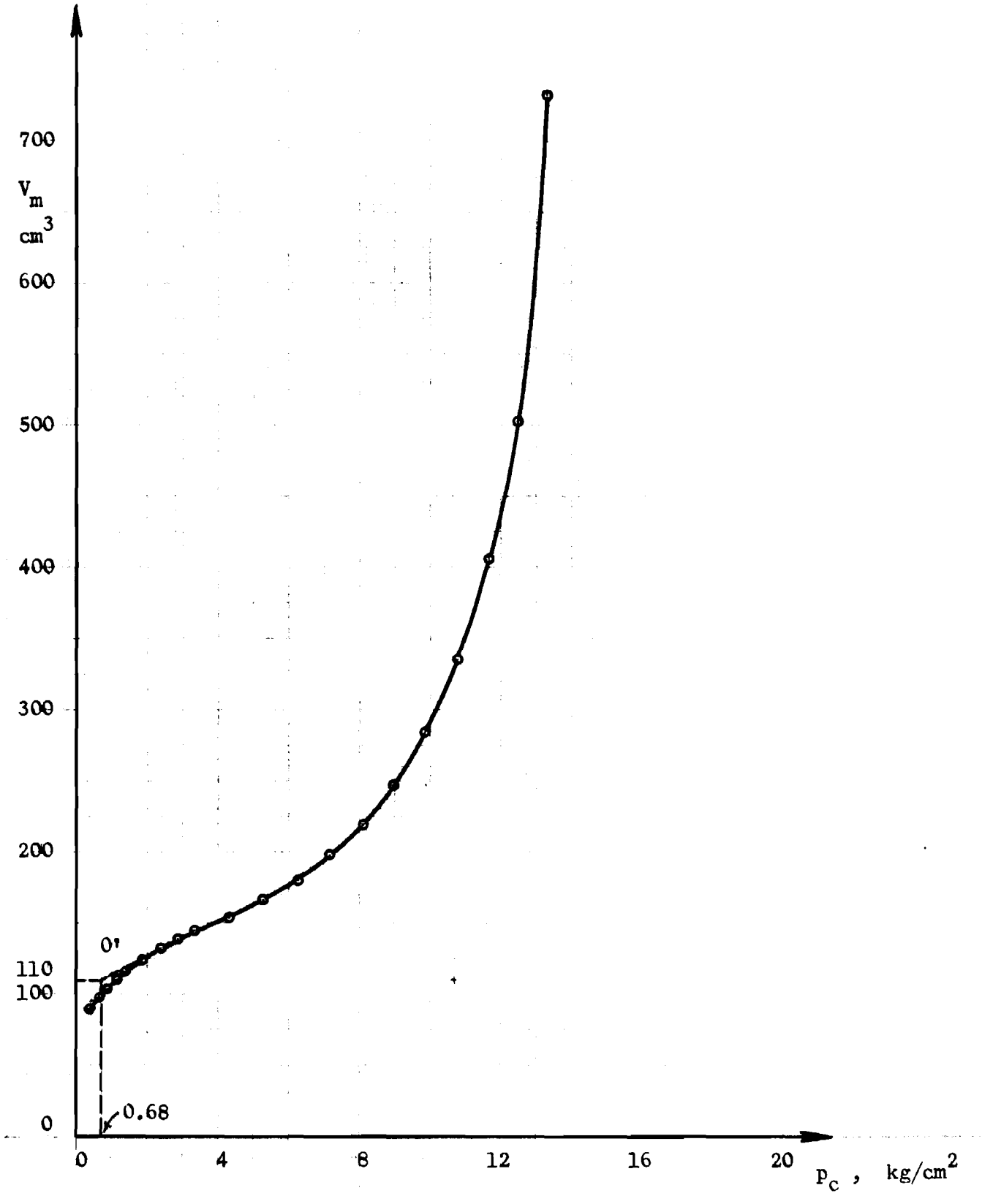

Fig. 53. Test 12 - 1. Pressuremeter curve. (Frozen clay).

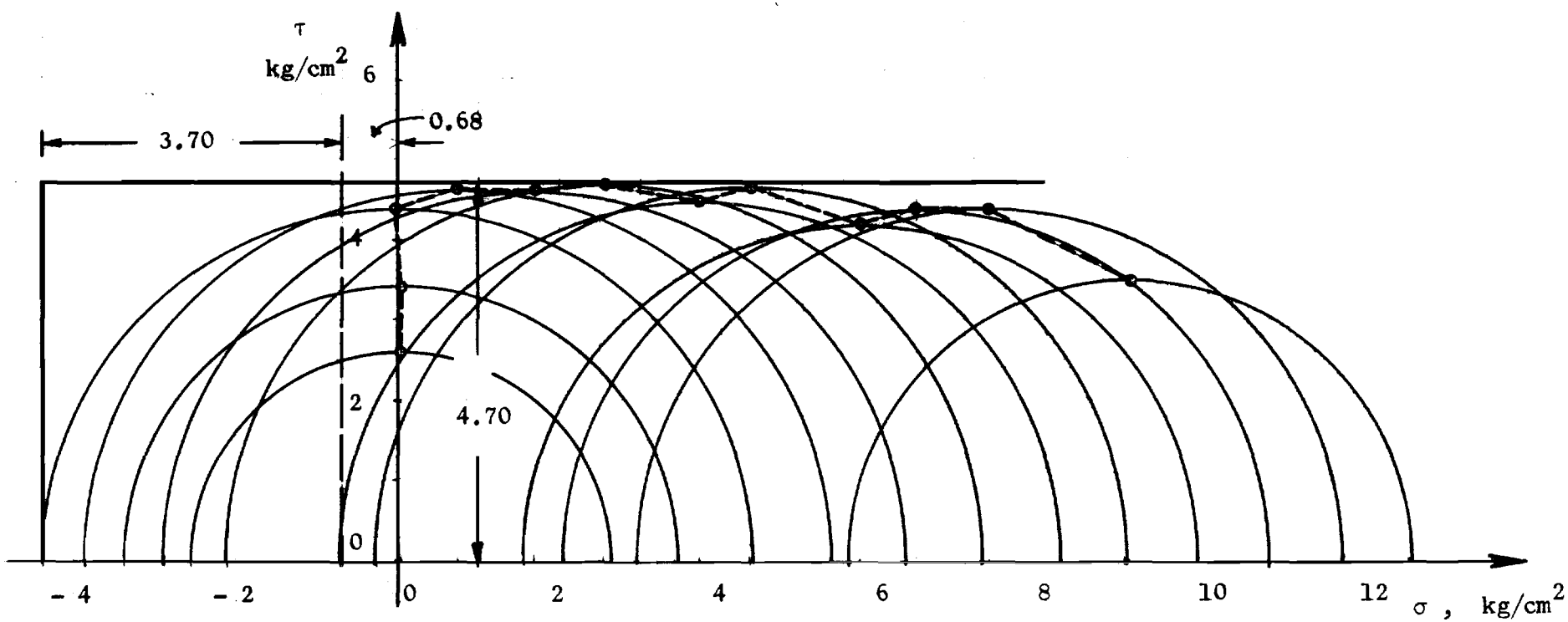

Fig. 54. Test 12 - 1. Vector curve. (Frozen clay).

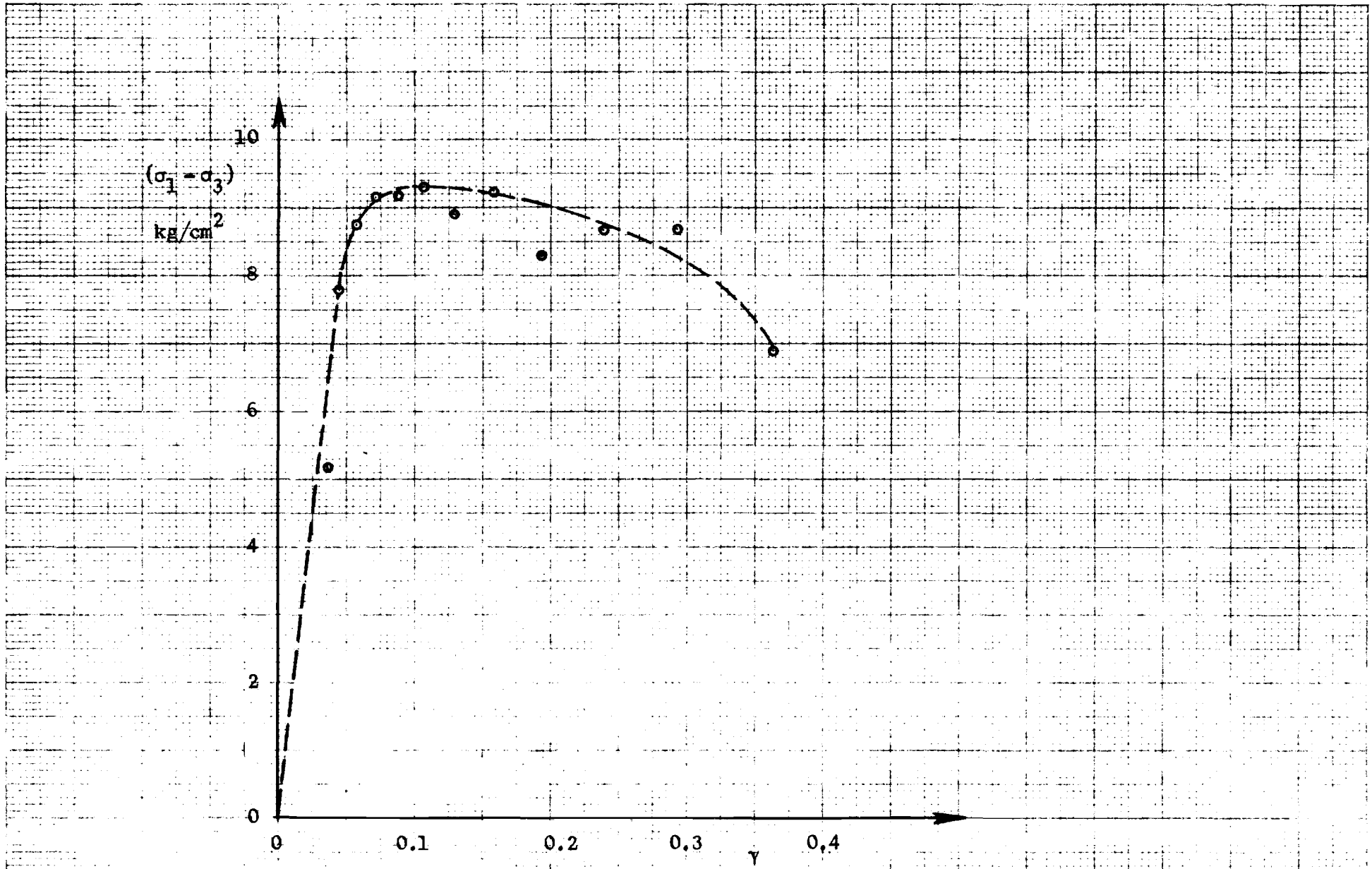

Fig. 55. Test 12 - 1. Stress-strain curve. (Frozen clay).

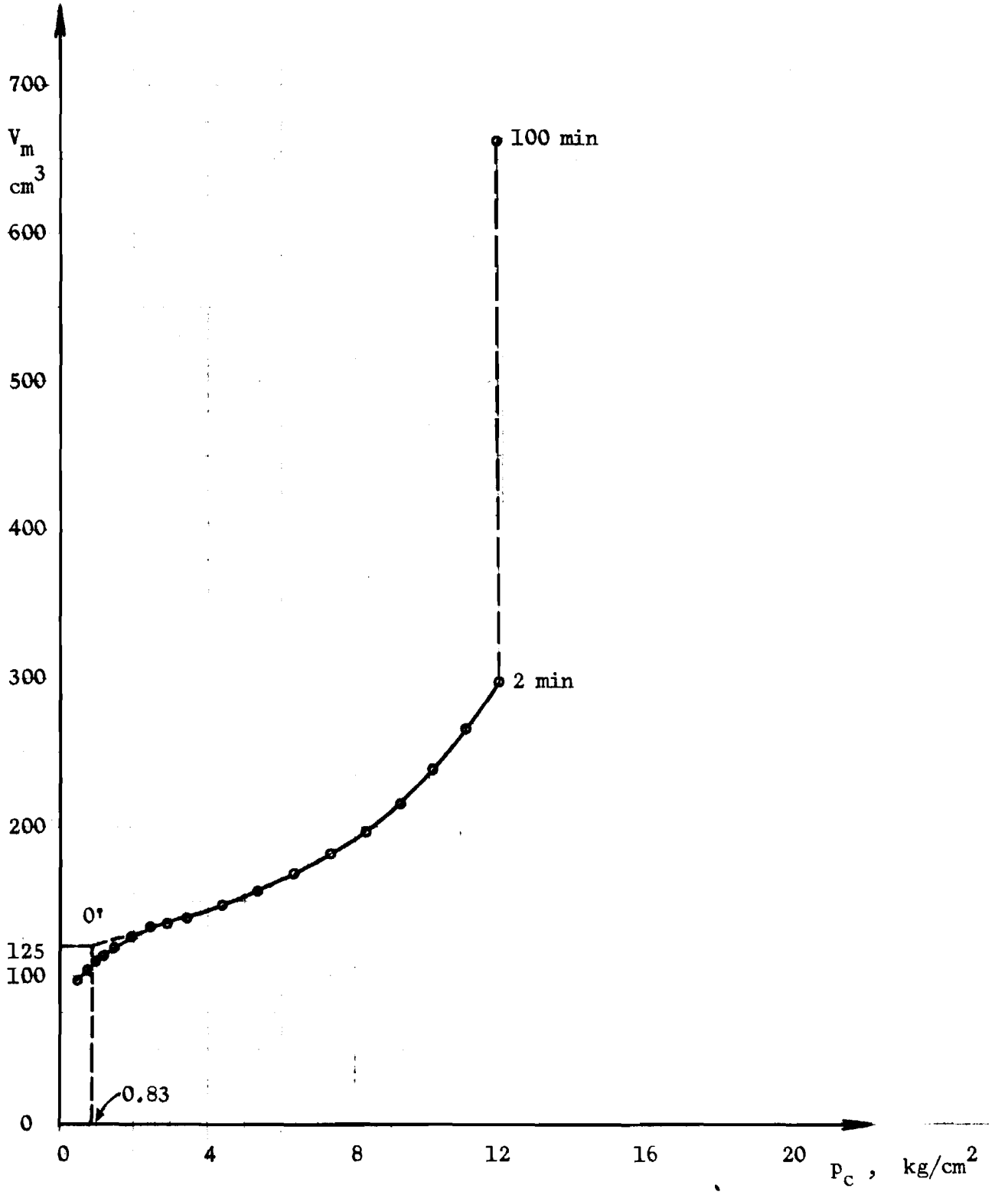

Fig. 56. Test 12 - 2. Pressuremeter curve. (Frozen clay).

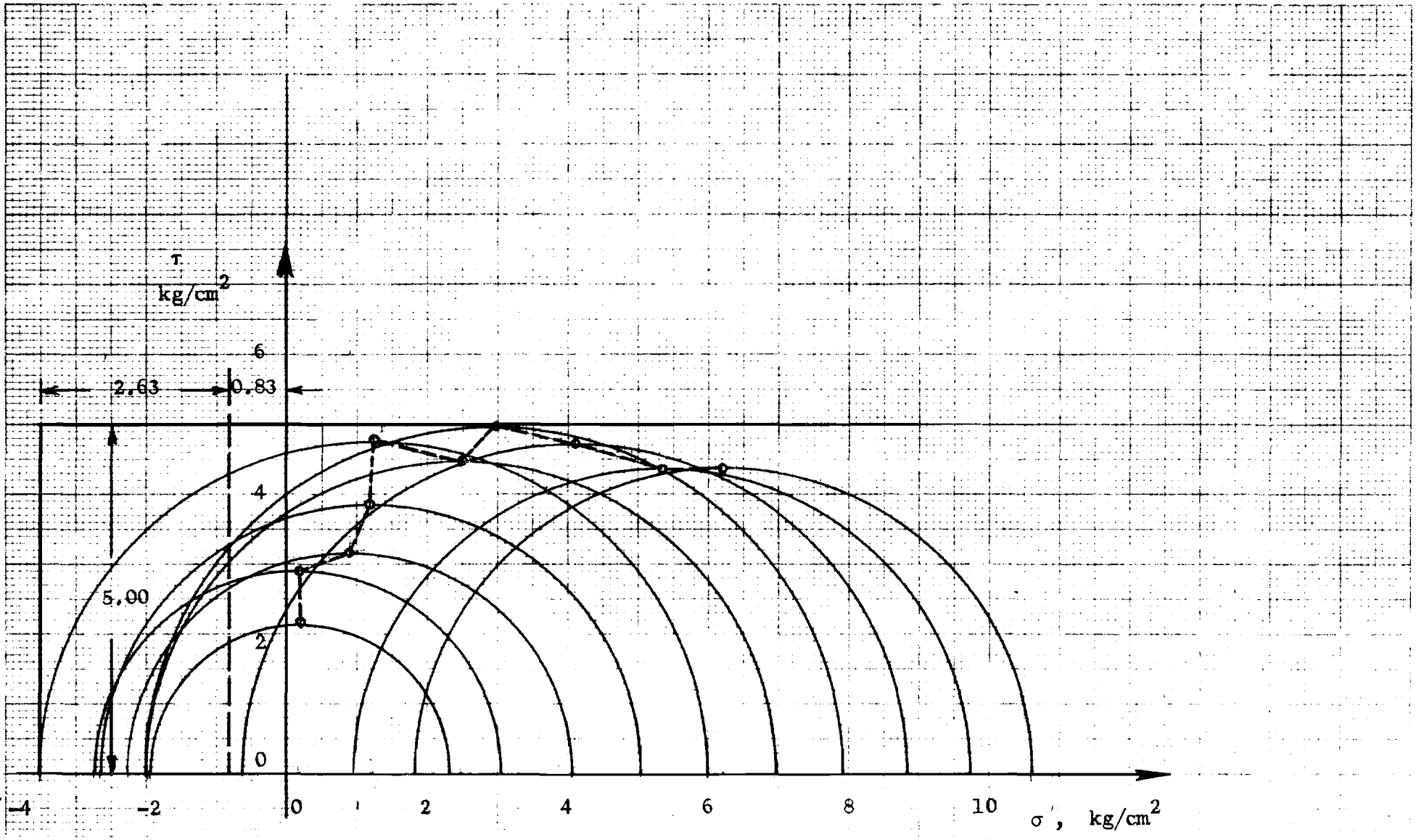

Fig. 57. Test 12 - 2. Vector curve.

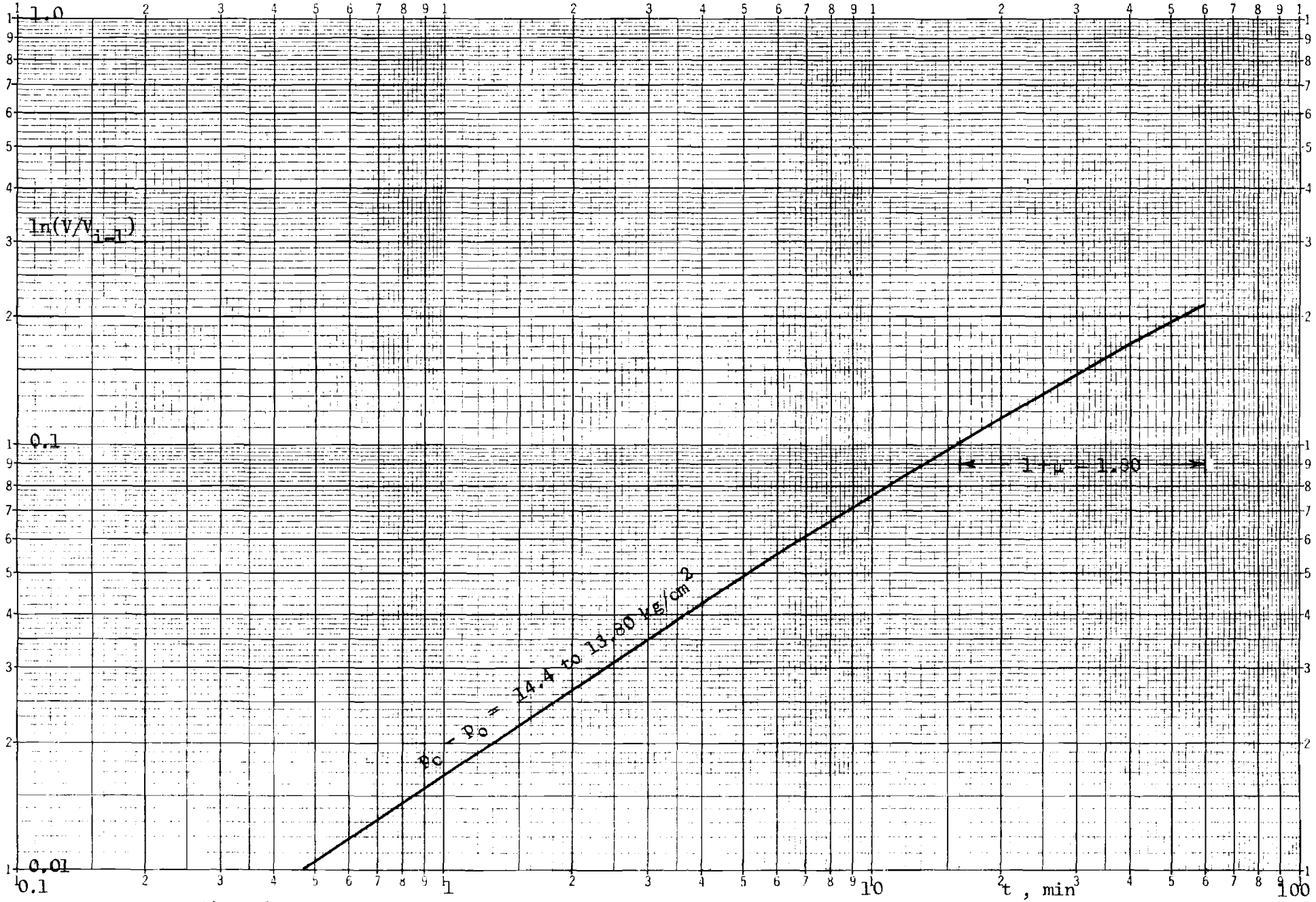

Fig. 58. Test 1 - 2. Creep curve.

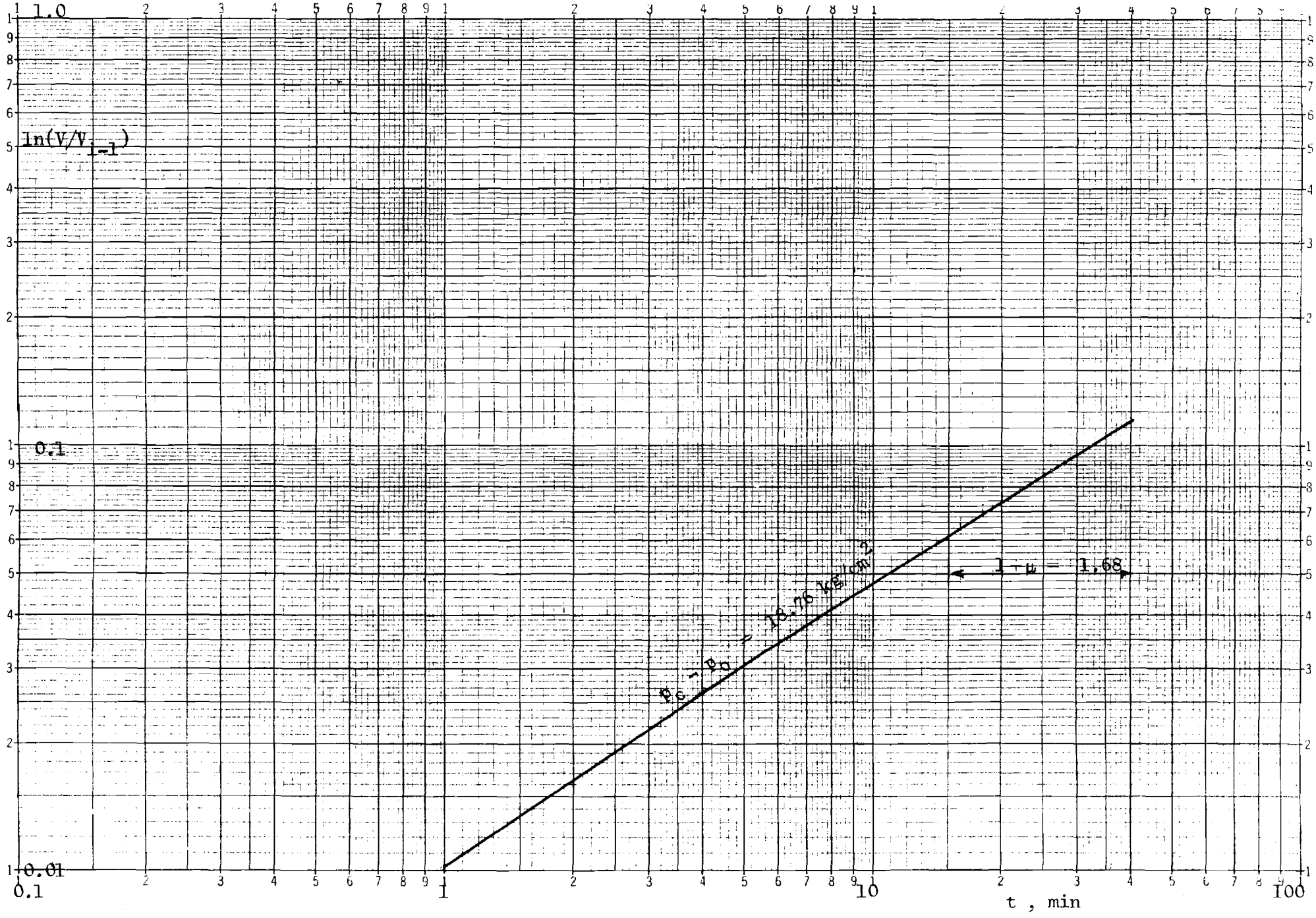

Fig. 59. Test 2 -3 . Creep curve.

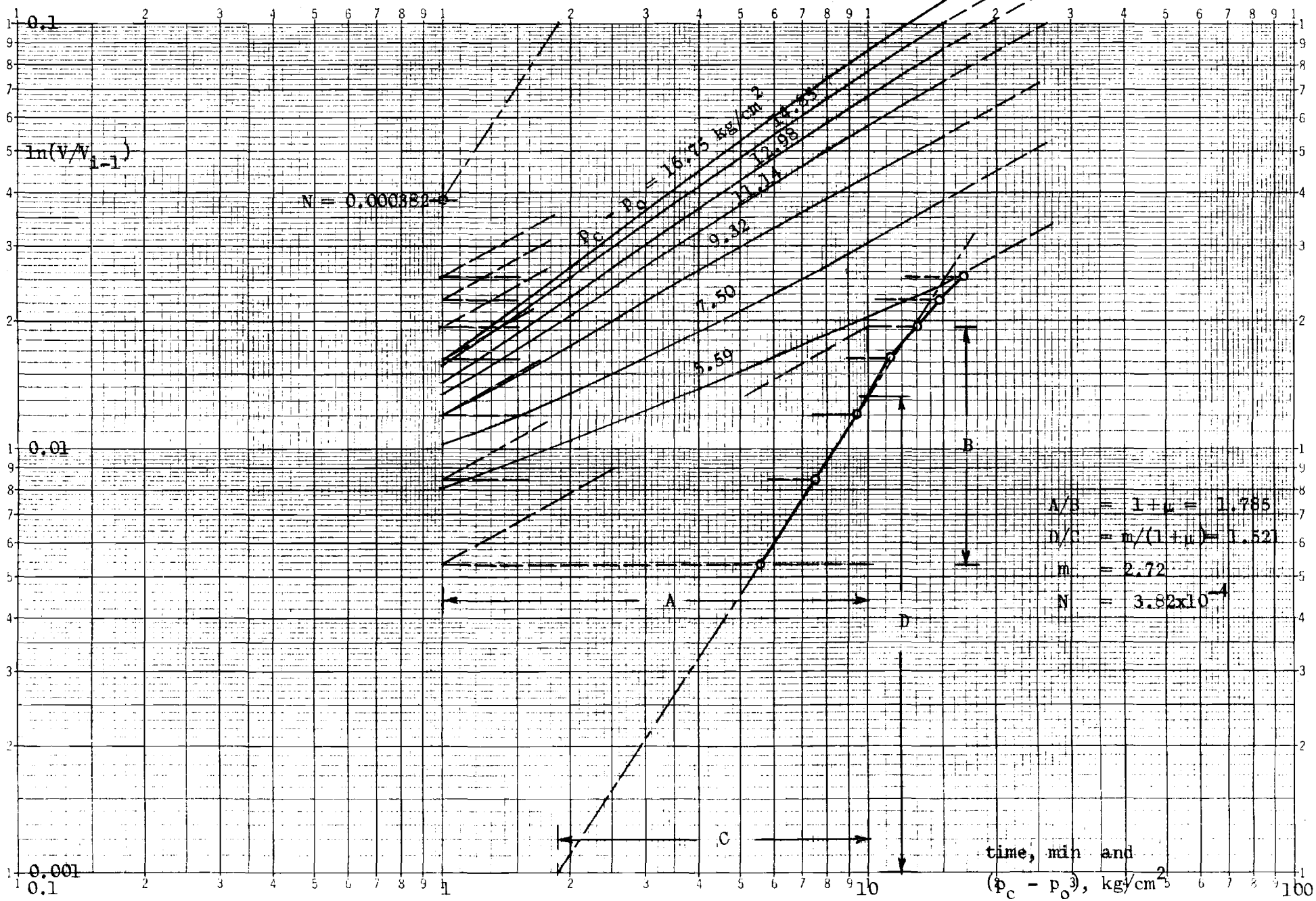

Fig. 60. Test 3 - 1. Determination of creep parameters.

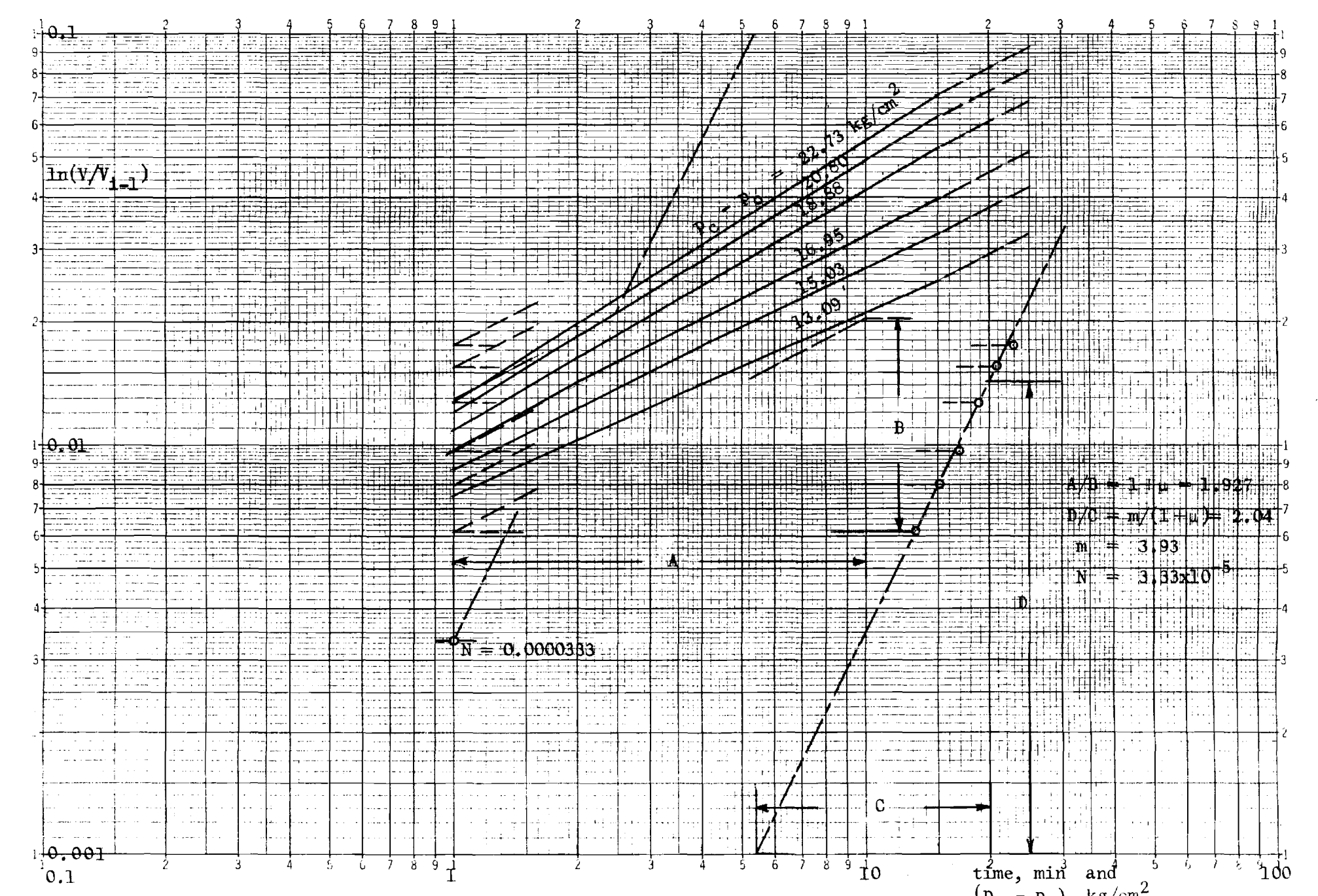

Fig. 61. Test 3 - 2. Determination of creep parameters.

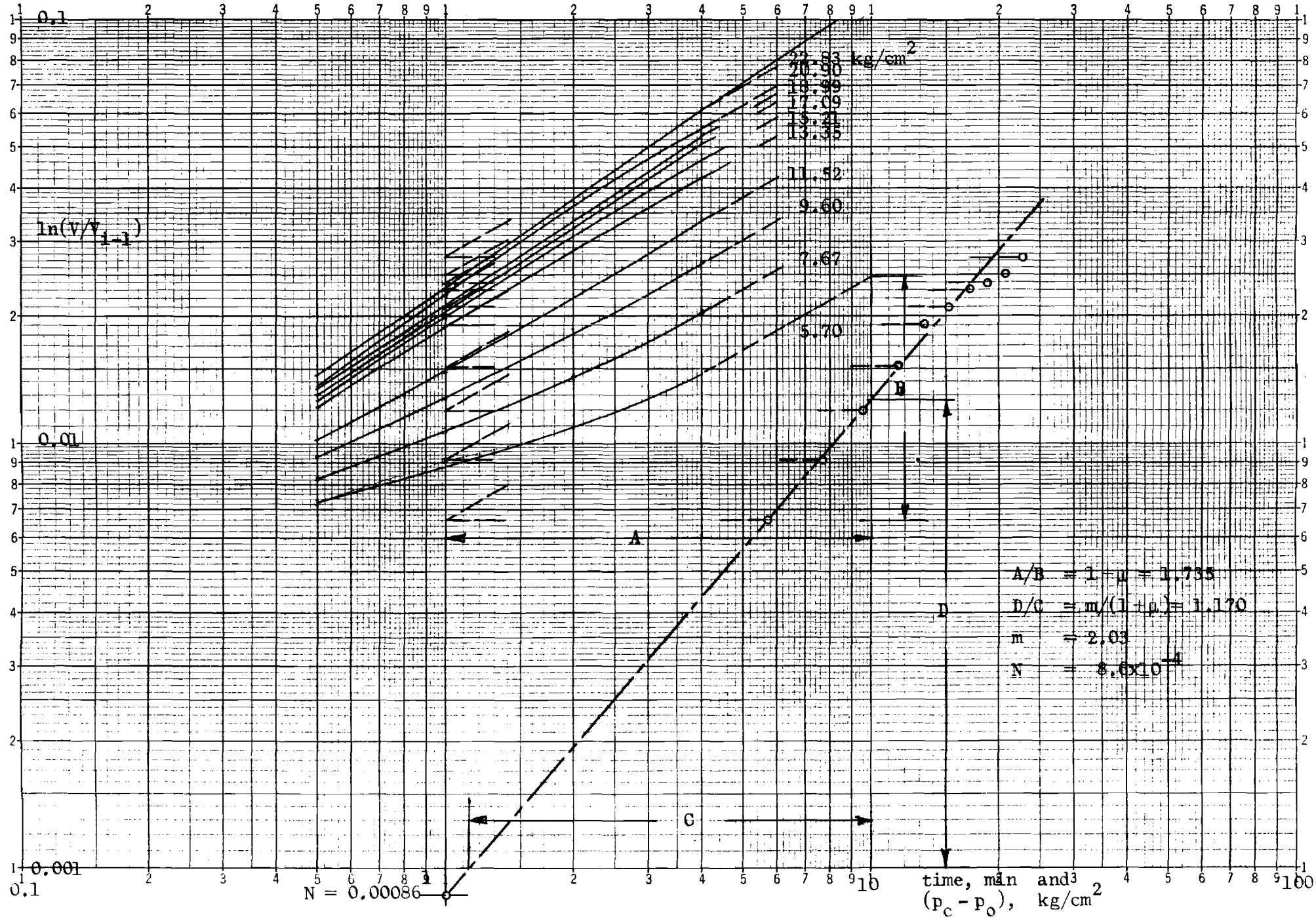

Fig. 62. Test 4 - 1. Determination of creep parameters.

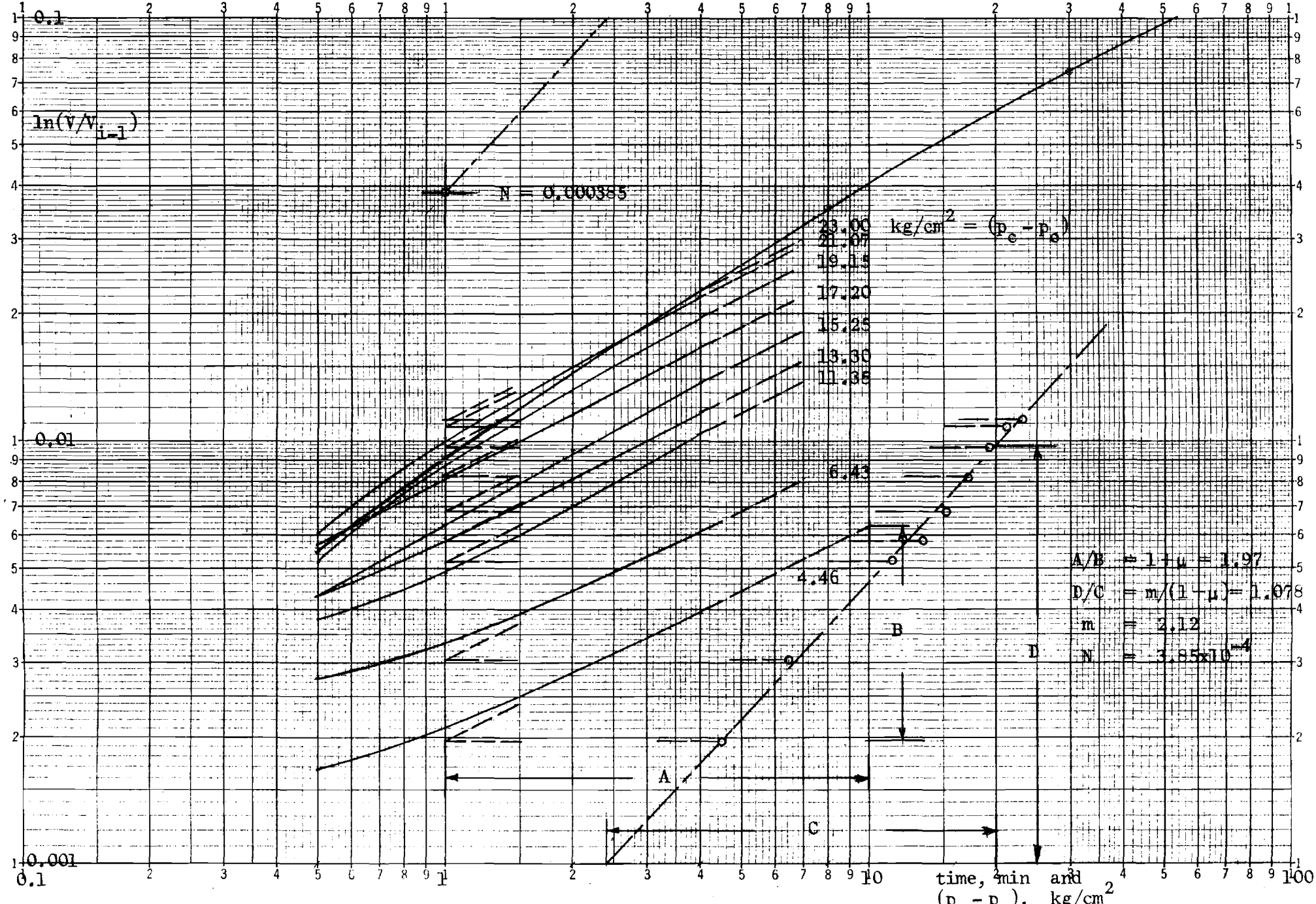

Fig. 63. Test 4 - 2. Determination of creep parameters.

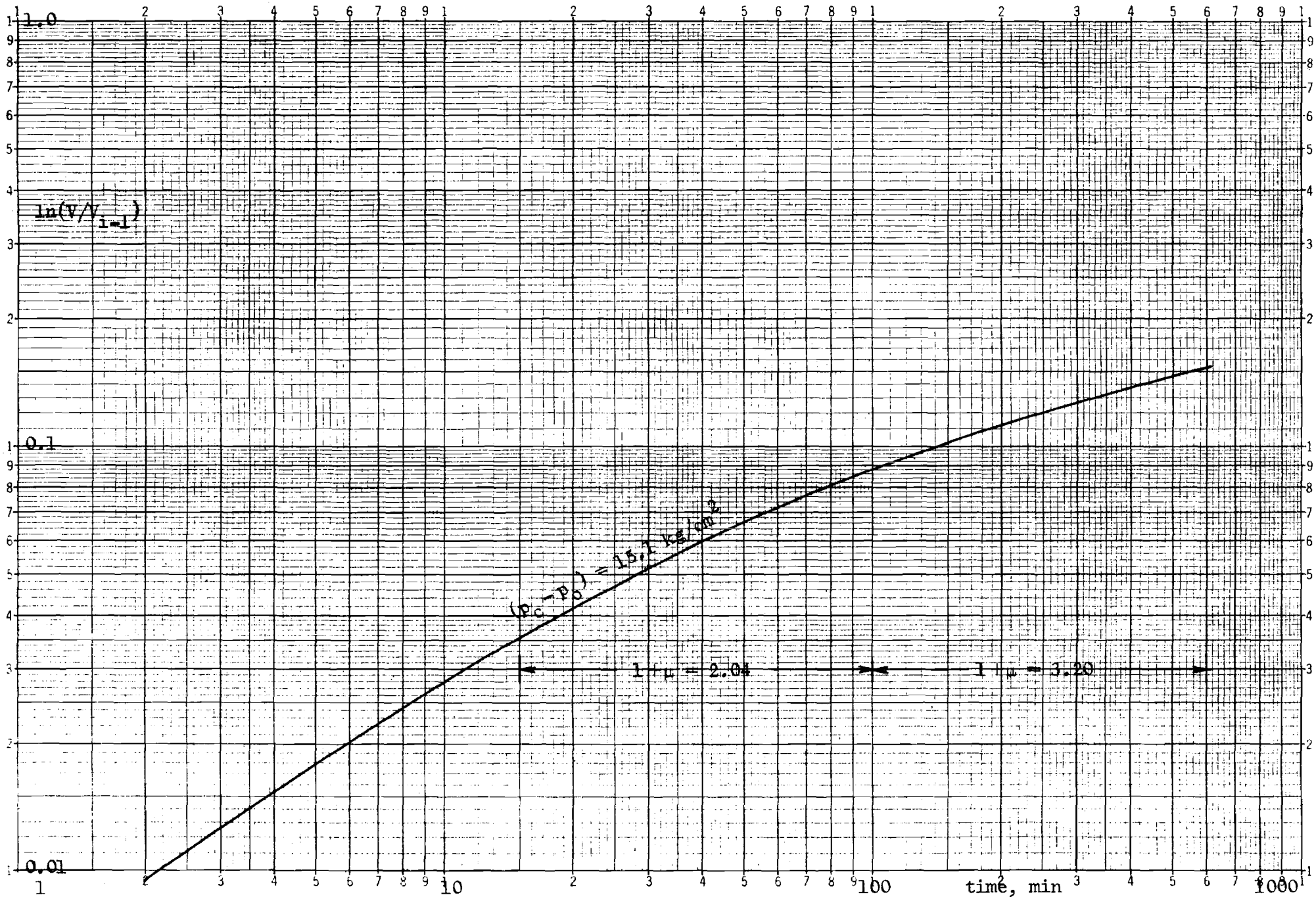

Fig. 64. Test 5 - 1. Creep curve.

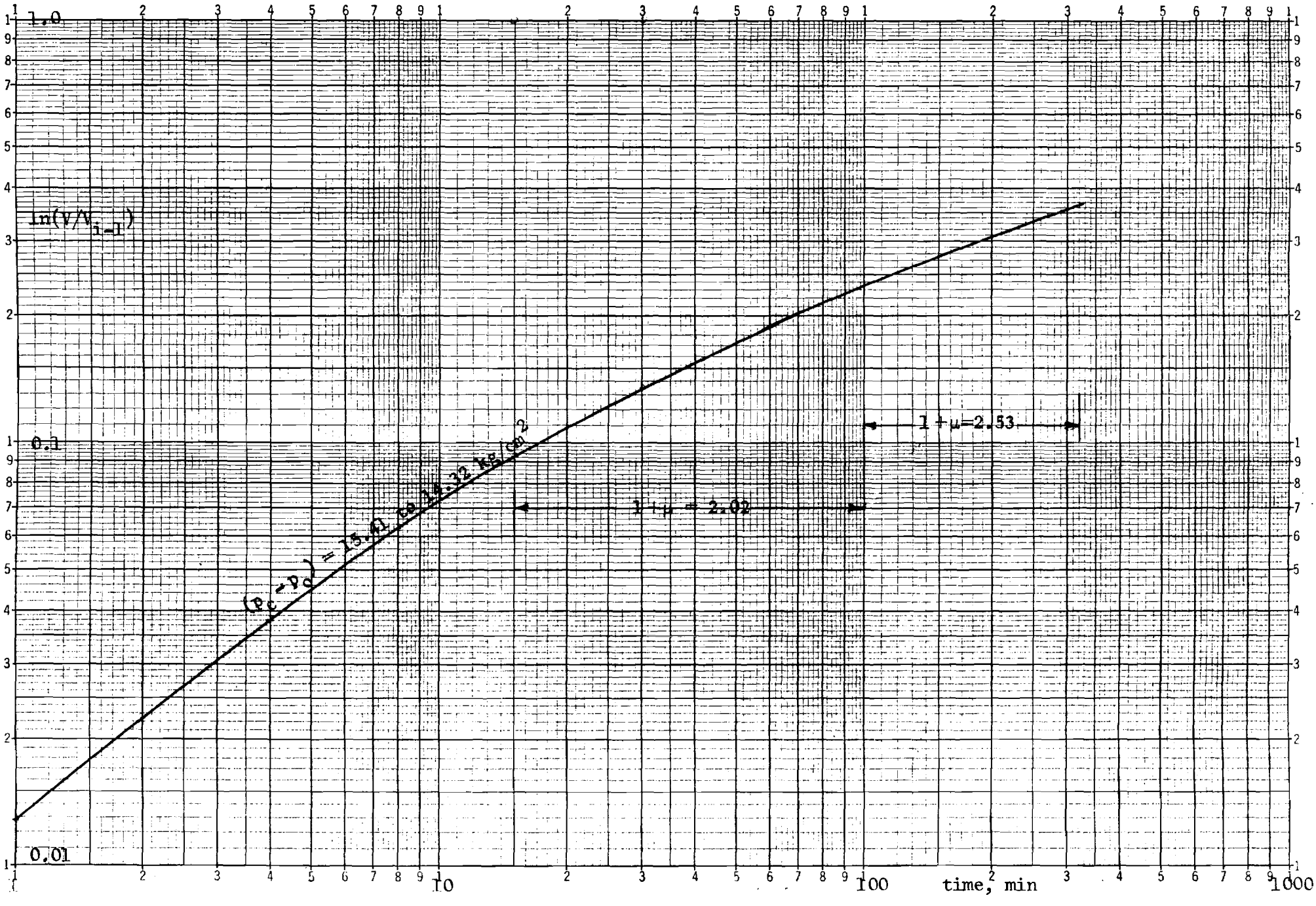

Fig. 65. Test 6 - 1. Creep curve.

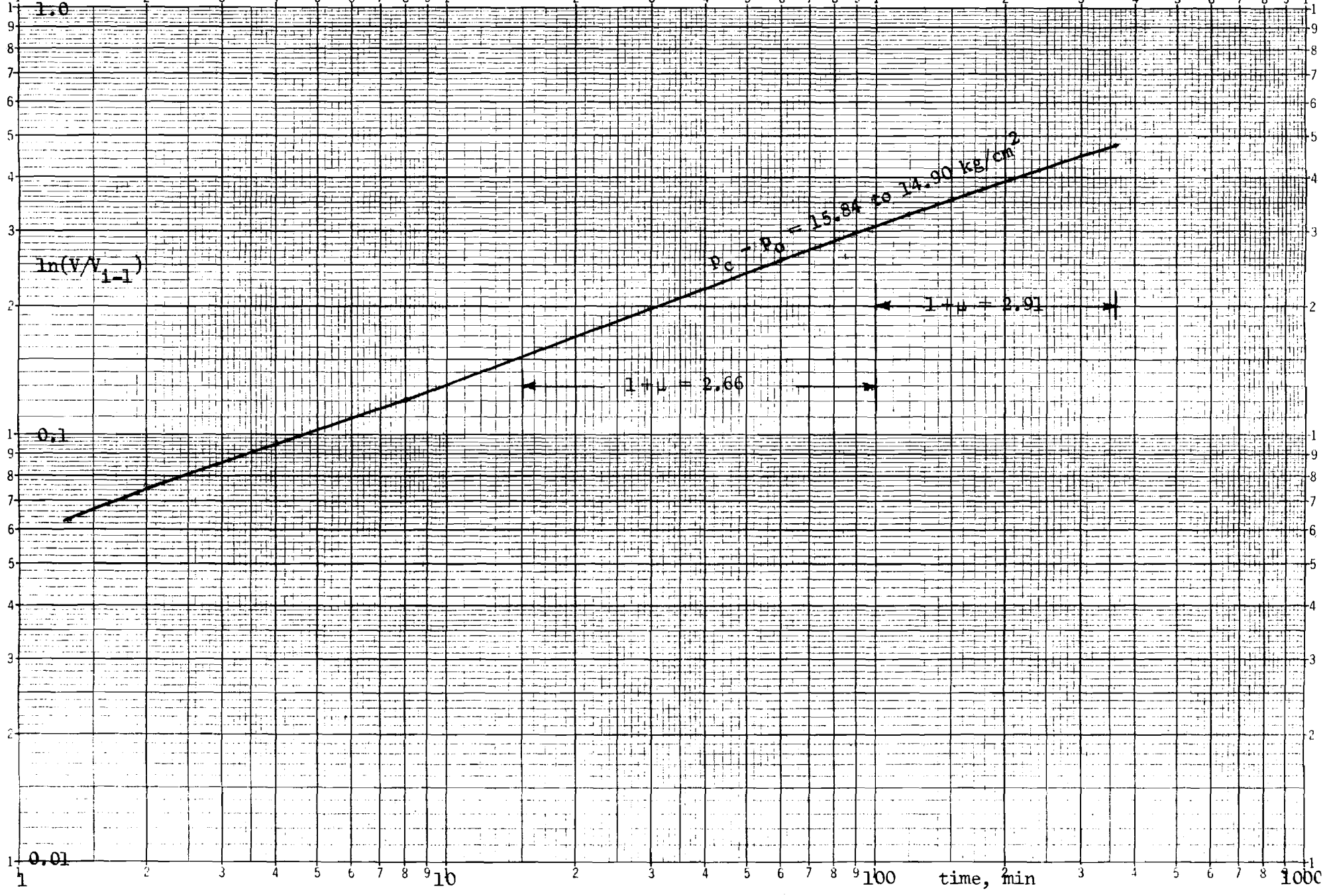

Fig. 66. Test 7 - 1. Creep curve.

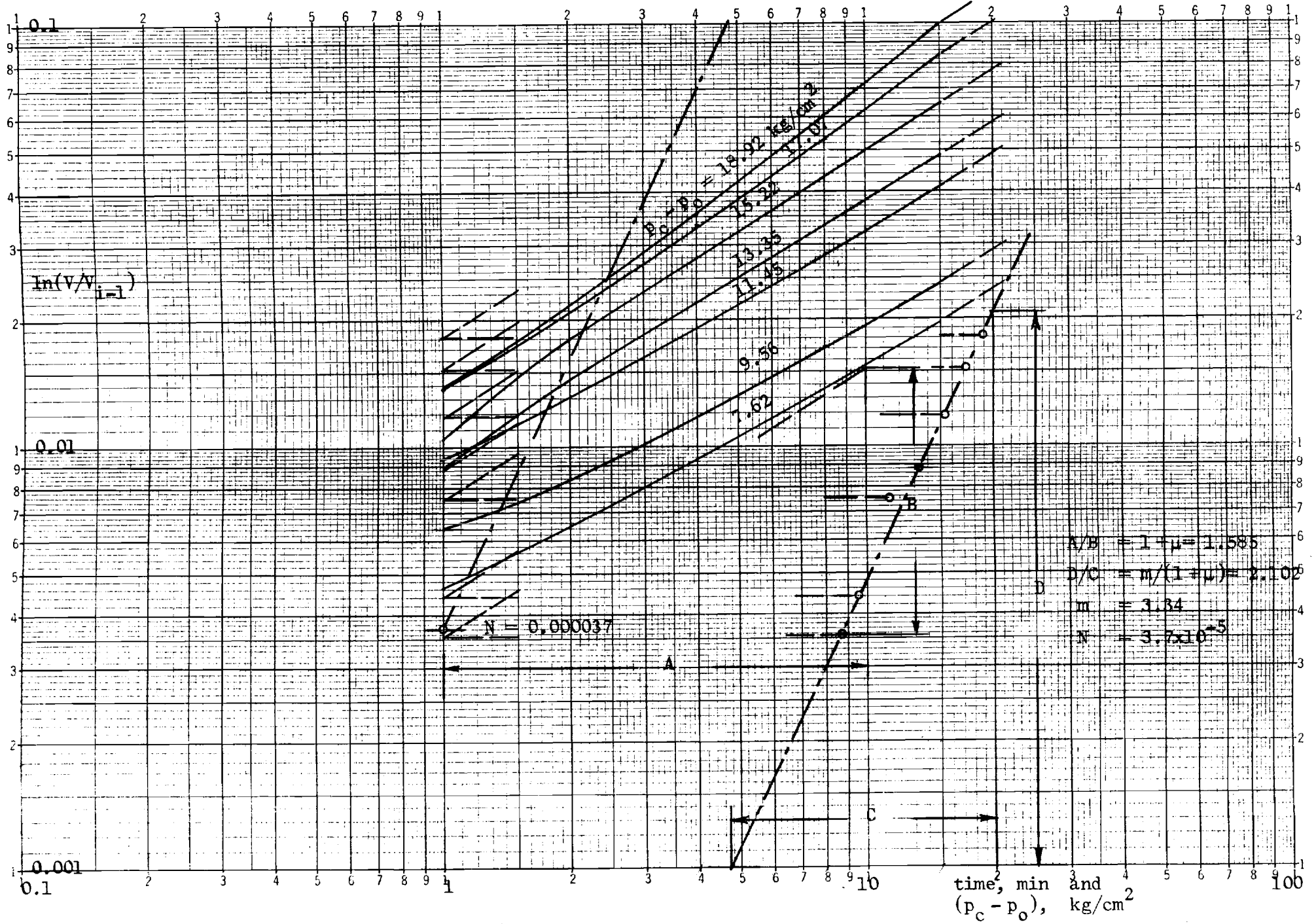

Fig. 67. Test 9 - 1. Determination of creep parameters.

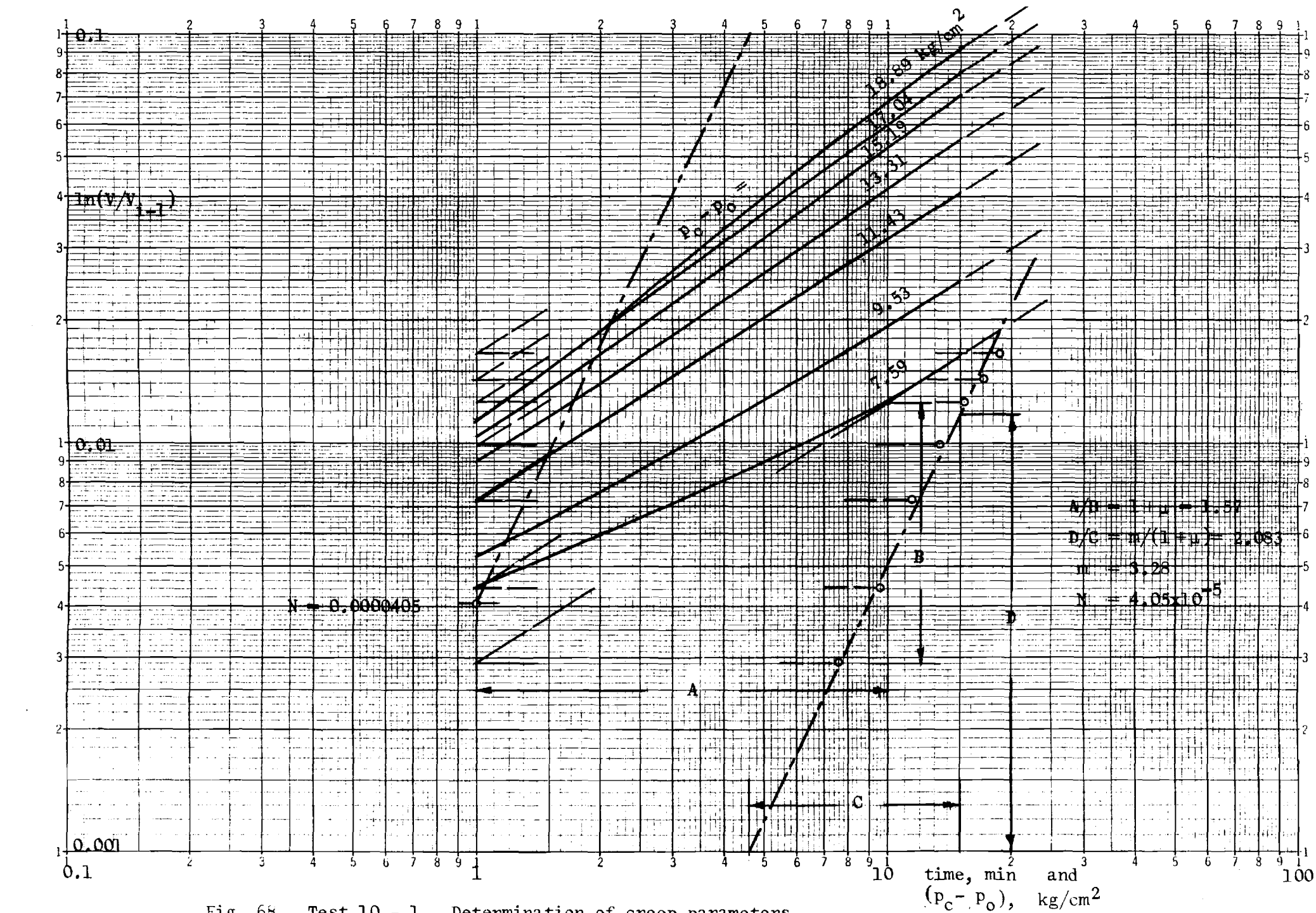

Fig. 68. Test 10 - 1. Determination of creep parameters.

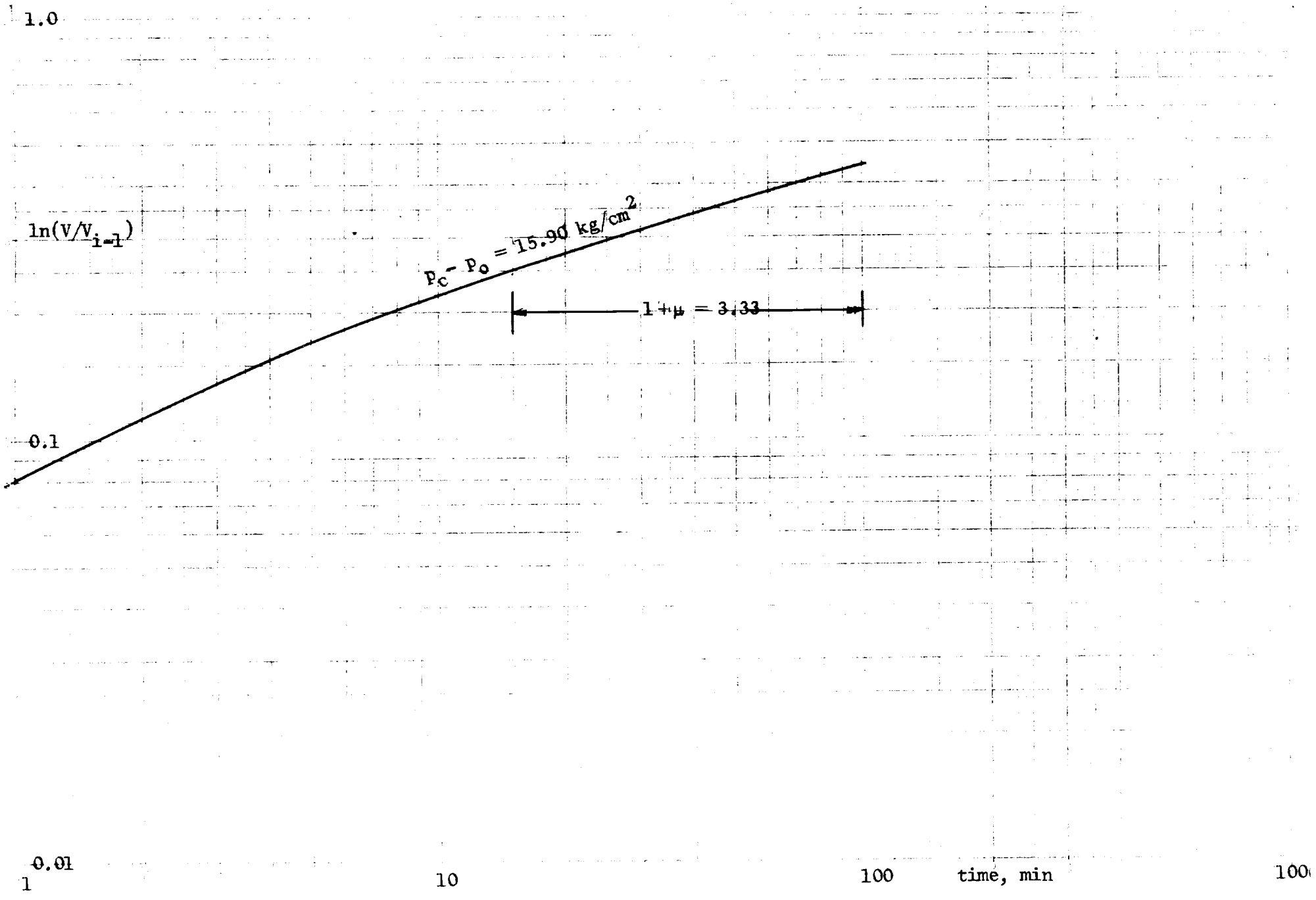

Fig. 69. Test 11 - 1. Creep curve.

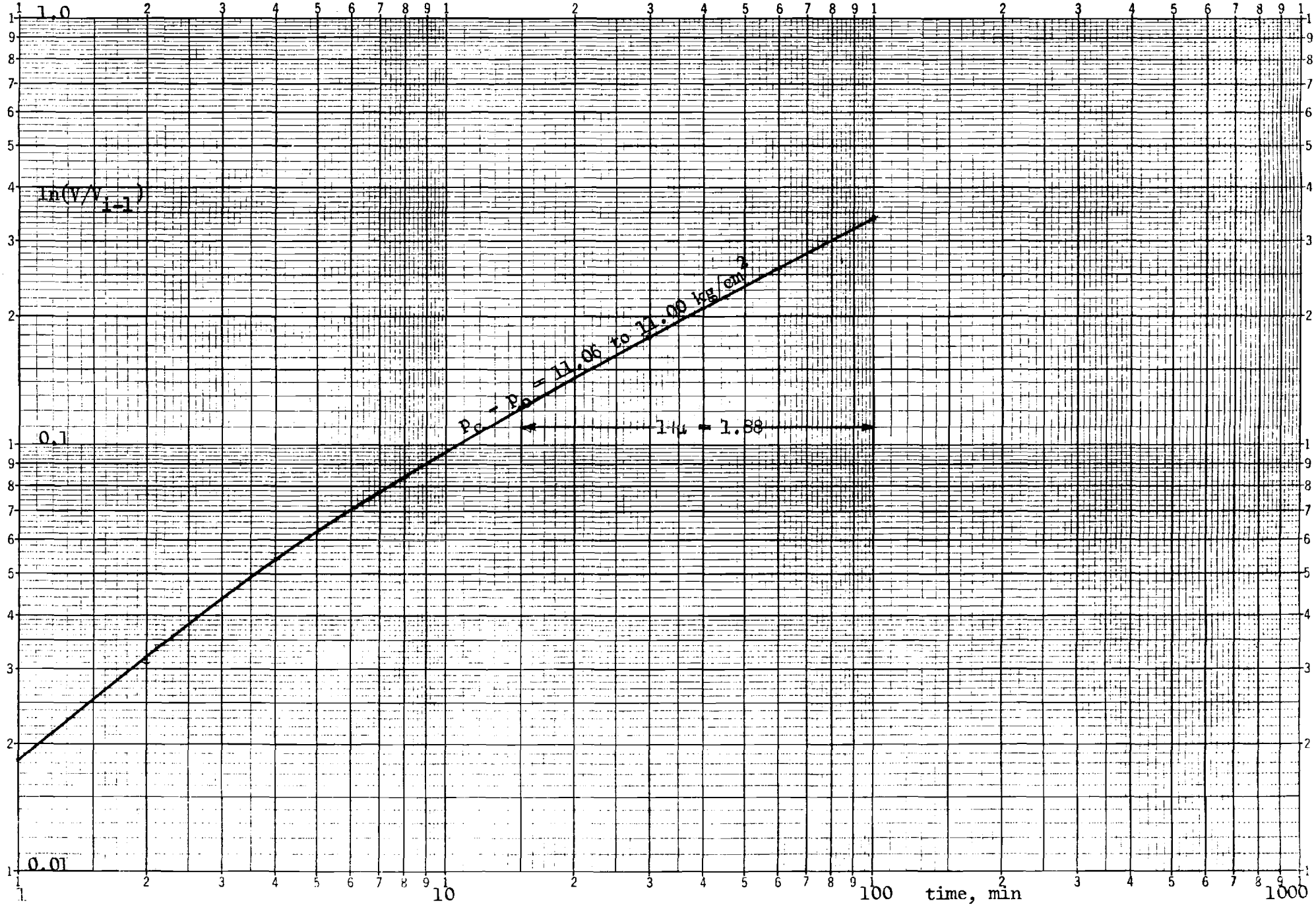

Fig. 70. Test 12 - 2. Creep curve.

APPENDIX A

EFFECT OF DISTURBED ZONE AROUND THE BOREHOLE ON THE RESULTS OF PRESSUREMETER TESTS

Due to drilling operations, destressing and temperature increase, it may be expected that a thin disturbed zone will be formed around a borehole in frozen soil. The presence of such a zone will influence the results of pressuremeter tests, and it may be interesting to try to estimate the importance of that influence on the parameters determined from the pressuremeter curve.

The presence of the disturbed zone makes the surrounding soil radially non-homogeneous in the immediate vicinity of the borehole. In reality, the degree of disturbance will decrease with distance from the hole and there will be a continuous variation of soil properties with distance. While such a problem can be solved by a numerical analysis (e.g., by the method used by Ladanyi, 1963a), only an approximate estimate of the effect of the non-homogeneity will be made here. The estimate is based on the assumption that all the disturbance is concentrated within a zone of finite thickness surrounding the borehole, while there is no disturbance outside of that zone.

The disturbed zone will affect the whole pressuremeter curve. As the most important portions of the curve, however, are those used for determining the pressuremeter modulus and the peak undrained shear strength of the soil, respectively, the analysis will be made only for the two extreme cases, viz.,

(1) For the pseudo-elastic portion of the curve, assuming elastic behavior both for the disturbed zone and the surrounding soil, and

(2) For the pseudo-plastic portion of the curve, assuming ideally plastic behavior of the disturbed zone.

The principle of consideration is described in the following.

If there is no disturbed zone, the plotting of the pressuremeter curve and the determination of parameters from the curve are usually made on the basis of net applied pressure, $p = p_c - p_o$, in the borehole of an initial volume V_o. Theoretically there is, however, no

reason why the pressuremeter curve could not be plotted in terms of the radial stress σ_r at any distance $r > r_o$ from the centre of the borehole, provided one replaces p by σ_r and V_o by V_r, the volume enclosed by the cylinder of radius r. Such a curve should give exactly the same values of parameters as the original one, if the soil is homogeneous.

If a disturbed zone of thickness t is present around the borehole, and if one can properly evaluate the properties of the disturbed soil in the zone, the correct pressuremeter curve for the undisturbed soil can be obtained by plotting the curve in terms of stresses and deformations outside of that zone, i.e., at $r = r_e$ (Figure A-1 (a)). The stress correction from p, applied at $r = r_o$, to p_e, applied to the undisturbed soil at $r = r_e$, will depend on the thickness of the disturbed zone and on its stress-strain and strength characteristics.

(1) Effect of Disturbed Zone on Pressuremeter Modulus, E_p

Assumptions:

(1) At small strains, the behavior of both the disturbed zone and the surrounding soil is linear-elastic with elastic constants ν_r and E_r for the zone, and ν and E for the surrounding soil;

(2) The soil deforms under plane-strain conditions.

From the Lamé's thick cylinder theory, and by equalizing radial displacements, at $r = r_e$, between the zone and the soil, it can be shown that p_e remains proportional to p and is governed by

$$p_e = \frac{p}{(a^2 - 1)B + 1} \qquad \text{(A-1)}$$

where

$$a = r_e/r_o = 1 + t/r_o \qquad \text{(A-1a)}$$

and

$$B = \frac{1}{2}\left[\frac{1 - 2\nu_r}{1 - \nu_r} + \frac{1+\nu}{1-\nu_r^2} \cdot \frac{E_r}{E}\right] \tag{A-2}$$

Assuming for an ice-saturated frozen soil that $\nu = \nu_r \approx 0.5$, one gets

$$B = E_r/E \tag{A-3}$$

and, since

$$a^2 - 1 = \frac{t}{r_o}\left(2 + \frac{t}{r_o}\right), \tag{A-3a}$$

$$p_e = \frac{p}{\frac{t}{r_o}\left(2 + \frac{t}{r_o}\right)\frac{E_r}{E} + 1} \tag{A-4}$$

The pressure p_e at $r = r_e$ refers to an initial volume

$$V_e = a^2 V_o \tag{A-5}$$

For example, in a typical case, one may have $t/r_o = 0.20$ and $E_r/E = 0.5$. Then, from (A-4) and (A-5), $p_e = 0.820p$ and $V_e = 1.44\, V_o$. According to Ménard (1957), the pressuremeter modulus for $\nu = 0.5$ is

$$E_p = 3\frac{\Delta p}{\Delta(\Delta V/V)} = 3\frac{\Delta p}{\Delta(\Delta V)}(V_o + \Delta V) \tag{A-6}$$

For example, in a pressuremeter test carried out in Leda clay, we can read from Figure 12, $\Delta(\Delta V) = 58.1\ cm^3$ for the pressure interval of 0 to 2 kg/cm^2. Since $V_o = 806\ cm^3$, uncorrected E_p is

$$E_p = 3\ \frac{2}{58.1}(806 + 58.1) = 89.4\ kg/cm^3 .$$

Assuming the presence of a weak zone with thickness $t/r_o = 0.20$, and with $E_r/E = 0.5$, one gets

$$\Delta p_e = 0.820 \times 2.0 = 1.640\ kg/cm^2 \quad \text{and}$$
$$V_e = 1.44 \times 806 = 1162\ cm^3 .$$

The corrected E_p is then

$$E_p = 3\ \frac{1.640}{58.1}\ (1162 + 58.1) = 103.3\ kg/cm^2 ,$$

which is an increase of 15.6 per cent over the uncorrected value. For the same thickness of the weak zone, the greatest difference would, obviously, appear for $E_r/E = 0$, giving

$$E_p = 126\ kg/cm^2 ,$$

which is an increase of 41 per cent.

This analysis shows that, with a reasonable care in borehole drilling, the effect of the disturbed zone on the pressuremeter modulus will probably not exceed about 20 per cent. Moreover, the effect can be eliminated by replacing in Eq. (A-6) Δp and V_o by Δp_e and V_e, according to Eqs. (A-4) and (A-5).

(2) Effect of Disturbed Zone on Undrained Shear Strength, c_u

Assumption:

At large strains, the disturbed zone is completely plastic with undrained cohesion $c_{ur} < c_u$.

In a completely plastic thick-walled cylinder, the stresses vary from the inside to the outside according to the equation (in terms of plane-strain information), (e.g., Drucker, 1967):

$$p_e = p - 2\, c_{ur} \ln(r_e/r_o) \qquad (A\text{-}7)$$

or

$$p_e = p - c_{ur} \ln(V_e/V_o) \qquad (A\text{-}7a)$$

In the pseudo-plastic region of the pressuremeter curve, the undrained compression strength and the corresponding average shear strain can be calculated from Eqs. (18) and (21), given in this report. If there is no disturbed zone, p in Eq. (18) denotes the pressure actually applied, while V_o in $V = V_o + \Delta V$ (Eq. 21) is actual initial volume of the borehole.

If a disturbed zone of thickness $t = r_e - r_o$ surrounds the borehole, one can, as before, remove the reference point to the outside of the zone by taking into account the resulting changes in p and V_o.

If, in Eq. (18), p_i and p_{i+1} are replaced by the corresponding p_e and p_{e+1} according to Eq. (A-7), there will be no change in the numerator, provided the thickness of the zone and the c_{ur} value do not change appreciably within this pressure interval. (Actually, t decreases with the hole expansion, as shown further). It also makes little difference if c_{ur} is small or even zero.

The main effect of the disturbed zone will, therefore, come from increasing the value of V_o to V_e. For illustration purposes, assume that $a = r_e/r_o = 1.20$. Then, from Eq. (A-7),

$$p_e = p_i - 0.368\ c_{ur}$$

$$p_{e+1} = p_{i+1} - 0.368\ c_{ur}$$

and

$$V_e = 1.44\ V_o$$

For the same pressuremeter test in Leda clay as before (Figure 12), it was obtained in the pseudo-plastic region:

$p_i = 3.0\ kg/cm^2$ $\qquad$ $\Delta V_i = 103.9\ cm^3$

$p_{i+1} = 2.5\ kg/cm^2$ $\qquad$ $\Delta V_{i+1} = 77.5\ cm^3$.

With $V_o = 806\ cm^3$ one gets: $(\Delta V/V)_i = 0.1140$ and $(\Delta V/V)_{i+1} = 0.0875$, from which

$$q_{i,i+1} = \frac{0.5}{\frac{1}{2} \ln(1140/875)} = 3.79\ kg/cm^2$$

for a strain of $\gamma_{i,\,i+1} = 0.1008$.

If V_o is replaced by $V_e = 1.44 \times 806 = 1162\ cm^3$, one gets,

$$(\Delta V/V)_i = 103.9/1268 = 0.0820 \quad , \text{ and}$$

$$(\Delta V/V)_{i+1} = 77.5/1239.5 = 0.0625 \ ,$$

and the new values of strength and strain are

$$q_{i,i+1} = \frac{0.5}{\frac{1}{2} \ln(820/625)} = 3.68 \text{ kg/cm}^2$$

at a strain of $\gamma_{i,\,i+1} = 0.0722$.

In other words, while the presence of a thin disturbed zone has only a small effect on the peak strength determined from the pressuremeter curve, it produces, nevertheless, a considerable shift of the stress-strain curve towards larger strains.

Figure A-1 (b) shows the whole stress-strain curve for the considered test in Leda clay (Figure 12), first calculated without, and then with taking into account a disturbed zone of a thickness $t_o = 0.2\ r_o$ (which amounts to $t_o = 7$ mm in the actual test). The calculation was made by assuming that the volume of the zone remained constant throughout the test, which leads to the approximate current thickness of the zone

$$t = t_o \left[V_o/(V_o + \Delta V)\right]^{\frac{1}{2}} \qquad \text{(A-8)}$$

from which,

$$V_e = V_o(1 + t/r_o)^2 \qquad \text{(A-9)}$$

and the corrected V is

$$V = V_e + \Delta V \qquad \text{(A-10)}$$

The corrected curve is seen to have higher modulus, lower strain at failure, and a little smaller peak strength. The new curve is assumed to be valid for the soil outside the disturbed zone.

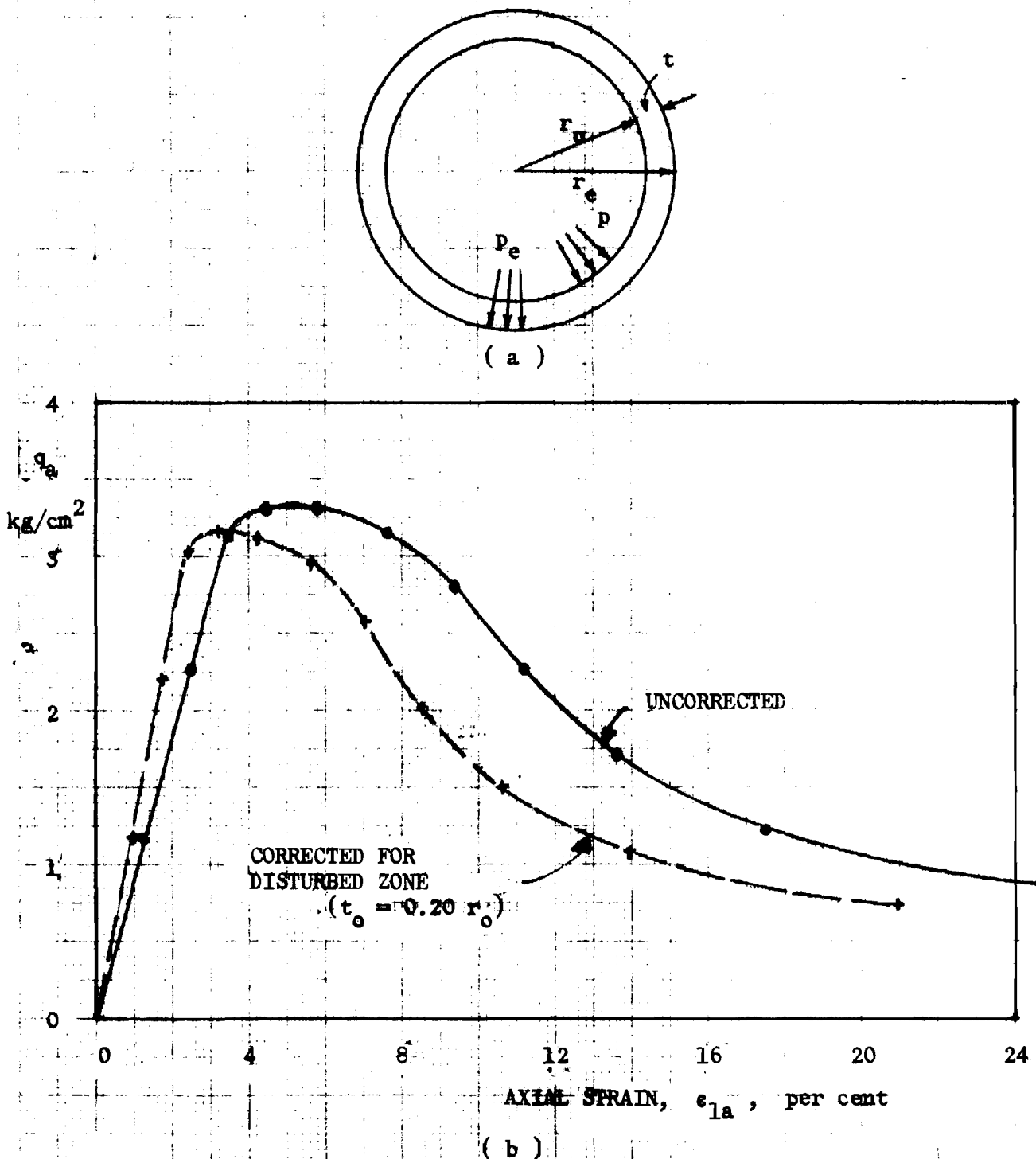

Fig. A - 1 . Effect of Disturbed Zone on Stress-Strain Curve.